Seasonal Variability of Iodomethane (CH_3I) Production in the Surface Ocean

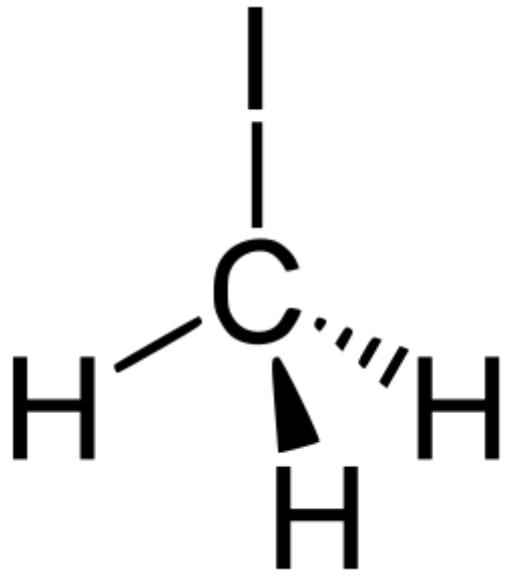

Qiang Shi

Seasonal Variability of Iodomethane (CH_3I) Production in the Surface Ocean

Dissertation
zur Erlangung des Doktorgrades
der Mathematisch-Naturwissenschaftlichen Fakultät
der Christian-Albrechts-Universität zu Kiel

vorgelegt von

Qiang Shi

Kiel 2012

Referent/in:	Prof. Dr. D.W.R. Wallace
Korreferent/in:	Prof. Dr. C. Marandino
Defence date:	29.01.2013

Table of contents

List of Figures

List of Tables

Abbreviations

°C	Degree Celsius
µl	Microliter
µm	Micrometer
µM	Micro mole per liter
$C_3H_3NaO_3$	Sodium pyruvate
$CaCl_2 \cdot 2H_2O$	Calcium Chloride Dihydrate
CCl_4	Tetrachloromethane
CDOM	Coloured Dissolved Organic Matter
CFCs	Chlorofluorocarbons
CH_3CCl_3	1,1,1-Trichloroethane
CH_3I	Methyl iodide
$CHBr_3$	Bromoform
$CHCl_3$	Chloroform
Chl *a*	Chlorophyll a
cm	Centimetre (10^{-2} metres)
$CoCl_2 \cdot 7H_2O$	Cobalt chloride heptahydrate
d	Day (as time unit)
dC	Daytime accumulation
DMS	Dimethyl sulfide
DOC	Dissolved organic carbon
DOI	Dissolved organic iodine
DOM	Dissolved organic matter
ECD	Electron capture detector
F	Filtered
$FeCl_3 \cdot 6H_2O$	Iron(III) chloride, hexahydrate
$F_{sea\text{-}air}$	Flux between ocean and atmosphere
GC	Gas chromatography
h	Hour (as time unit)
H_3BO_3	Boric acid
HDEP	High-density polyethylene bottles
He	Helium
HEPES	4-(2-hydroxyethyl)-1-piperazineethanesulfonic acid

HMDE	Hanging mercury drop electrode
HOI	Hypoiodous acid
HOI	Hypoiodous acid
hν	Light
I^-	Iodide
I_2	Molecular iodine
I_2O_2	Diiodide dioxide
IO	Iodide oxide
IO_3^-	Iodate
KCl	Potassium chloride
KI	Potassium iodide
KIO_3	Potassium iodate
L	Liter
$L_{(air\text{-}sea)}$	Loss rate sea-to-air flux
$L_{(Mix)}$	Loss rate diffusion
$L_{(other)}$	Loss rate others
$L_{(SN2)}$	Loss rate SN_2
MED 4	Mediator complex subunit 4
$MgCl_2$	Magnesium chloride
$MgSO_4 \cdot 7H_2O$	Magnesium sulfate heptahydrate
min	Minute (as time unite)
mm	Millimetre
NaCl	Sodium chloride
$NaEDTA \cdot 2H_2O$	Ethylenediaminetetraacetic acid, disodium dihydrate
NaH_2PO_4	Monosodium phosphate
$NaHCO_3$	Sodium bicarbonate
NF	Non-filtered
$(NH_4)_2SO_4$	Ammonium sulfate
nm	Nanometre
nM	Nano mole per liter
O_2	Oxygen
P	Pre-purged samples
P_{gross}	Gross production
P_{net}	Net production
pM	Pico mole per liter

SN_2	Bimolecular nucleophilic substitution
SSS	Surface seawater salinity
SST	Surface seawater temperature
Tg	Tetagram (10^{-12} grams)
UV	Ultraviolet light
V	Volt
VHOC	Volatile halogenated organic compounds
WCOT	Wall-coated open tubular
yr	Year (as time unit)
$ZnSO_4 \cdot 7H_2O$	Zinc Sulfate Heptahydrate
$^{63}_{28}\mathrm{Ni}$	Radioactive Nickel-63

Author contributions

Chapter 3: The seasonal cycle of methyl iodide in the Kiel Fjord.

Qiang Shi wrote the manuscript and performed all experimental work about methyl iodide. Kathrin Wuttig and Mirja Dunker provided additional experimental data about CDOM and iodine. The data about chlorophyll *a,* SSS and SST was provided by FB2-BI department (Annegret Stuhr and Catriona Clemmesen-Bockelmann). FB1-ME provided all the meteorological data. Wallace and Marandino contributed the discussion.

Chapter 4: Results and discussion from the Kiel Fjord incubation experiments

Qiang Shi conducted all the incubation experiments for natural seawater, performed the calculations, evaluated the data and wrote the manuscript. Hansup Nam Koong provided the data for the incubation experiments for artificial seawater. Wallace contributed the discussion.

Appendix: SHIVA Sonne Cruise: Results and Discussion

Qiang Shi collected all Data about CH_3I using GC-ECD during SHIVA Sonne cruise, performed the calculations, and wrote the manuscript. Kathrin Wuttig provided additional experimental data about iodine. The concentrations of chlorophyll *a* and phytoplankton pigments, including Zeaxanthin, were analysed by colleagues from the Alfred Wegener Institute (AWI). Marandino and Quack contributed the discussion.

Summary

Methyl iodide is a major carrier of gas phase iodine from the ocean into the atmosphere. In the atmosphere, methyl iodide is photodissociated by near-UV light, and participates in ozone destruction and aerosol formation in the troposphere. In the ocean, the production sources and sinks, including air-sea flux, of methyl iodide must be investigated to improve the understanding of the methyl iodide global cycle.

From October 2008 to November 2010 methyl iodide concentrations were measured in the Kiel Fjord. They showed a repeating seasonal cycle of CH_3I with highest concentrations in summer (June and July) and lowest concentrations in winter (December to February). The correlations of methyl iodide concentration with corresponding biological and physical parameters (e.g. solar radiation) in the Kiel Fjord were investigated. The strongest positive correlation was observed between CH_3I and solar radiation, and implied that CH_3I production in the Kiel Fjord is controlled primarily by the amount of solar radiation reaching the sea surface and likely by a photochemical mechanism.

“Whole-bottle” (quartz-flask) long-term (57 hours) incubation experiments were conducted to examine production of methyl iodide from July 2009 to July 2010 in the context of the time-series. A clear diurnal variation of methyl iodide was observed in the samples exposed to natural light. The concentration of methyl iodide in the “sunlit” samples increased from 08:00 to 17:00, and decreased from 17:00 to 08:00 of the second day. Compared to the “sunlit” samples, the CH_3I concentration in the “dark” samples varied only slightly. This implied that solar radiation played an important role in the CH_3I production process, and is consistent with the CH_3I production by a photochemical mechanism.

No significant difference was observed between filtered and non-filtered samples with the natural sunlight incubations for incubation experiments conducted in the same month. The daytime accumulation of methyl iodide (from 08:00 t0 17:00) was not affected by filtration. Hence, the CH_3I

production pathway does not appear to be directly biological but rather photochemical in nature.

However, methyl iodide loss during the night was larger in the samples that were incubated under daylight. As a result, the daily net production of methyl iodide over 24 h was low in the incubation flasks. During our incubation experiments, loss by a sea-to-air flux was excluded because the flasks were sealed. The mean chemical loss rate of 0.047 pmol L^{-1} day^{-1} was calculated, and this was 1-2 orders of magnitude lower than the observed loss rate of CH_3I during the night in the incubation experiments, which averaged 2.98 pmol L^{-1} day^{-1}. There are two main possibilities for this additional loss pathway. One is bacterial degradation, the other is chemical oxidation by compounds that are produced during the day and which accelerate the degradation of CH_3I during the night.

Using the annual cycle of monthly mean concentrations in Chapter 3, a mass balance for CH_3I in the Kiel Fjord was calculated. Based on the gas exchange relationship of Nightingale et al. [2000] the calculated sea-to-air flux in this study averaged 3.1 nmol m^{-2} day^{-1}. The daily net production rates of CH_3I could be estimated from the field time-series data. They had strong seasonal variability and ranged from 0 to 0.15 pmol L^{-1} day^{-1}. By combining loss rates estimated from the incubation experiments with net production rates estimated from the field time-series data, the gross production rates for CH_3I were calculated on a monthly basis. These calculations imply highest gross production rates in summer and much lower production rates in winter and are consistent with a seasonal cycle of CH_3I that is driven primarily by variations in light intensity.

Zusammenfassung

Methyliodid ist ein Haupttransportträger des Jods vom Ozean in die Atmosphäre. Im Zeitraum von Oktober 2008 bis November 2010 wurde die Konzentration des Methyliodids in der Kieler Förde bestimmt. Die Konzentration zeigte eine sich wiederholende saisonale Schwankung mit einem Maximum im Sommer und einem Minimum im Winter.

Dieser Zusammenhang wurde anhand von Inkubations-Experimenten zwischen Juli 2009 und Juli 2010 untersucht. Die Experimente wurden in mit „Fördewasser“ gefüllten Quarzflaschen (300 mL, kein Headspace) über eine Dauer von bis zu 57 h in 50 cm Wassertiefe am Pier des Helmholtz-Zentrums für Ozeanforschung Kiel (GEOMAR) durchgeführt. Als Negativkontrolle wurden parallel Dunkelproben analysiert.

Die Lichtproben zeigten eine deutliche Schwankung bezüglich der Methyliodidkonzentration. Täglich nahm die Konzentration über die Lichtperiode zu um dann in der Dunkelperiode wieder abzufallen. Eine Filtration der Wasserproben mit einem 0,2 mm Filter, was die Konzentration der Bakterien in den Quarzflaschen minimierte, nahm keinen Einfluss auf die Methyliodidkonzentration. Das lässt darauf schließen, dass die Produktion des Methyliodids primär photochemisch erfolgt. Diese Vermutung wird durch die Dunkelproben bestätigt, in denen die Methyliodidkonzentration nur schwache oder keine Schwankungen aufwies. Des Weiteren findet in der Dunkelperide ein erhöhter Abbau des Methyliodids statt. Sowohl die Produktion unbekannter chemischer Substanzen innerhalb der Lichtperiode, als aich Bakterien, die nicht durch die Filtration entfernt wurden, könnten für diesen Abbau verantwortlich sein. Insgesammt zeigte sich die Nettoproduktion des Methyliodids als gering.

Der Vergleich der saisonalen Variabilität des Methyliodids mit der Oberflächentemperatur zeigte eine direkte positive Korrelation bezüglich der Produktionsrate. Neben einem dirketen Effekt, könnte dieser Zusammenhang

indirekten Ursprungs sein, in dem die Oberflächentemperatur die Bildung von Vorstufen des Methyliodids beeinflusst.

Chapter 1
Introduction and Research Questions

1.1 Background

Halogenated methanes are commonly found in the marine environment and the atmosphere. This group of compounds is often referred to as halocarbons or volatile halogenated organic compounds (VHOC), for instance, methyl iodide. Numerous halocarbons are produced by industry and are intermediates for the manufacture of various products. Halocarbons are used as solvents for dry cleaning and degreasing in the mechanical industry (Klick, 1992). Some halocarbons are toxic, for example tetrachloroethylene from cleaning solvents, which is toxic in the respiratory system and the liver. On the other hand, chlorofluorocarbons (CFCs) and many other halocarbons that have been used widely as refrigerants, propellants and solvents since the early to middle twentieth century, are non-toxic. CFCs and long-lived halocarbons in the atmosphere can result in the depletion of stratospheric ozone and can act as greenhouse gases (Anderson, Toohey, & Brune, 1991; Crutzen & Arnold, 1986; Grob & Habich, 1983; Newman, Daniel, Waugh, & Nash, 2007; Solomon, 1990).

Until the beginning of the 1970s, it was assumed that halogens occur only as inorganic gases in the atmosphere and in this form participate in natural biogeochemical cycles. Between 1971 and 1975, J. E. Lovelock and colleagues detected VHOC with gas chromatography (GC) coupled to the highly sensitive and selective electron capture detector (ECD), which they developed. They discovered that halocarbons have not only anthropogenic but also natural sources, including production by marine organisms. The oceans have been implicated as one of the main natural sources, where organisms such as macroalgae and microalgae can release large quantities of VHOC to the ocean surface where they can exchange with the atmosphere. In

recent years, intensive research into VHOC answered only some of the questions about their sources, sinks and cycling in the ocean and atmosphere. More investigation is needed in order to understand the global cycling of halocarbons.

One specific halocarbon, methyl iodide (CH_3I), an ocean-derived iodocarbon, is a major carrier of iodine to the atmosphere. In the atmosphere, methyl iodide is photodissociated by near-UV light, with a maximum absorption at 260 nm (Roehl, Burkholder, Moortgat, Ravishankara, & Crutzen, 1997) and generates iodide atoms, which participate in ozone destruction and aerosol formation in the troposphere. In the ocean, the production sources and sinks, including air-sea flux, of methyl iodide must be investigated to improve the understanding of the methyl iodide global cycle.

1.2 Methyl Iodide Cycle

Miyake and Tsunogai [1963] explained the main source of iodine to the atmosphere as the vaporization of free iodine which is formed from the solar irradiation of iodide in the seawater. In turn, the atmosphere supplies iodine via precipitation to marine and terrestrial environments (Miyake & Tsunogai, 1963). It was Lovelock and Maggs [1973] who first detected methyl iodide in the atmosphere and ocean using an electron capture detector. They proposed that methyl iodide is produced in the ocean and is a key compound in the natural cycle of iodine (Lovelock & Maggs, 1973). In addition, methyl iodide has been thought of as the major organic iodine compound in the atmosphere (Heumann, Gall, & Weiss, 1987; Rasmussen, Khalil, Gunawardena, & Hoyt, 1982b). However, several studies suggest that other iodinated compounds, such as chloroiodomethane and diiodomethane, may supply a significant fraction of atmospheric iodine (Carpenter et al., 1999; Klick & Abrahamsson, 1992; Moore & Tokarczyk, 1992).

Compared to methyl chloride and methyl bromide, the carbon-iodine bond is relatively weak (Solomon, Garcia, & Ravishankara, 1994). This bond can be easily broken by solar UV radiation (260-360 nm) (Tsao and Root 1972) to yield methyl and iodine radicals (Equation 1).

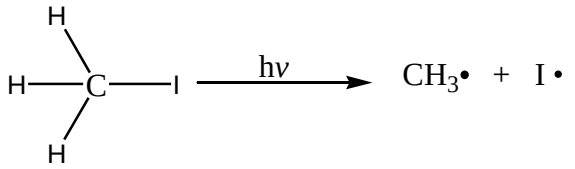

(1)

The iodine radicals can catalytically destroy tropospheric ozone (Davis et al., 1996; Solomon et al., 1994) to form oxygen molecules and IO radicals (see equation 2 and 3), which in turn photodissociate again and regenerate iodine atoms (Carpenter et al., 1999).

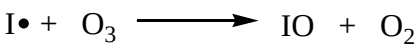

(2)

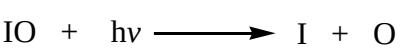

(3)

Iodine monoxide can react with nitrogen oxide, water vapour or itself and yield $IONO_2$, HOI and I_2O_2 respectively (O'Dowd et al., 2002) (see Figure 1.1). These species (IO, I_2O_2 and HOI etc.) are either oxidized or photolyzed, regenerating iodine atoms, or lost via dry and wet deposition and /or to aerosols (McFiggans et al., 2000).

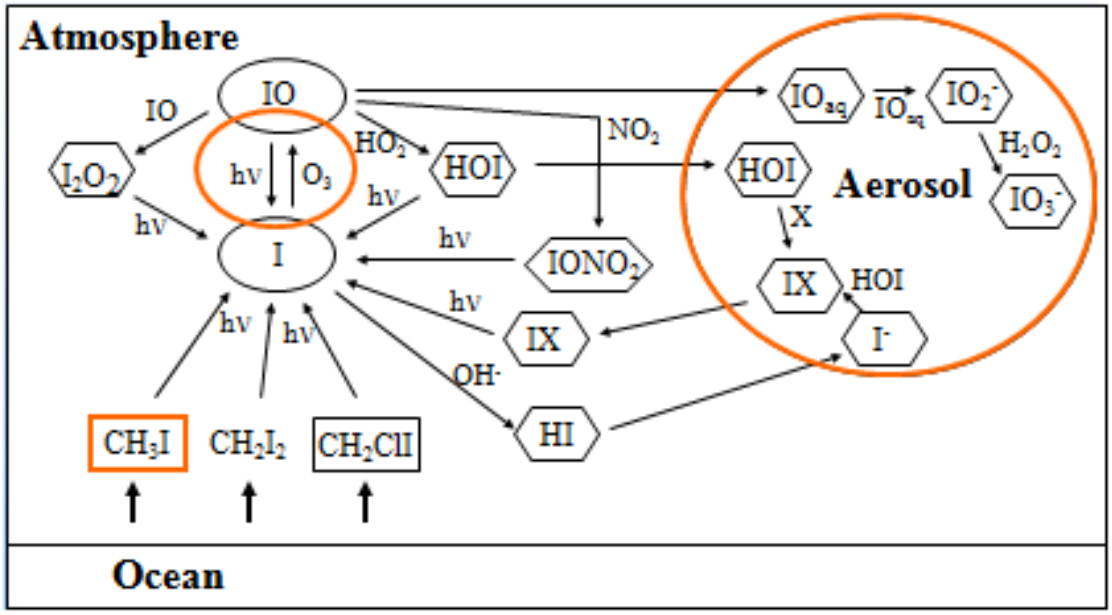

Figure 1.1: Photolysis of methyl iodide in atmosphere (O'Dowd et al., 2002; Vogt, Sander, Von Glasow, & Crutzen, 1999)

During rain, snow and other precipitation events the iodine species re-enter the ocean. It is known that hypoiodous acid (HOI) and molecular iodine (I_2) react with marine dissolved organic matter (DOM) to produce dissolved organic iodine (DOI). Garland [1980] suggested that the methyl iodide in the surface seawater could result from the oxidation of iodide by ozone and the subsequent reaction of HOI with organic molecules (Garland, Elzerman, & Penkett, 1980). Several investigations have attempted to evaluate the role of algae and phytoplankton in producing methyl iodide (Brownell, Moore, & Cullen, 2010; Hughes, Franklin, & Malin, 2011; Smythe-Wright et al., 2006). In the recent literature the possibility of abiotic production via photochemistry has also been proposed, and has been suggested to be of primary importance in the production of CH_3I [Happell and Wallace, 1996; Moore and Zafirou, 1994; Richter and Wallace, 2004]. The main sinks of methyl iodide in seawater are thought to be sea-to-air flux and nucleophilic substitution reaction with chloride and bromide. Other identified loss pathways include hydrolysis and photolysis (see Figure 1.2).

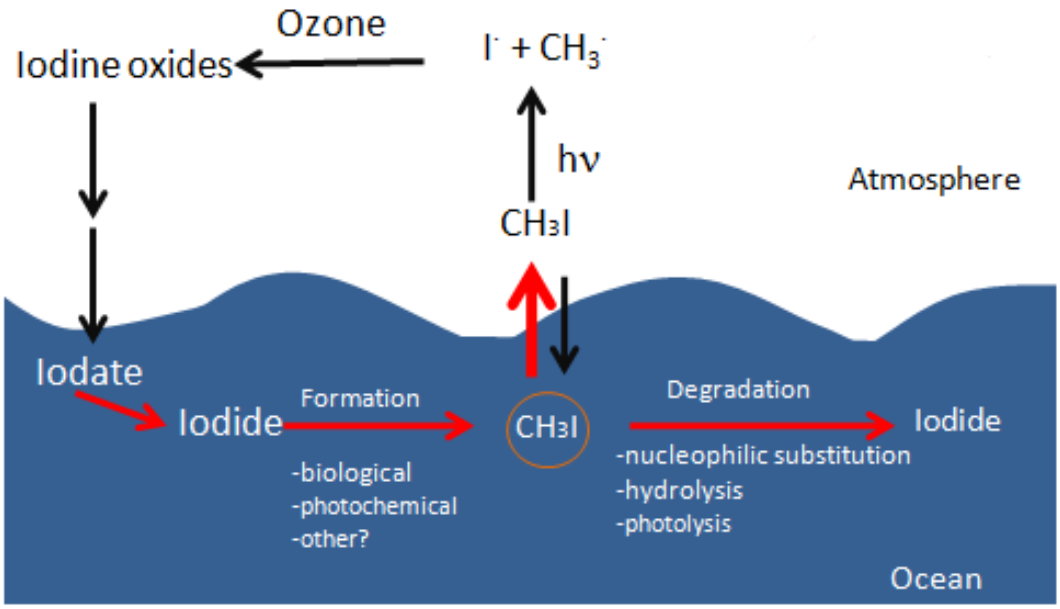

Figure 1.2: Schematic of the methyl iodide cycle

1.3 Methyl Iodide in the Atmosphere

Since the first detection of methyl iodide in the atmosphere by Lovelock et al [1973], many investigations have been performed to detect its source. The main source of methyl iodide for the atmosphere is thought to be the sea-to-air flux of CH_3I from the ocean. The first estimate of the global flux from the ocean to the atmosphere was calculated by Liss and Slater [1974] as 0.27 Tg yr^{-1} using the two-layer model and the data set (atmospheric and marine concentration of CH_3I) from Lovelock et al [1973]. Singh et al. [1983] estimated a similar flux of 0.3-0.5 Tg yr^{-1} based on their own measurements of atmospheric and marine concentrations of CH_3I in the eastern Pacific. Rasmussen et al. [1982] calculated a global flux of 1.3 Tg yr^{-1} based on their own atmospheric concentrations and the costal water data from Lovelock [1975]. These 1975 measurements for the region off SW Ireland were higher than previous measurements, leading to higher fluxes of methyl iodide. Reifenhäuser and Heumann [1992] estimated a flux of 0.8 Tg yr^{-1} by

extrapolation of their measurements of CH_3I near Antarctica to the global ocean. Moore and Groszko [1999] extrapolated data from the Pacific to the global ocean which yielded a flux of 0.3 Tg yr^{-1}. Based on the data from the tropical Atlantic, a global flux of 0.19-0.41 Tg yr^{-1} was calculated by Richter and Wallace [2004]. The differences between the reported fluxes are quite large, mainly due to the temporally and spatially sparse data sets of marine CH_3I (see Table 1).

Table 1.1: Sources of methyl iodide to the atmosphere

Sources	Tg yr^{-1}	Gmol yr^{-1}	Referece
Oean	0.27	1.90	(Liss & Slater, 1974)
(sea-to-air flux)	1.3	9.16	(Rasmussen et al., 1982b)
	0.3-0.5	2.11-3.52	(Singh, Salas, & Stiles, 1983a)
	0.8	5.64	(Reifenhauser & Heumann, 1992)
	0.3	2.11	(Moore & Groszko, 1999)
	0.21	1.48	(Bell et al., 2002)
	0.19-0.41	1.22-2.89	(Richter & Wallace, 2004)
Rice paddies	0.025	0.18	(Muramatsu & Yoshida, 1995)
	0.071	0.50	(Redeker et al., 2000)
Biomass burning	0.003-0.008	0.24-0.06	(Andreae et al., 1996)
Volcanic emission	<0.003	<0.018	(Jordan et al., 2000)
Peatland ecosystems	0.001	0.01	(Dimmer et al., 2001)

Several other potential terrestrial sources from were reported in recent years. Muramatsu and Yoshida [1995] reported that 0.025 Tg yr^{-1} of methyl iodide can be produced by rice paddies, while Redeker et al. [2000] estimated the emission to be ca. 0.071Tg yr^{-1}. Andreae et al. [1996] reported elevated CH_3I concentrations in smoke from Savanna fires in Africa and estimated the global emission of CH_3I from biomass burning between 0.003 and 0.008 Tg yr^{-1}. Other potential sources are emissions from volcanoes at < 0.003 Tg yr^{-1} (Jordan, Harnisch, Borchers, Le Guern, & Shinohara, 2000) and peatland

ecosystems with 0.001 Tg yr^{-1} (Dimmer, Simmonds, Nickless, & Bassford, 2001), both insignificant when compared with the oceanic source.

Photolysis is the main sink of methyl iodide in the atmosphere, because the carbon-iodine bond is easy broken by solar UV radiation (see in section 1.2). The mean lifetime of methyl iodide against photolysis in the troposphere has been estimated to be about 4 to 8 days (Zafiriou, 1974). The total loss rate of CH_3I due to photolysis in the atmosphere was estimated by Chameides and Davis [1980] to be about 1.5 Tg yr^{-1} using an average lifetime of eight days and an atmospheric concentration of 5-10 ppt. The sinks of methyl iodide in the atmosphere must be similar in magnitude to the sources in order to maintain observed levels. In recent years methyl iodide has been detected in the range of 1-3 ppt over the open ocean (Moore & Tokarczyk, 1993; Rasmussen, Khalil, Crawford, & Fraser, 1982a; Rasmussen et al., 1982b; Singh, Salas, & Stiles, 1983b; Yokouchi, Nojiri, Barrie, Toom-Sauntry, & Fujinuma, 2001; Yokouchi et al., 2008), and not in the range of 5-10 ppt used by Chameides and Davis [1980]. Using these refined values, their sink reduces to roughly 0.3 Tg yr^{-1}. Bell et al [2002] reported a similar sink of 0.3 Tg yr^{-1} from model calculations.

1.4 Methyl Iodide in the Ocean

As discussed above, there are more than 0.2 Tg yr^{-1} (or 2×10^{11} g yr^{-1}) of CH_3I transferred into the atmosphere, which is produced in the ocean. Biological production in the ocean surface waters has generally been considered to be the major source for oceanic methyl iodide. Macro algae, including kelp and some red and green seaweed, were identified to produce CH_3I (Lovelock, 1975; Laturnus, 1995; Manley et al., 1992; Nightingale et al., 1995). Some evidence from laboratory studies showed biological production of CH_3I by phytoplankton (Manley & delaCuesta, 1997; Moore & Tokarczyk, 1993). Phytoplankton is considered to be potentially even more important than macro algae in terms of global CH_3I production. In the open ocean, marine

cyanobacteria are ubiquitous and were shown to produce the trace gas in laboratory culture (Shaw, Chisholm, & Prinn, 2003). Smythe- Wright et al. [2006] reported that some *Prochlorococcus* species were an important source of methyl iodide. Brownell et al. [2010] and Hughes et al. [2011] confirmed the CH_3I production from *Prochlorococcus* however with widely ranging rates (see chapter 3, section 3.3.2.) The annual production rates of CH_3I by macro algae in coastal waters is less than 3.0×10^8 g yr^{-1}, and the mean production rate by the phytoplankton (not including *prochlorococcus*) was calculated to be 1.2×10^9 g yr^{-1} by Manley and de la Cuesta [1997], while the production rate by bacteria under laboratory conditions could be in the range of 1.0×10^7-1.2×10^8 g yr^{-1} (Amachi, Kamagata, Kanagawa, & Muramatsu, 2001). The sum of these production rates seem to be insufficient to account for the global flux (2×10^{11} g yr^{-1}). The only reported biological production rate (5.3×10^{11} g yr^{-1}) that can account for the global methyl iodide flux was calculated/measured by Smythe-Wright et al. [2006] based on *Prochlorococcus* cultures (MED4). However Brownell [2010] calculated a global CH_3I production rate of only 8.5×10^7 g yr^{-1} (0.03% of the estimated global CH_3I sea-to-air flux) by extrapolation of their own results with the same strain in culture (MED4). Their rates were 1000-fold lower than that reported by Smythe-Wright et al [2006]. Hughes et. al. [2011] suggested that previous discrepancies in the rate of CH_3I production by *Prochlorococcus* in culture could be due to the cell physiological status under the different culture conditions based on the large reported range of rates of CH_3I production per cell reported from *Prochlorococcus* culture (Brownell et al., 2010; Hughes et al., 2011; Smythe-Wright et al., 2006).

Since biological production appears not to be sufficient to balance the flux, the involvement of another source of CH_3I production in the surface seawater, such as photochemical production (Happell & Wallace, 1996; Moore & Zafiriou, 1994; Richter & Wallace, 2004; Yokouchi et al., 2001), has been inferred. Moore and Zafiriou [1994] reported methyl iodide production from filtered seawater samples under irradiation and proposed photochemical production. Addition of iodide to the samples enhanced the production of

methyl iodide in the oxygen-free seawater. Based on the analysis of factors influencing the saturation anomaly of CH_3I at high and low latitudes, a photochemical production pathway of methyl iodide was also proposed by Happell and Wallace [1996]. Richter and Wallace [2004] and Wang and Moore [2009] supported the photochemical production of methyl iodide in the open ocean via a set of incubation experiments under natural light conditions.

The main sink of methyl iodide in the ocean is its flux to the atmosphere, which was already described in section 1.3 as the main source of CH_3I in the atmosphere. Another sink of CH_3I in the seawater is the nucleophilic substitution reaction with chloride and bromide. Zafiriou [1975] first presented the rate of these reactions. Subsequently, Elliott and Rowland [1993] calculated the chemical loss rate of methyl iodide dependent on the seawater temperature. Moore [2006] estimated the chemical loss of CH_3I with chloride assuming a pseudo first order reaction and using data from incubation experiments. Using a model, Bell et al. [2002] calculated a global loss of 2.6 10^{11} g yr^{-1} with an assumption that the marine source was photochemical with a production rate dependent on both light flux and the modelled concentration of dissolved organic carbon (DOC). A third known sink of methyl iodide in the seawater is diffusion via mixing, either lateral or vertical, with lower concentrations of CH_3I. In open ocean waters, where CH_3I concentrations decrease below the euphotic zone, the downward mixing loss has been shown to be negligible in comparison with sea-to-air flux (e.g. Richter and Wallace, 2004).

1.5 Goal of this Study

The review of the literature shows there are different potential sources of methyl iodide in the ocean. However, the major oceanic sources of CH_3I still remain under debate. The goal of this study was to evaluate the major sources of methyl iodide in the surface seawater and the relative importance of photochemical production of methyl iodide compared to biological

production. A set of incubation experiments was designed to identify and quantify the sources of methyl iodide in the marine environment using a GC-ECD system. The experimental study was conducted in the context of a seasonal time-series of measurement of CH_3I concentration together with other parameters (e.g. concentration of iodine species /chlorophyll *a* etc.) in order to examine the factors influencing the CH_3I production in the surface seawater.

Chapter 2 describes the instruments and procedures used in this thesis. In Chapter 3 the seasonal variation of methyl iodide in the Kiel Fjord is presented and discussed. In Chapter 4 the incubation experiments investigating the source of methyl iodide in the ocean will be described and discussed. Chapter 5 presents the conclusions based on the collected data, ideas and suggestions for the future research.

Chapter 2
Methods

2.1 Overview of the Analytical System

Concentrations of the dissolved halogenated carbon compounds in seawater were measured in this study using gas chromatography and an electron capture detector (ECD). Sample extraction was achieved using a home-made purge and trap apparatus (Figure 2.1). Detailed description of the procedure is given in section 2.2.

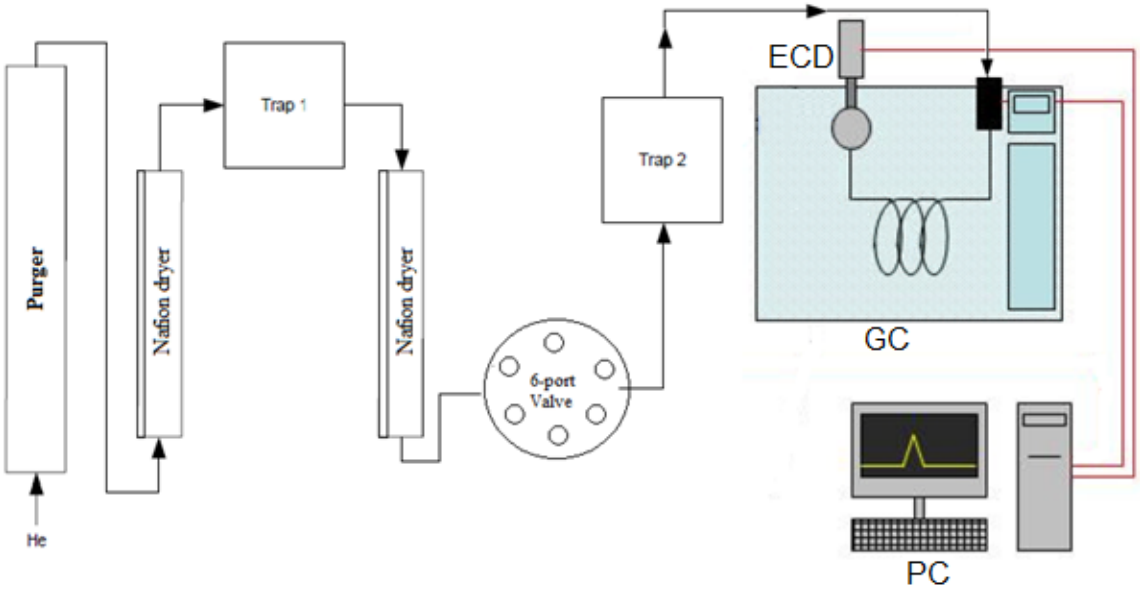

Figure 2.1: Experimental set-up for purge and trap system coupled to gas chromatography with an ECD detector.

2.2 Analytical System

2.2.1 Gas Chromatography System with ECD Detector

For all measurements a FISONS 8000 gas chromatograph was used, equipped with a column and ECD (see Figure 2.2).The principle of gas chromatography is based on the distribution of components between a mobile phase and a stationary phase. The mobile phase is a carrier gas, usually an inert gas such as helium or nitrogen (helium was used in this study), and the stationary phase is often a polymer on an inert solid support, which is filled in a GC-column.

Figure 2.2: FISONS 8000 gas chromatograph with ECD detector was used for discrete samples analysis. GC-column (right side) parameters: 60m, 0.25mm, RTX-VGC.

The column used in this study was a 60 m long, wall-coated open tubular (WCOT) type with a RTX-VGC (coating: 1.4 µm, column diameter: 0.25 mm). Samples were injected from trap into the GC via a 6-port Valco valve and transported through the column by the flow of the carrier gas. Depending on the various chemical and physical properties of the analytes, they exit the column at different times (retention times). A substance with high vapor

pressure and / or low solubility in the stationary phase is eluted quickly and, consequently, the retention time within the column is short. A substance with low vapor pressure and / or high solubility is eluted late, and has a longer retention time. Additional key parameters affecting the retention time include the flow rate of the carrier gas and the column temperature.

The temperature program of the GC oven was software controlled. The initial temperature was 25 °C, which was held for 6 minutes, then temperature increased to 150 °C at 6 °C/min, and was held at 150 °C for 1 min. At the end of the analysis, the temperature decreased rapidly to 25 °C.

The other end of the column was connected to the detector, so that after passing through the column, the analytes can be detected and quantified. The ECD is ideal for the measurement of halogenated organic substances. It is more sensitive than almost any other GC detectors for molecules containing electronegative atoms such as chlorine, bromine, iodine (Lovelock, 1974; Maggs, Joynes, Davies, & Lovelock, 1971).

An ECD consists of a stainless steel cylinder containing radioactive Nickel-63 ($^{63}_{28}Ni$), a cathode and an anode (see Figure 2.3). In our configuration, the carrier gas (He) was supplemented by a makeup gas (N_2) added at the detector base. The Nickel-63 emits beta particles (electrons) which collide with the makeup gas molecules (N_2) (Reaction 1). Some makeup gas molecules are ionized and form a stable cloud of free electrons in the ECD cell. When halogenated compounds, e.g. methyl iodide, enter the cell, they react with some of these free electrons (Reaction 2-a, 2-b), temporarily reducing the number remaining in the electron cloud. The detector electronics are set to maintain a constant current (of about 1 nanoampere) through the electron cloud. A pulsed potential is applied across the cell and the pulse rate is varied to compensate for the decreased number of free electrons in order to maintain a stable value of the current. The pulse rate is proportional to the concentration and is converted to an analog output that is connected to a data acquisition system (Lovelock, 1974; Pellizza.Ed, 1974). The final step in the

reaction sequence is the neutralization of the negative ions formed by capture (Reaction 3).

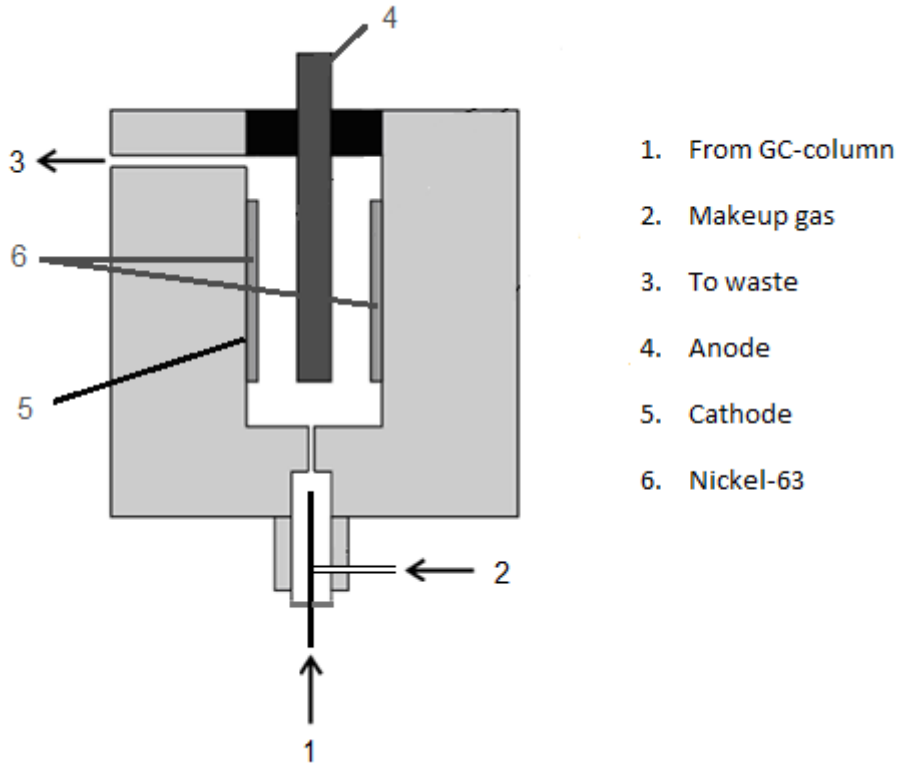

Figure 2.3: A schematic diagram of an ECD-cell (adapted from University of Mainz, Fortgeschrittenen-Praktikum Analytische Chemie)

$$\beta\text{–radiation} + N_2 \longrightarrow N_2^+ + e^- \qquad (1)$$

$$R\text{-}X + e^- \longrightarrow R\text{-}X^- \qquad (2a)$$

$$R\text{-}X + e^- \longrightarrow R^\bullet + X^- \qquad (2b)$$

$$R^\bullet + N_2^+ \longrightarrow R^+ + N_2 \qquad (3)$$

2.2.2 Purge and Trap System

The analytical procedure for measuring halocarbons can be divided into three main steps: a) extraction from the matrix and pre-concentration, b) separation of the different compounds and c) detection. For the volatile halocarbons in seawater the dynamic headspace method is often used to extract the compounds from the matrix.

The purge and trap method is the dynamic headspace method used in this work (see Figure 2.4). The volatile organic carbons are released from the liquid into the gaseous phase by continuous gas flow at a given purge temperature. The purged chemicals are trapped by freezing, adsorbing, or both. After all volatiles have been purged out of the liquid and trapped, they are released at high temperature and injected into the gas chromatography (GC).

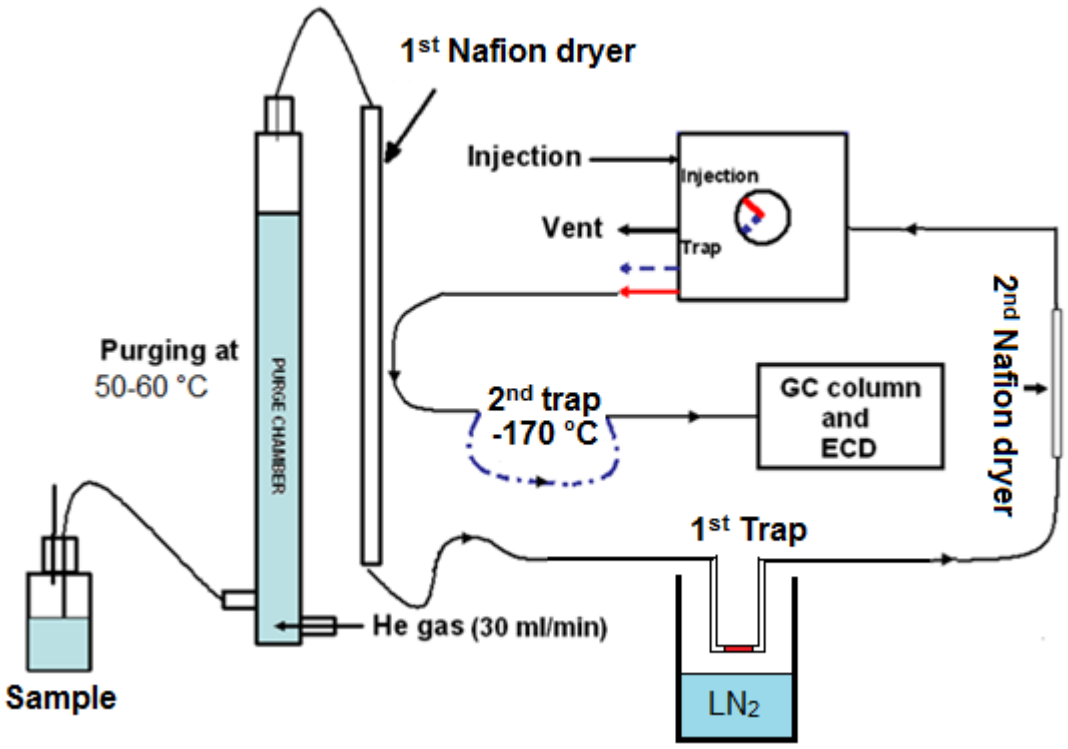

Figure 2.4: Schematic of the purge and trap system used in this study.

The purge chamber (50 ml) was made of glass and could be heated to 50-60 °C. Analytes were extracted into a flowing stream of helium that was bubbled through the water sample. The helium-flow was 30 ml/min for 40 minutes. A Nafion dryer (50 cm length) was used to dry the purged gas stream. The purged gases were trapped in a glass tube (¼´´ID) filled up to 25 mm length with “Unify” glass beads. The tube was placed in the headspace immediately overlying liquid nitrogen (N_2) and the trap temperature was kept at -100 °C. To desorb the analytes, the valve was switched to the “Trap” position and the liquid nitrogen dewar was removed and replaced with boiling water for 3 minutes. The gases were trapped on a second trap constructed of a 50 cm length of capillary tubing immersed in liquid N_2 (-170°C).The second trap was used because there was a relatively long desorption time off the first trap, which would result in peak tailing if injection onto the GC occurred directly. The second trap focused the peaks since the release time was only ca. 2-5 seconds, resulting in much better resolution of the chromatograms.

2.3 Standardization of Halocarbon Analysis

For quantification of halocarbons in seawater, it is necessary to calibrate the measurements by comparison with peak areas from injections of liquid standards. Three stock standard solutions were prepared in pentane. The final standards for calibration were then prepared by serial dilutions of the stock solutions into methanol.

The first stock solution (A-I) contained 5 µl of methyl iodide and 10 µl of CH_2ClI in 10 ml pentane. The second stock solution (A-II) contained 10 µl of $CHCl_3$ and 10 µl of CCl_4 in 10 ml pentane. And the third stock solution (A-III) contained 10 µl of each brominated compounds (CH_2Br_2, $CHBr_2Cl$, $CHBr_3$) in 10 ml pentane. For the final calibration, a common solution (B-I) was prepared as a mixture of the three stock solutions (see Table 1). From this common solution four dilutions were prepared: 1:1,000,000; 1:500,000; 1:250,000;

1:100,000. All of the listed chemicals were purchased from Merck, and all stock solutions were stored at -20 °C.

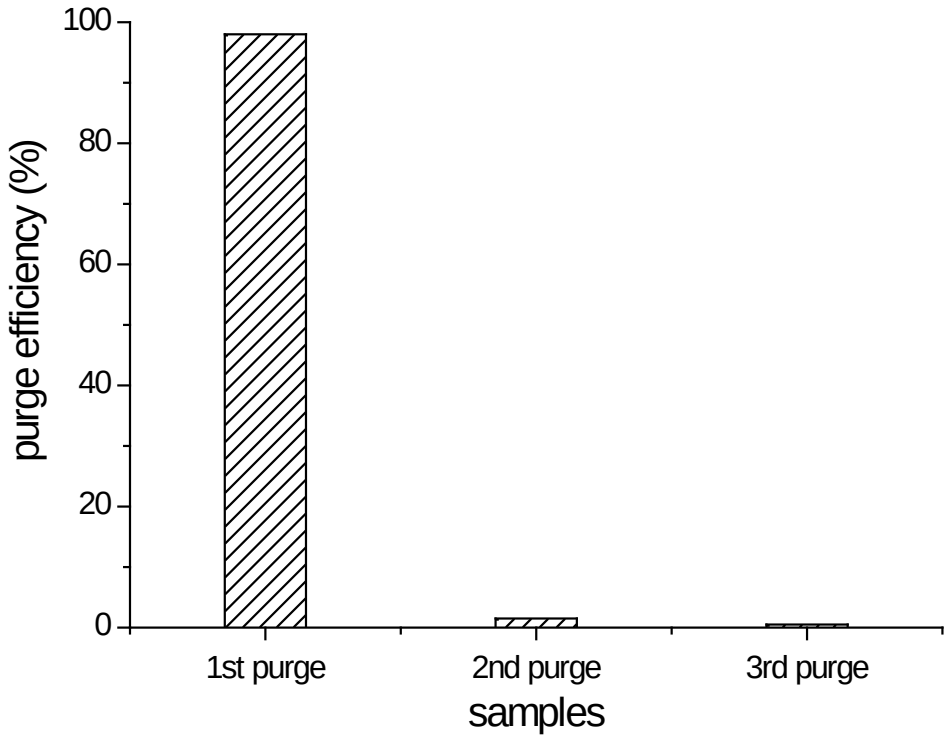

Figure 2.5: Recovery of methyl iodide in one repeatedly purged seawater sample. Purge efficiency is calculated by dividing the peak area of each purge sample by the total peak area of methyl iodide from the repeated purging (three times) of a sample.

A system blank was analyzed before every standard-measurement. In this study, analyte-free water for the blank measurement was prepared by bubbling 30 ml of seawater for at least 1 hour at 60°C in the purge chamber. The methyl iodide free seawater sample was analyzed in the same manner as the standards. Results showed that 98-99% of methyl iodide was driven out of the seawater during the first purge and trap cycle (Figure 2.5). For the second and third purging there was no significant change and these values were considered as a blank.

Calibrations were performed by injecting microliter volumes of the working standards, via a septum port, into the purge vessel containing pre-purged tap water and analyzed in the same way as seawater samples. For later analysis,

the injection volume was normalized. Every working standard was measured 3 times. The standard deviation of triplicate measurements ranged from 13% to 23%.

Table 2.1: Example of standard concentrations and peak areas of measured halogen compounds in a calibration.

	Concentration	Peak area	Standard	Linear Regression		
	(pM)	(mean)	deviation	Slope	Intercept	R^2
CH_3I	0.32	948 052	224140	1205833.4	513191.6	0.97
	0.64	1 495 073	325940			
	1.60	2 026 076	271295			
	3.20	4 533 733	986733			
$CHCl_3$	0.51	1 591 811	696331	136898.1	1537480.9	0.94
	1.01	1 623 186	488577			
	2.40	1 971 934	1448908			
	5.06	2 191 731	1835871			
CH_2Br_2	0.58	863 985	207191	710624.9	610389.7	0.97
	1.15	1 331 417	169916			
	2.80	3 020 679	759882			
	5.81	4 574 357	1036118			
CH_2ClI	0.55	1 543 678	292858	825102.5	1290001.9	0.97
	1.11	2 127 836	303237			
	2.80	4 083 714	1337217			
	5.64	5 742 200	1776757			
$CHBr_2Cl$	0.48	677 620	119179	600247.6	501751.8	0.99
	0.96	1 106 701	37935			
	2.40	2 097 372	121655			
	4.85	3 341 261	764331			
$CHBr_3$	0.46	363 550	64106	352465.2	195427.6	1.00
	0.92	537 158	45390			
	2.40	1 004 896	155932			
	4.67	1 854 875	105509			

The results of the standard measurements in one calibration are shown in Table 1. Using linear regression we calculated the concentrations of halogen compounds in the seawater samples. The linear regression of methyl iodide showed a good linear relationship between peak area and concentration (R^2 = 0.97).

2.4 Analysis of Other Variables

In order to investigate the factors influencing methyl iodide production in the ocean, seasonal seawater samples of the coloured dissolved organic matter (CDOM), inorganic iodine species and chlorophyll *a* were collected from the Kiel Fjord. The optically active fraction of coloured dissolved organic matter (CDOM) plays a major role in determining underwater light availability in the ocean. CDOM is also a primary reactant in the photoproduction of CO_2, H_2O_2 and OCS and is a photosensitizer in the photolysis of dimethyl sulphide (DMS). Iodide (I^-) is mainly found in surface seawater within the euphotic zone (Kennedy & Elderfield, 1987; Luther, Wu, & Cullen, 1995; Wong, 1991). It can be readily oxidized by many photochemical oxidants in surface seawater and can provide a significant source of I atoms (Mopper & Zhou, 1990). Chlorophyll *a* measurements provide a useful estimate of algal biomass and its spatial and temporal variability.

2.4.1 Coloured Dissolved Organic Matter (CDOM) Analysis

Dissolved Organic Matter (DOM) can be a source of methyl radicals in seawater [Moore and Zafirou, 1994; Richter, 2003; Yokouchi et al.,2008]. Coloured dissolved organic matter (CDOM) can be the main light absorbing substance in the ocean and represents an important chromophore in the UV region (Nelson, Siegel, & Michaels, 1998; Siegel & Michaels, 1996; Siegel, Michaels, Sorensen, Obrien, & Hammer, 1995). CDOM plays an important role in light availability for photochemical reactions (Dister & Zafiriou, 1993).

The absorption of light by water, suspended material (phytoplankton and other particles including non-living detritus), and CDOM controls the propagation of solar radiation through the water column. CDOM absorbs primarily UV and blue light, and is also fluorescent. The absorption spectra of CDOM are typically in the visible (400-700 nm) and UV-A (320-400 nm) regions, declining exponentially with wavelength. Because of this, CDOM spectra are commonly parameterized as exponential functions (Bricaud, Morel, & Prieur, 1981; Green & Blough, 1994), such that:

$$\alpha(\lambda) = \alpha(\lambda_0)e^{-S(\lambda-\lambda_0)} \qquad (4)$$

where $\alpha(\lambda)$ is the absorption coefficient at wavelength λ (m^{-1}), $\alpha(\lambda_0)$ is the absorption coefficient at a reference wavelength λ_0 (m^{-1}), and S is the exponential slope parameter (nm^{-1}).

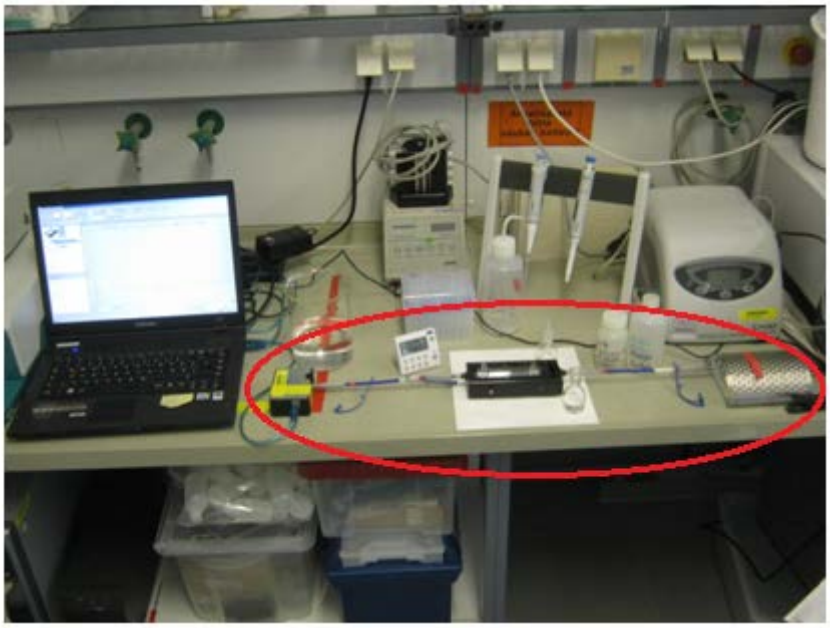

Figure 2.6: Ocean Optics USB4000 UV-VIS spectrophotometer (within red circle) used to analyze CDOM

Seawater has a higher refractive index and thus transmits more photons through the waveguide than pure water, leading to lower apparent optical

absorbance at certain wavelengths. Based on these, CDOM in the seawater was measured using a LWCC-2100 100 cm path length liquid waveguide cell (Word Precision Instruments, Sarasota, Florida) and an Ocean Optics USB4000 UV-VIS spectrophotometer in conjunction with an Ocean Optics DT-MINI2-GS light source, scanning the absorption spectrum from 250 nm to 750 nm (see Figure 2.6) (Heller & Croot, 2010; Nelson, Carlson, & Steinberg, 2004; Nelson et al., 2007; Steinberg, Nelson, Carlson, & Prusak, 2004). All measurements required one of the 10 cm cuvettes to be filled with Milli-Q water as a blank solution and one of the cuvettes was filled with seawater samples at room temperature. The resulting dimensionless optical density spectra were converted to absorption coefficient α(λ) (m^{-1}):

$$\alpha(\lambda) = 2.303 A\lambda / \ell \qquad (5)$$

where 2.303 converts decadal logarithmic absorbance to base e, and l is the effective optical path length of the waveguide (here 103.8 ± 0.5 cm).

The water samples were taken from the pier, in front of GEOMAR´s west shore building and all samples were syringe filtered through 0.2 µm filters (SARSTEDT AG). All samples were stored in white high-density polyethylene bottles (HDPE, from Thermo Scientific Nalgene) at -20°C until laboratory analysis.

2.4.2 Inorganic Iodine Analysis

Cathode stripping square wave voltammetry, described by Campos [1997], was used to determine the concentration of iodide in seawater without changing the pH value. Iodide reacts with mercury in an one-electron process according to the equation 6 (Turner & Deitz, 1975):

$$Hg + I^- \rightleftharpoons 0.5\ Hg_2I_2 + e^- \qquad (6)$$

This method is fast and precise (+/- 5% relative standard deviation). We used the cathode stripping square wave voltammetry with the hanging mercury drop electrode (HMDE) (Campos, 1997; Luther, Swartz, & Ullman, 1988).The drop size was medium in order to prevent dislodging by larger drops. The purge time of samples was 230 seconds using nitrogen. The scan was performed from -1.2 to -0.1 V under the following conditions: deposition potential = -0.05 V; deposition time = 60 s; equilibration time = 5 s; scan rate = 200 mV/s; amplitude = 0.02 V; frequency = 100 Hz. The detection limit of this method is 0.5-1.0 nM (Figure 2.7).

All samples were collected in 125 ml brown HDEP bottles (from Thermo Scientific Nalgene) and filtered through 0.2 µm Nuclepore filters (SARSTEDT AG). The filters were stored at -20°C in dark until laboratory analysis. 20 ml of sample was added to the flow cell following the addition of 100 µl 0.2% Triton X-100 as surfactant. Samples were purged 230 seconds with nitrogen gas. Every sample was measured 3 times. A 50 µl standard was added to the sample after each triplicate. The iodide standard was prepared in deionized water from potassium iodide (20 µM). At least two standard additions were done.

Iodate was measured using spectrophotometry (Truesdale, 1978). Under acidic conditions, iodate reacts with excess iodide producing I_3^-, which is then measured spectrophotometrically at 350 nm. A 10 ml sample (filtered through 0.2 µm Nuclepore filter) was added in a graduated, stoppered cylinder following the addition of 250 µl 1.5 M sulphamic acid. The mixture was stirred, reacted for 2.5 minutes, and then mixed with 750 µl of a 10% potassium iodide solution. After an additional 2.5 minutes reaction time, the mixtures were measured at a wavelength of 350 nm. During the preparation and measurement the samples were kept under subdued light.

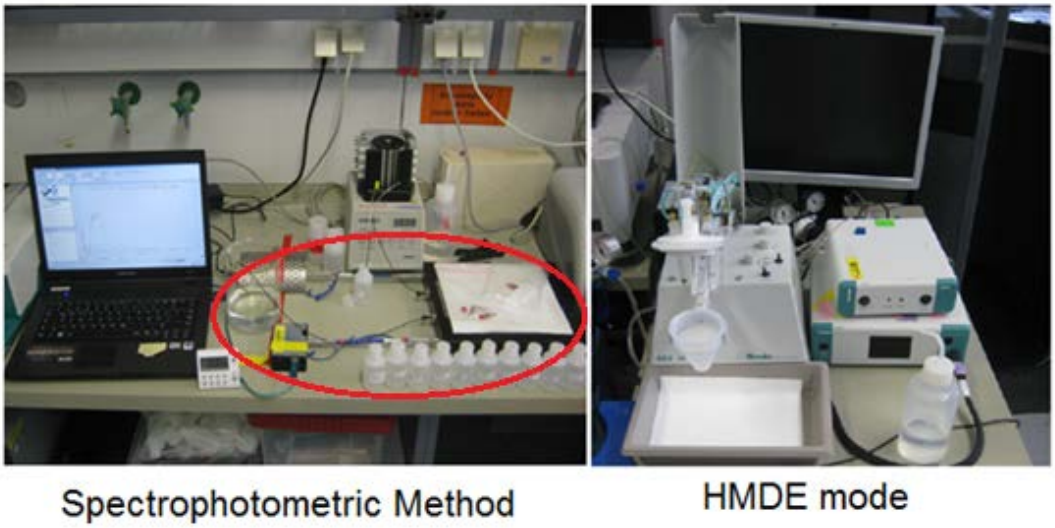

Figure 2.7: Instruments for iodate (left, within red circle) and iodide (right) measurements

2.4.3 Chlorophyll *a*

The water samples were taken from the same position, in front of GEOMAR´s west shore building. One litre of sample water was filled in polyethylene bottles. The samples were vacuum filtered through 25mm GF/F filters (Whatman) immediately after sampling with a pressure of less than 0.2 atmospheres. The filters were kept in the dark and kept frozen at -20 °C prior to analysis. The analytical procedure was the same as described in the protocols for the Joint Global Ocean Flux Study (JGOFS) core measurements, released from UNESCO in 1994.

2.5 Experiments

2.5.1 Artificial Seawater

In order to conduct experiments related to photochemical reaction pathways for CH_3I, artificial seawater was irradiated under natural light conditions (see Chapter 4, section4.1). In spring of 2009, a set of incubation experiments of

artificial seawater were conducted. The preparation of artificial seawater was as described by Harrison and Berges in 2004 and by Moore et al. in 2007. The chemical composition of the artificial seawater is shown in Table 2. All the chemicals were purchased from MERCK. Here potassium iodide and potassium iodate were added as the iodine source in the artificial seawater.

The general steps to make the artificial seawater were as follows:

1: All substances of Turk's Island Salt Mix and macronutrients were added into the Milli-Q ultrapure water (ELGA Purelab ULTRA), and mixed well until the pH-value of the medium was 7.9.
2: The medium was sterilized by steam autoclaving for 20 minutes at 120 °C. After autoclaving, the medium was cooled for 12 hours in the sterile bench.
3: For the buffer solution, trace metals and other substances were sterilized by filtration with a 0.2 µm filter, which was further added to the autoclaved medium.
4: Autoclaved quartz bottles (250 ml) were filled with the artificial seawater without headspace on the sterile bench.
5: The quartz bottles were incubated on the roof of GEOMAR under natural light conditions (light samples), the remaining bottles were kept in a box out of sunlight (dark samples).

In this study, 3 types of artificial seawater media were used to examine their influence on methyl iodide formation. The so-called "normal medium" contained only artificial seawater without potassium iodide (KI), potassium iodate (KIO_3) and sodium pyruvate ($C_3H_3NaO_3$) added. The second medium type was artificial seawater with added KI or KIO_3, up to 470 nmol L^{-1} (a total concentration of 400 to 500 nmol L^{-1} has been found in the most oceanic regions (Campos, Farrenkopf, Jickells, & Luther, 1996; Chance, Malin, Jickells, & Baker, 2007; Elderfield & Truesdale, 1980; Farrenkopf, Dollhopf, Ni Chadhain, Luther, & Nealson, 1997; Jickells, Boyd, & Knap, 1988)). The last medium type was artificial seawater with KI + $C_3H_3NaO_3$ or KIO_3 + $C_3H_3NaO_3$, where the pyruvate concentration was 11 µmol L^{-1}. Here sodium pyruvate was

used as a methyl group donor because it is photolyzed at a significant rate by wavelengths in the solar spectral region (Moore & Zafiriou, 1994).

Table 2.2: The chemical composition of the artificial seawater the medium (Berges, Franklin, & Harrison, 2004; Moore et al., 2007)

components	Concentration
Macronutrients:	
NaH_2PO_4	50 µM
$(NH_4)_2SO_4$	400 µM
Turk´s Island Salt Mix:	
NaCl	481 mM
$MgSO_4 \cdot 7H_2O$	28 mM
$MgCl_2$	27 mM
KCl	9 mM
$CaCl_2 \cdot 2H_2O$	10 mM
Buffers:	
HEPES-NaOH	1 mM
$NaHCO_3$	6 mM
Trace metals:	
$NaEDTA \cdot 2H_2O$	117 nM
$FeCl_3 \cdot 6H_2O$	118 nM
$ZnSO_4 \cdot 7H_2O$	0.8 nM
$CoCl_2 \cdot 7H_2O$	0.5 nM
Others:	
H_3BO_3	20 mM
Pyruvate	11 µM
KI	470 nM
KIO_3	470 nM

2.5.2 Experimental Design

A major question underlying this dissertation is: How important is photochemical production compared to biological production for CH_3I formation? To answers this question a series of incubation experiments was designed (Figure 2.8).

We conducted “whole-bottle” incubation experiments to examine production of methyl iodide, as well as several other halocarbons (chloroform, dibromomethane, chloriodomethane, dibromchloromethane and bromoform). The experiments involved long-term incubations (57 hours) of natural seawater samples at natural light levels. The natural seawater samples were treated in 3 different ways: untreated or original (O), pre-purged with synthetic air (P) to remove all volatile iodinated organics, filtered (F) to remove most phytoplankton. The filtered samples were also pre-purged for 3 hours using the synthetic air after the filtration.

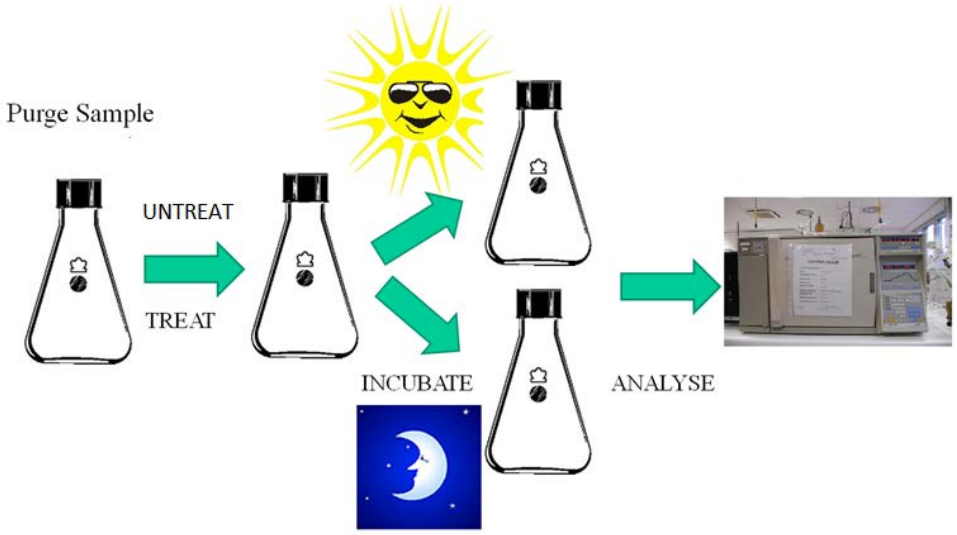

Figure 2.8: Experimental design

Half of the samples (untreated and treated) were irradiated under natural sunlight, the other half of the samples were kept in the dark for comparison. Every 24 hours, 4 “light samples” and 2 “dark samples” were analyzed using

the purge and trap method coupled to the GC-ECD. Every sample was analyzed in triplicate. The measurement times were 8:00, 12:00, 17:00 and 22:00 every day. In this study, the filtered samples were the samples filtered through 0.2 µm membrane filters. The “pre-purged samples” were those which were bubbled for 5 hours with synthetic air to remove volatile iodinated organics (time-zero samples). Detailed descriptions are given in the following section (2.5.3).

2.5.3 Experimental Details

From 2009 to 2010 the incubation experiments of natural seawater were conducted at the pier in the Kiel Fjord (IFM-Geomar, now GEOMAR), and the seawater was sampled directly from the surface (0.5 meter deep) of the Kiel Fjord, in front of GEOMAR’s west shore building (54.3°N, 10.1°E; see Figure 2.9).

Figure 2.9: GEOMAR sampling location, western Kiel Fjord (red mark).

a) Artificial Seawater Incubations

Month-long incubations with artificial seawater were performed in summer 2009. The “light” samples of the different media (see section 2.5.1) were irradiated under natural light on the roof of IFM-GEOMAR (Figure 2.10). The “dark” samples for comparison were incubated in a box.

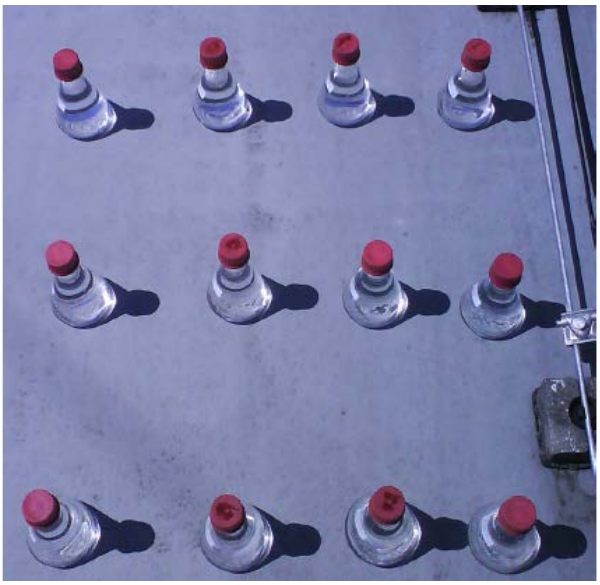

Figure 2.10: Artificial seawater incubation on the roof of IFM-GEOMAR.

b) Long-term Incubation with Natural Seawater

From summer 2009 to winter 2010 the long-term incubation experiments were conducted in the Kiel Fjord. The type of seawater samples consisted of original samples (untreated, O), pre-purged samples (P) and filtered samples (F). The incubation experiments were repeated from spring to winter. The “filtered seawater samples” were natural seawater samples filtered stepwise through 20 µm, 5 µm and finally 0.2 µm membrane filters (Figure 2.11). After filtration, most of the plankton had been removed from the samples (the size of pico-planktons is from 0.2 µm to 2 µm). Some bacteria (< 0.2 µm) could have remained in the samples, which were not axenic.

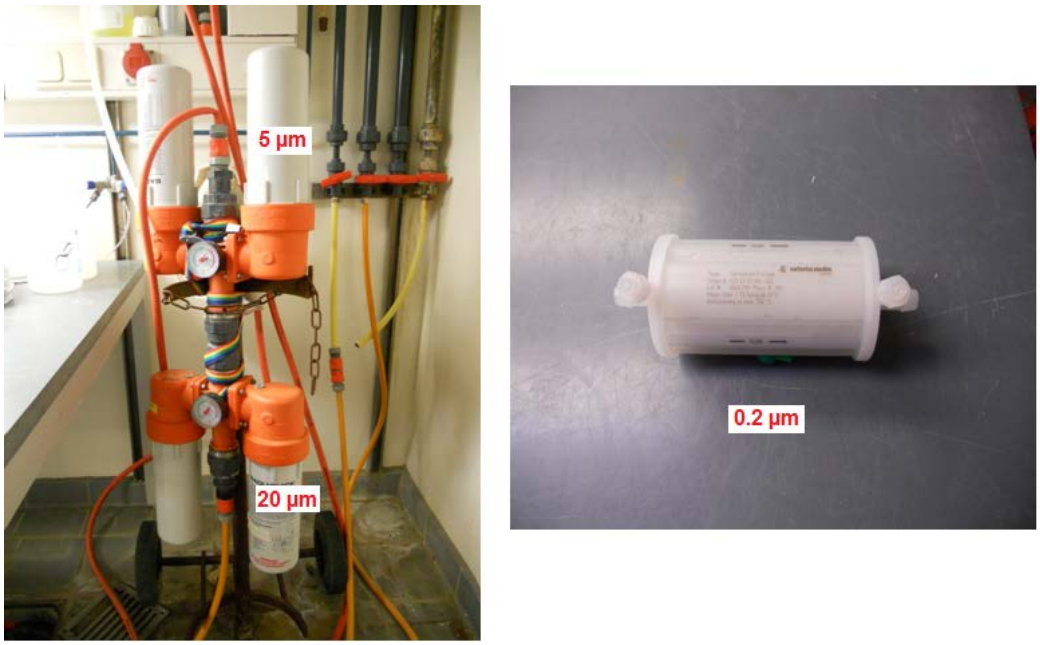

Figure 2.11: The filtration instrumentation used in this study.

The seawater samples (7L) were bubbled for 5 h with synthetic air (flow: 35-45 ml min^{-1}, 12-14L) to reduce the initial concentration of volatile iodinated organic compounds (zero-sample: 20-30% of methyl iodide left in the seawater compared with original seawater), but dissolved oxygen and CO_2 remained in the seawater (O_2: 150 µmol L^{-1} in original seawater; O_2: 138 µmol L^{-1} after 5 h purge).

During the incubations the quartz-flasks were immersed under the sea surface in order to keep the production under conditions as close to natural conditions as possible (Figure 2.12), especially with natural temperature and natural light ("light samples"). The "dark samples" were kept in a box, which was full of water but without light. The production rates of compounds were monitored with the purge and trap method described above.

Figure 2.12: Incubation experiments in Kiel Fjord

Chapter 3
The Seasonal Cycle of Methyl Iodide in the Kiel Fjord

3.1 Introduction

In parallel with incubation experiments discussed in Chapter 4, surface water samples from the Kiel Fjord were analyzed over an annual cycle for methyl iodide, other halogenated compounds, and additional parameters that are potentially related to CH_3I production. Long-term, time-series observations can reveal indications about the processes controlling concentrations (e.g. through correlation). Methyl iodide measurements were made in the Kiel Fjord (54.3°N, 10.1°E, in Figure 2.9) from October 2008 until July 2010. All samples were collected from the pier at a water depth of 0.5 metre and were analyzed using the purge & trap GC-ECD method, which was described in Chapter 2.

3.2 The Annual Cycle of Methyl Iodide Concentrations

3.2.1 Seasonal Variation of Methyl Iodide Concentrations

The concentrations of dissolved methyl iodide obtained from the Kiel Fjord are plotted in Figure 3.1. The mean concentration over the entire time-series was 5.00 pmol L^{-1} (ranging from 0.45-11.20 pmol L^{-1} from Oct. 2008 to Dec. 2010). The concentrations of methyl iodide showed a pronounced seasonal cycle. The concentrations of CH_3I increased gradually from February through June, with maximum concentrations in summer, and then decreased during August and September reaching minimum values during the winter months. Figure 3.2 shows the monthly mean concentrations calculated from all the data collected over the 3 years of the study. The mean concentration of methyl iodide increased from 0.99 pmol L^{-1} in February to 8.93 pmol L^{-1} in June, than decreased to 1.43 pmol L^{-1} in December.

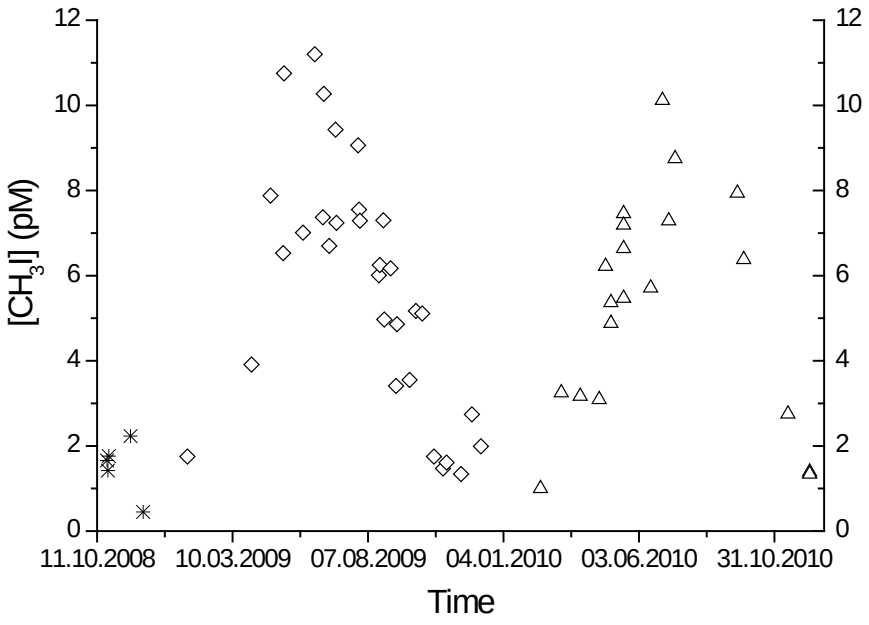

Figure 3.1: The concentrations of methyl iodide in the Kiel Fjord between October of 2008 and December of 2010. Stars (*) indicate 2008, diamonds (◊) indicate 2009, and triangles (Δ) indicate 2010.

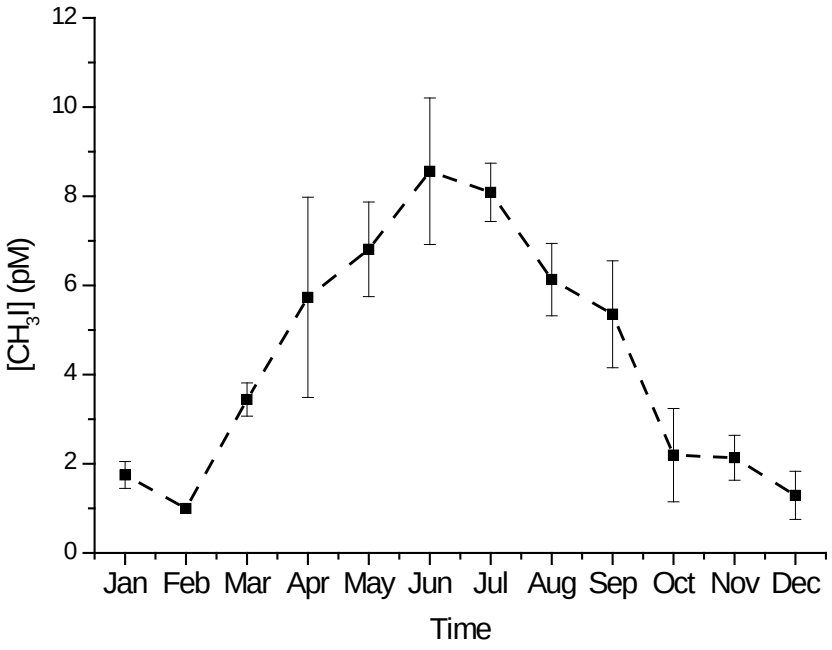

Figure 3.2: The annual cycle of methyl iodide in Kiel Fjord based on monthly means calculated from the entire data set. The error bars represent the 95% confidence interval.

3.2.2 Seasonal Variation of Other Parameters

Figure 3.3 depicts the monthly mean surface concentration of methyl iodide (from Figure 3.2) together with time-series of sea surface temperature (SST), solar radiation, salinity (SSS), chlorophyll *a*, CDOM, iodide [I^-], iodate [IO_3^-] and [NO_3^-] from the same sampling location. SST, SSS and solar radiation are measured routinely close to the sampling location by members of the Maritime Meteorology research unit at GEOMAR. The CDOM, iodide and iodate procedures are described in Chapter 2, sections 2.3 and 2.4.

Monthly mean SST remained at <6 °C from November to April, and increased rapidly at the end of April to a maximum of approximately 20 °C in late July. There was a noticeable time lag between the seasonal patterns of solar radiation and SST, with the maximum of surface irradiance occurring in June (Figure 3.3a and c). The maximum of CH_3I also occurred in June, prior to the maximum in SST (Figure 3.3a). Lower salinity was observed in summer (S=13-14) compared with winter (S=16) (Figure 3.3b). This may be related to seasonal variation of freshwater discharge from the nearby Schwentine River. The highest concentrations of chlorophyll *a* (5-8 µg L^{-1}, Figure 3.3d) occurred between June and late September with a minimum (0.99 µg L^{-1}) in January.

CDOM absorption varied between 4.2 to 4.6 m^{-1} from December to May, and fell to 3.5 m^{-1} in June. From July to November the level increased back to its starting value (Figure 3.3e). The concentration of iodate in the Kiel Fjord ranged from 100 nmol L^{-1} to 165 nmol L^{-1} (Figure 3.3f). The variation in iodide was small from January to August (ranging from 100 nmol L^{-1} to 130 nmol L^{-1}), but concentrations increased rapidly in September from 120 nmol L^{-1} to 240 nmol L^{-1} (Figure 3.3g). Nitrate decreased from January to April (54 µg L^{-1} - 6 µg L^{-1}), and then varied between 4 µg L^{-1} and 10 µg L^{-1} from May to December (Figure 3.3h).

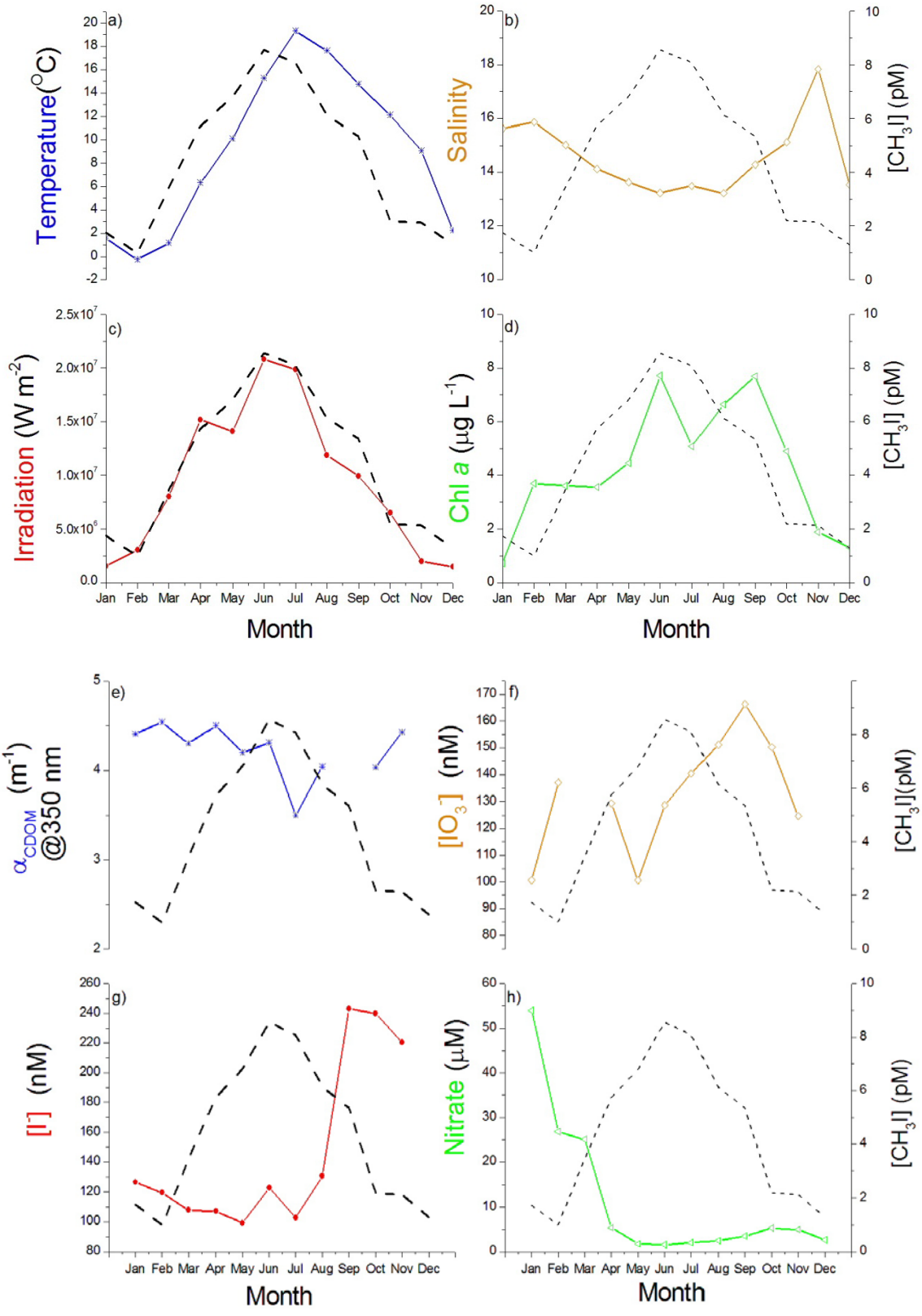

Figure 3.3: Annual variation of (a) SST, (b) SSS, (c) solar radiation, (d) Chlorophyll a, (e) CDOM, (f) iodate, (g) iodide, and (h) nitrate in the Kiel Fjord. The black dashed line depicts the annual cycle of methyl iodide. The data presented are monthly mean values for data collected over the time period from Oct. 2008 to Dec. 2010.

3.2.3 Correlations of Methyl Iodide with Other Parameters

The correlations of the seasonal variability of CH_3I in the Kiel Fjord with corresponding biological and physical data may provide information useful for understanding the factors that influence oceanic production of methyl iodide. A simple statistical approach using scatter plots and Spearmann´s Rank correlations was used to investigate the relationship between the monthly mean values of the surface water concentrations of methyl iodide and the parameters shown in Figure 3.3 (see Figure 3.4 and Table 3.1). Table 3.1 also includes correlations for additional halocarbon compounds that were measured at the same time in the same samples (they will be discussed in chapter 4, section 4.4).

Table 3.1: Spearmann´s Rank Correlation coefficients for the monthly mean data. The red marked values denote the significant correlation between CH_3I and other parameters. The correlations for additional halocarbon compounds will be discussed in chapter 4, section 4.4.

	CH_3I	CH_2ClI	$CHBr_2Cl$	$CHBr_3$
Irradiation	0.93	0.49	0.92	0.87
SST	0.79	0.83	0.65	0.77
Chl *a*	0.68	0.33	0.83	0.78
SSS	-0.72	-0.31	-0.50	-0.65
CDOM	-0.61			
Nitrate	-0.73	-0.33	-0.48	-0.69
iodide	-0.44			
iodate	0.13			

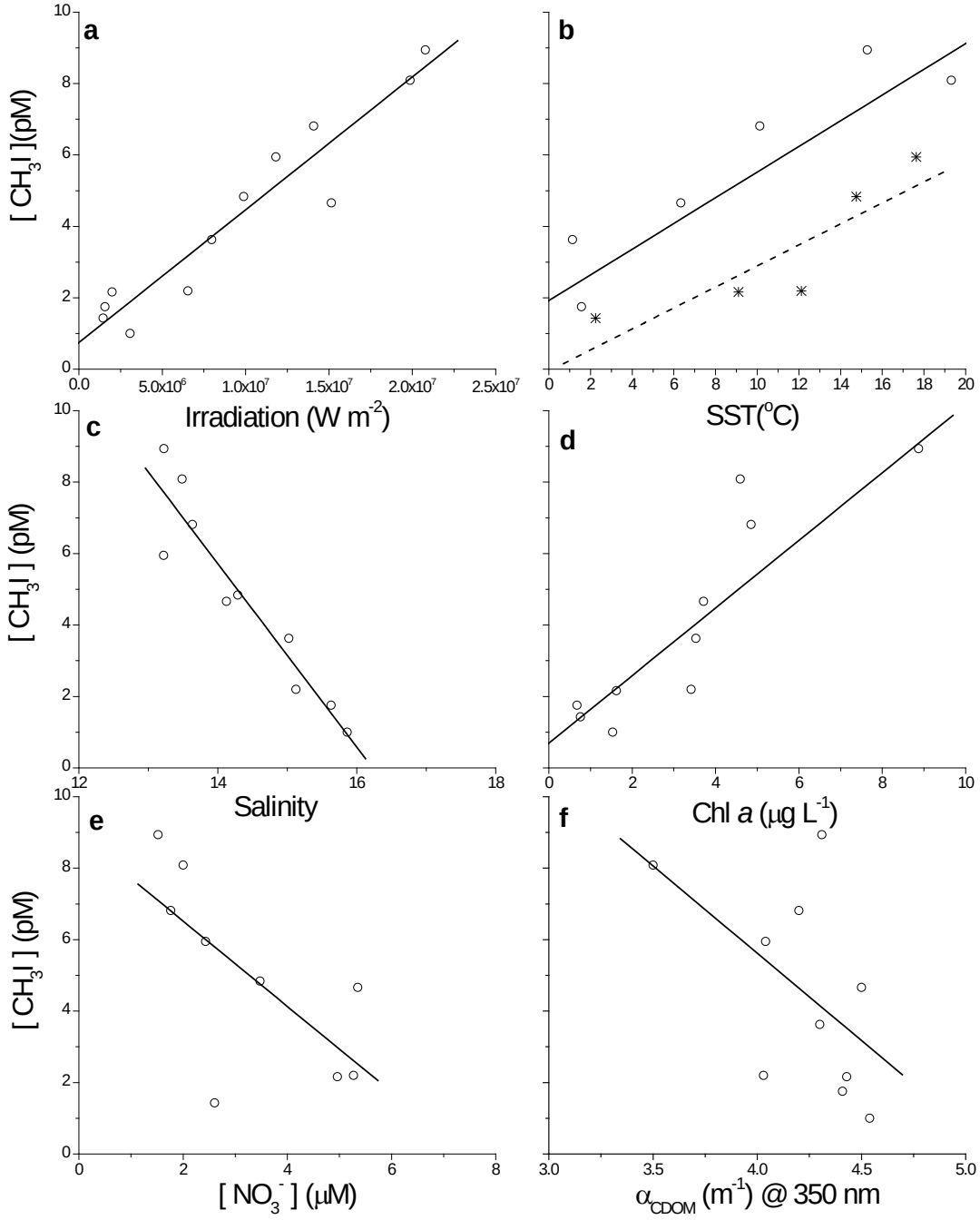

Figure 3.4: Scatter plots of monthly mean CH_3I concentrations versus the monthly means of the other parameters shown in Figure 3.3. In panel b, circles represent data collected from January to July, and stars denote data collected from August to December.

Based on this analysis, the seasonal variation of methyl iodide appears to be most strongly correlated with solar radiation followed by SST and chlorophyll *a*. The correlation coefficient of monthly mean CH_3I concentrations with incident solar radiation was very high (R = 0.96) for the Kiel Fjord (Figure 3.4a and Table 3.1). Correlations with temperature (R= 0.79) and chlorophyll *a* (R= 0.68) were highly significant but weaker. Strong inverse correlations were observed with salinity (R= -0.72), nitrate (R= -0.73), and CDOM (R= -0.61). No correlations were observed with iodide and iodate. Figure 5b indicates that there were two separate, linear relationships observed between CH_3I concentration and SST. One was for the period of warming (winter to summer, circles, regression slope = 0.36), and the other for the period of cooling (summer to winter, stars, regression slope = 0.3).

3.2.4 Long-term Accumulation and Loss of Methyl Iodide

The increase of CH_3I from winter to summer in 2010 is equivalent to a daily accumulation rate ($\Delta[CH_3I]_{24hr}$) of 0.07 $pmol \cdot L^{-1} \cdot day^{-1}$, and the corresponding accumulation rate ($\Delta[CH_3I]_{24hr}$) in 2009 was 0.05 $pmol \cdot L^{-1} \cdot day^{-1}$. Based on the average annual cycle (in Figure 3.3) the averaged accumulation (or loss) rates in different seasons ranged from -0.09 to 0.09 $pmol \cdot L^{-1} \cdot day^{-1}$ (Figure 3.5). In March the net accumulation of CH_3I increased rapidly with rate of ca. 0.09 $pmol \cdot L^{-1} \cdot day^{-1}$, the net accumulation rates kept increasing from April to June with rates of ca. 0.04 $pmol \cdot L^{-1} \cdot day^{-1}$, 0.07 $pmol \cdot L^{-1} \cdot day^{-1}$ and 0.07 $pmol \cdot L^{-1} \cdot day^{-1}$, respectively. The very rapid increase of CH_3I in March corresponds with a very rapid increase in irradiance (Figure 3.3c). After July the CH_3I concentration in Kiel Fjord decreased to the winter minimum. The maximum loss rate of methyl iodide was observed on October with ca. 0.09 $pmol \cdot L^{-1} \cdot day^{-1}$.

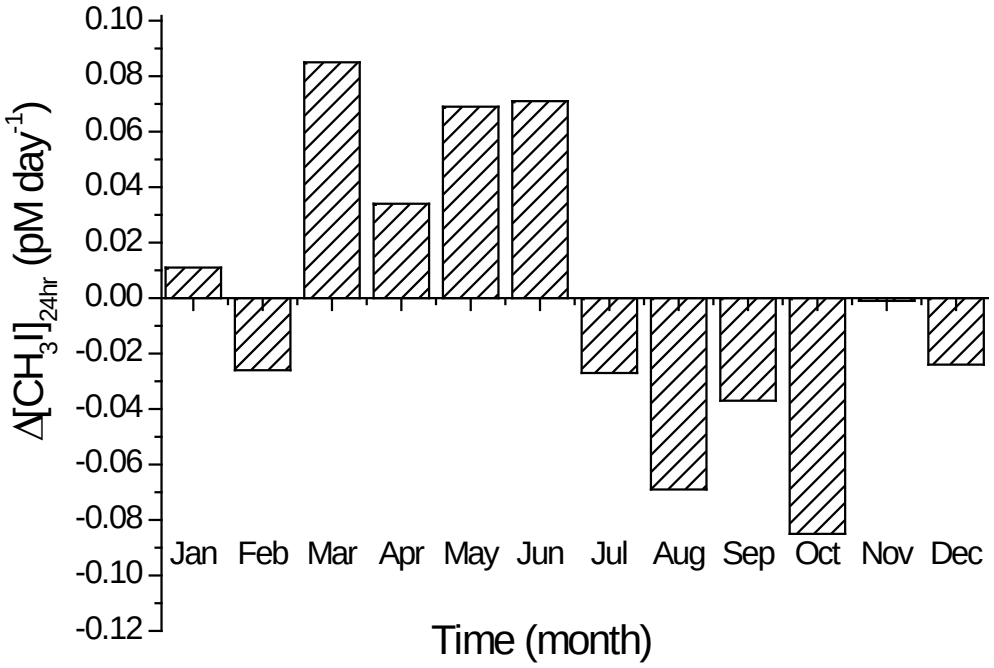

Figure 3.5: Monthly-average values of the daily accumulation/loss rates ($\Delta[CH_3I]_{24hr}$) of CH_3I based on the time-series data set (Oct.2008-Dec.2010) shown in Figure 3.3.

3.3 Discussion

3.3.1 CH_3I Concentration Ranges and their Seasonality

Concentrations of methyl iodide in coastal and shelf sea environments are generally reported to range from 0.6 to 61 pmol L^{-1} (Table 3.2). CH_3I concentrations measured from October 2008 to December 2010 in Kiel Fjord fall within this range (0.45 to 11.20 pmol L^{-1}), but are generally lower than those reported previously from similar latitudes in the Labrador Sea (15.5-61 pmol L^{-1}) (Moore & Tokarczyk, 1993) and from coastal waters of Mace Head (mean: 15.07 pmol L^{-1}) (Carpenter, Malin, Liss, & Kupper, 2000). The concentrations measured in the Kiel Fjord are however similar to those measured from the shelf seas of the western English Channel (0.6-14.6 pmol L^{-1}) (Archer, Goldson, Liddicoat, Cummings, & Nightingale, 2007).

Table 3.2: CH_3I concentration in the coastal seawater and open ocean seawater from this and previous studies

			[CH_3I] (pM)	
Reference	Latitude	Site	Range	Mean
Coastal:				
(Lovelock, 1975)		Kimmeridge (England)	19-55	
(Manley, Goodwin, & North, 1992	33°N	Laguna (California)	2.6-9.9	6.3
(Moore & Tokarczyk, 1993)	52°N-60°N	Grank banks	15.5-61.0	
(Happell & Wallace, 1996)		Greenland/Norwegian Seas	0.85-2.5	1.3
(Carpenter et al., 2000)	53.3°N	coastal of Mace Head		15.1
Open ocean:				
(Moore and Tokarczyk, 1993)	52°N-60°N	NW Atlantic	0.7-7.0	
	19°S	tropical Atantic	6.0-12	8
(Happell and Wallace, 1996)	8°N - 1°S	tropical Atantic	1.0-2.8	1.8
(Moore & Groszko, 1999)		eastern Atlantic off Ireland	1.2-8.2	3.4
	41°N-61°N	NW Atlantic	0.7-7.0	
	40°S-50°N	Pacific	2.0-6.0	
(Carpenter*, et al.*,2000)	53.3°N	offshore of Mace Head		9.7
(Chuck, Turner, & Liss, 2005)	50°N-65°S	Atlantic and Southern ocean	0.2-18.7	4.4
(Archer et al., 2007)	50.25°N	western English Channel	0.6-14.6	6.1
(Wang, Moore, & Cullen, 2009)	36.8°N-59.3°N	NW Atlantic	0.6-12.8	
This study:				
2009-2010	54.3°N	Kiel Fjord	0.45-11.2	5
2011	16.9°N	Mindelo	6.7-8.8	
SONNE Cruise (2011)	1°N-15°N	tropical Pacific	1.0-10.0	4.56

Table 3.3: Seasonal variation of CH_3I in surface water and atmosphere from this and previous studies. Here Spring is defined as being from March to May, Summer was from June to September, October and November were the Fall, and the remaining months (from December to February) were Winter.

			[CH_3I] (pM)(mean)			
Reference	Latitude	Site	Spring	Summer	Fall	Winter
In Water:						
(Tessier, Amouroux, Abril, Lemaire, & Donard, 2002)		Scheldt Estuary	24.0	2.4	9.2	3.2
		Gironde Estuary		3.5	1.3	1.4
(Archer et al., 2007)	50.25°N	Rhine Estuary	5.6		2.9	2.7
		western English Channel	4.9	11.1	6.5	1.8
(Wang et al., 2009)	43.4°N	Labrador sea	1.3	12.8	7.8	
	46.5°N	NW Atlantic	0.9	7.1	3.6	
This Study:						
2009-2010	54.3°N	Kiel Fjord	5.03	6.95	2.18	1.39
In Air:				[CH_3I] (ppt)(mean)		
(Carpenter et al., 1999)	53.2°N	Mace Head	0.43	3.4		
(Krummel, et al. ,2007)	40.4°S	Cape Grim	0.84	1.20	1.43	1.21
(Yokouchi et al., 2008)	43.2°N	Cape Ochi-ishi	0.7	2.9	1.5	0.6

Archer [2007] reported CH_3I concentrations in the western English Channel that increased gradually from February to the summer maximum in July and then decreased to winter-minimum levels, showing a clear seasonal pattern (Table 3.3). Wang and Moore (2009) reported the seasonality of methyl iodide in the open ocean for the first time. They found CH_3I in the surface mixed layer had an obvious variation between different seasons with a maximum in summer (Summer: 12.8 pmol L^{-1}; Spring: 1.3 pmol L^{-1}; Fall: 7.8 pmol L^{-1}; Labrador Sea; Table 3.4) (Wang et al., 2009).

A seasonal variation of atmospheric CH_3I (based on 9 observation stations from 82.5°N to 68.5°S) was reported by Yokouchi et al (Yokouchi et al., 2008). The seasonality was interpreted to imply that there was a seasonal variation of the oceanic source of methyl iodide with the maximum inferred sea-to-air flux in summer-autumn.

3.3.2 Correlations of CH_3I with Other Parameters

a) Solar Radiation

The strongest positive temporal correlation was observed between CH_3I and incident solar radiation (R= 0.93, Table 3.1). This is in agreement with the spatial correlations reported by Happell and Wallace [1996], who reported a linear relationship between open ocean CH_3I saturation anomaly and incident photosynthetically active radiation (PAR) (R = 0.88). This was interpreted to suggest that CH_3I production in the open ocean was controlled primarily by the amount of solar radiation reaching the sea surface and likely by a photochemical mechanism. The lack of a clear correlation with biomass (e.g. chlorophyll *a*) suggested that CH_3I might be produced via a light-dependent, abiotic pathway. Wang and Moore [2009] observed a moderate positive correlation of CH_3I and PAR (R = 0.58) and suggested also that solar radiation may be responsible for the production of CH_3I.

However, it is also possible that solar radiation could correlate with the growth of specific CH_3I-producing phytoplankton species, for instance the *Prochlorococcus* (Brownell et al., 2010; Hughes et al., 2011; Smythe-Wright et al., 2006). Smythe-Wright et al. [2006] suggested that CH_3I production by a high light adapted strain of P. marinus (MED4) in their laboratory cultures could be associated with cell senescence. Brownell et al. [2010] observed that the CH_3I production ceased when the cultures of *Prochlorococcus. marinus* reached stationary phase, and further suggesting CH_3I production was associated with growth of *Prochlorococcus marinus* (but at a much lower rate per cell). Hughes et. al. [2011] investigated the production of CH_3I by another

high light adapted P. marinus strain (CCMP 2389) and suggested that the rate of CH_3I production depended on physiological state of cell.

b) SST

A strong positive correlation was also observed between CH_3I and SST (R= 0.79). This might suggest that SST plays a role for the production process of CH_3I in the surface ocean. However since the temporal (and geographical) variation in SST is determined strongly by the input of solar radiation to the sea surface, the positive correlation with SST could also be due to the influence of light and remain consistent with a photochemical mechanism. This hypothesis was proposed by Chuck et al. [2005], when they found marine CH_3I was correlated spatially with SST (R = 0.87) during two cruises from Grimsby (UK) to Montevideo (Uruguay) and from Bremerhaven (Germany) to Cape Town (South Africa). Wang and Moore [2009] also observed a positive temporal correlation between SST and CH_3I although it was weaker (R=0.61), than that observed in this work or reported by Chuck et al. [2005].

Groszko [1999] observed that the sea-air concentration anomaly of methyl iodide increased with temperature for surface waters with temperatures less than 15 °C. Above 18 °C, methyl iodide had no strong trend with temperature. He used an empirical fourth-order polynomial function to fit the concentration anomaly data with SST below 15°C (R= 0.79). In this study, CH_3I concentrations continued to increase with SST for waters >18 °C (the maximum SST in Kiel Fjord was 21.7°C), and the empirical fourth-order polynomial function of Groszko [1999] did not fit the collected data for waters < 15 °C. Using linear regression a strong correlation of CH_3I with SST was observed based on all collected data, throughout the temperature range encountered in this study (R= 0.79).

SST can also influence the accumulation of methyl iodide through its control on the chemical loss reaction rate of methyl iodide (Elliott & Rowland, 1993;

Moore, 2006). In addition, higher SST decreases the solubility, so that warming can lead to an increase of the sea-to-air loss of methyl iodide (DeBruyn & Saltzman, 1997; Yamamoto, Yokouchi, Otsuki, & Itoh, 2001; Yokouchi et al., 2001; Yokouchi et al., 2008). Increased temperature also tends to enhance the growth rate of phytoplankton and bacteria (up to a temperature limit) (Eppley, 1972; Ratkowsky, Olley, Mcmeekin, & Ball, 1982; Rhee & Gotham, 1981). A role of increased SST on the growth rate of phytoplankton and bacteria, which might produce methyl iodide in seawater (Amachi et al., 2001; Brownell et al., 2010; Hughes et al., 2011; Smythe-Wright et al., 2006) must also be considered.

c) Chlorophyll a

A moderately strong positive correlation between chlorophyll *a* and CH_3I (R= 0.68) was observed, which might imply that CH_3I production involves a biological pathway. However, such a correlation was not observed by Chuck et al [2005] or by Happell and Wallace [1996]. The observed correlation between chlorophyll *a* and CH_3I concentration may be spurious because the seasonal chlorophyll level in the Kiel Fjord is also correlated with solar radiation, density stratification, etc.

Some laboratory studies show biological production of CH_3I by macroalgae (Laturnus, 1995; Manley et al., 1992; Nightingale et al., 1995), by phytoplankton (Smythe-Wright et al., 2006), and by bacteria (Amachi et al., 2001). However, when compared with an estimated annual sea-to-air flux of 1.3-3.6 × 10^{11} g yr^{-1} (Moore & Groszko, 1999), the limited annual production rates of CH_3I by these biota do not appear to be sufficient: macro algae in coastal waters ≤ 3.0 × 10^{8} g yr^{-1} [Manley and Dastoor, 1988; Manley et al., 1992; Nightingale et al., 1995]; phytoplankton ≈ 1.2 × 10^{9} g yr^{-1} [Manley and de la Cuesta,1997]; bacteria under laboratory conditions ≈ 1.0 × 10^{7}-1.2 × 10^{8} g yr^{-1} (Amachi et al., 2001). As a result the involvement of another source of CH_3I production in the surface seawater, such as photochemical production (Happell & Wallace, 1996; Moore & Zafiriou, 1994; Richter & Wallace, 2004;

Yokouchi et al., 2001), has been inferred. The only reported biological rate that can account for the global methyl iodide flux is 5.3×10^{11} g yr^{-1} (Smythe-Wright et al., 2006), assuming that *Prochlorococcus* is the sole biological source of CH_3I. In 2010 Brownell et. al. calculated a global CH_3I production rate of only 8.5×10^7 g yr^{-1} by extrapolation of their own results using the same stain of *Prochlorococcus* (MED4) as was used by Smythe-Wright et al [2006]. Their rates were 1000-fold lower than those reported by Smythe-Wright et al [2006] and the associated flux accounts for only 0.03% of the global CH_3I sea-to-air flux estimated by Moore and Groszko [1999]. Hughes et. al. [2011] conducted further culture experiments and noted a very wide range of CH_3I production rates. They suggested that earlier disagreement in the rate of CH_3I production by *Prochlorococcus* could be attributed to different cell physiological status in the different culture conditions (Brownell et al., 2010; Hughes et al., 2011; Smythe-Wright et al., 2006). The highest CH_3I production rates reported by Hughes et al. [2011] took place after their cell culture had crashed. Given this, it is unclear why the observed CH_3I increase was attributed to production by the *Prochlorococcus* cells rather than to photochemical or other production processes which might have increased rapidly following cell lysis.

d) CDOM

In this study a seasonal variability of CDOM was measured and a negative correlation between CH_3I and CDOM ($R = -0.61$) was observed. This might suggest that higher concentration of CDOM can slow down the CH_3I formation in the seawater. As a source of methyl radicals in the seawater (Moore and Zafirou, 1994; Richter, 2003; Yokouchi et al., 2008), increased dissolved organic matter (DOM) would be expected to enhance the rate of CH_3I formation in the seawater. However CDOM represents only a small part of the DOC pool in the ocean which might help to explain the observed, but unexpected, negative correlation between CH_3I and CDOM in this study.

e) Inorganic Iodine (Iodide and Iodate)

With respect to the photochemical pathway of CH_3I production via a radical mechanism (Moore and Zafirou, 1994; Happell and Wallace, 1996; Richter and Wallace, 2004), it has been suggested that the iodine atoms are formed from the oxidation of iodide.

$$I^- \xrightarrow{\text{Oxidation}} I_2 \longrightarrow I\cdot$$

In support of this, Manley [1994] and Moore et al. [1994] found that the addition of iodide enhanced CH_3I production during incubations. Manley [1994] showed there was positive relationship between CH_3I accumulation and iodide in laboratory experiments. However, in this Kiel Fjord study, no significant correlation between CH_3I and iodide was observed. One possible reason for the lack of correlation in our study is that the concentration of iodide (>100 nmol L^{-1}) was always at least 10000 times higher than the CH_3I concentration (maximum of 10 pmol L^{-1}).

Similarly, over the annual cycle no correlation between iodate and CH_3I was observed. If iodate participates in the production of methyl iodide in the seawater, iodate need first be reduced to molecular iodine (I_2). As noted above, there was always enough iodide available in the Kiel Fjord (100 nmol L^{-1}) to produce the low levels of methyl iodide measured.

f) Nitrate

A strong, inverse correlation between CH_3I and nitrate (R= -0.73) might be consistent with higher concentrations of nitrate reducing the rate of CH_3I formation in surface seawater. Chuck et al. [2005] also found a strong negative correlation (R = -0.85) between surface CH_3I concentration and nitrate during the second leg of the ADOX cruise (Cape Town to Polar Front then back to Cape Town) and explained the lower CH_3I concentration in the

high-nitrate low-chlorophyll waters of the pelagic Southern Ocean as being the result of low biological activity or, alternatively, being related to the I^- concentration given that the I^- concentration could be a controlling factor during the process of CH_3I photochemical formation. However, I^- concentrations were not measured during their cruise. Campos et al. [1999] proposed that nitrate reductase enzymes preferentially reduced nitrate but also can reduce iodate (IO_3^-) to iodide (I^-), based on their observation that dissolved iodide concentration (I^-) in surface seawater decreased and the nitrate concentration (NO_3^-) increased from the subtropical front to the polar front. Thus higher nitrate concentration might be associated with lower iodide production in surface seawater. However CH_3I concentrations were not analyzed on their cruise. There is therefore a possibility that CH_3I production is associated with nitrate reductase activity which might contribute to the strong negative correlation between CH_3I and nitrate in our study. However, the lack of a significant correlation between iodide and CH_3I in this study (section 3.3.2.5) argues against this being an important control.

3.3.3 Multiple Regression Analysis

As discussed above, there are multiple correlations of CH_3I with potentially related parameters and it is possible that multiple parameters control the CH_3I concentration in surface seawater.

To explore these multiple correlations further, a multiple linear regression analysis between the CH_3I concentrations and SST, solar radiation, salinity, iodide, iodate, nitrate, CDOM and chlorophyll *a* was performed. The monthly average values of all collected data (shown in Figure 3.3) were fit to the following regression equation:

$$[CH_3I] = a + b[\text{irradiation}] + c[SST] + d[\text{chlorophyll}] + e[SSS] + f[\text{iodide}] + g[\text{nitrate}] + h[CDOM] \quad (1)$$

where a, b, c, d, e, f, g and h are constants. After step wise linear multiple regression analysis the constants “a”, “d”, “f”, “g” and “h” were set to zero because of a higher correlation coefficient and t-test for CH_3I. The best-fit constants, correlation coefficient (R^2) are given in the followed equation 2:

$$[CH_3I] = 3.291E\text{-}7[\text{irradiation}] + 0.071[\text{SST}] + 0.034[\text{SSS}] \quad (R^2 = 0.98) \qquad (2)$$

Using this equation and the data (SST, SSS, irradiation) collected from 2009 to 2010, the methyl iodide concentrations were predicted. The residuals (predicted – observed) obtained after applying equation 2 are plotted in Figure 3.6. This shows that the seasonal variation of CH_3I in both years is very well explained by SST, SSS and solar radiation.

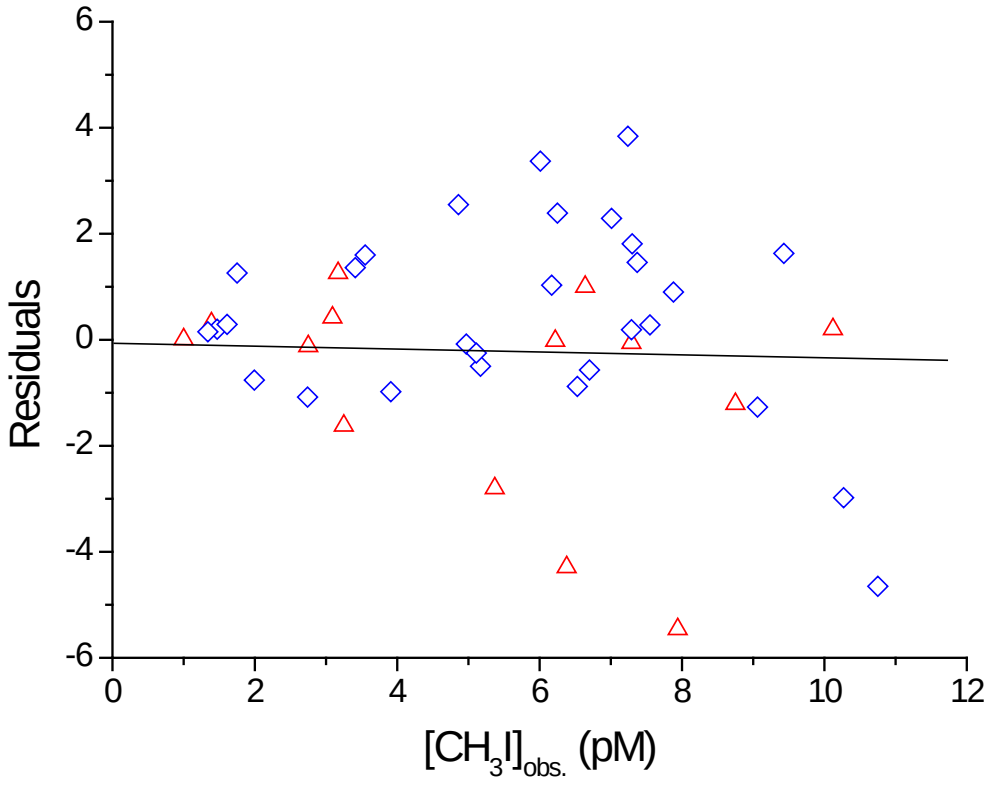

Figure 3.6: Residuals versus observed (obs.) dissolved CH_3I in the Kiel Fjord using equation 2; solid line indicates results of regression analysis for all data from 2010 and 2009. Residuals from 2010 are marked as red triangles, 2009 data are represented with blue diamonds.

3.3.4 The Seasonal Mass Balance of CH_3I in the Kiel Fjord

Using the annual cycle of monthly mean concentrations shown in Figure 3.3, we can examine monthly and seasonal variations in the mass balance of CH_3I in the Kiel Fjord according to:

$$\Delta[CH_3I]_{24hr} = P_{net} - L_{sea-air} - L_{SN_2} - L_{Mix} \qquad (3)$$

Where:

$\Delta[CH_3I]_{24hr}$ is the average daily accumulation or loss of CH_3I which is calculated from the changes of the monthly mean concentrations shown in Figure 3.3.

P_{net} represents the average daily net production of CH_3I and is solved for using equation 3, the measured accumulation and estimates of the (known) loss terms. Conceptually, P_{net} represents the difference between gross (or total) production of CH_3I (e.g. due to photochemical and/or biological processes) and losses due to any additional, uncharacterized loss processes that are not represented in the mass balance equation (e.g. microbial degradation; see Chapter 4).

$L_{sea-air}$ is the average daily sea-to-air flux of CH_3I calculated with the gas exchange relationship of (Nightingale et al., 2000) using 24 hour averages of wind speed as measured at GEOMAR, and assuming a constant atmospheric CH_3I mole fraction of 3 x 10^{-12}. The net sea-to-air flux of methyl iodide has been calculated using the transfer velocity parameterization corrected for the temperature-dependent Schmidt number by Groszko [1999]. Based on this approach the calculated sea-to-air flux in this study averaged 3.1 nmol m^{-2} day^{-1} and ranged from -0.4 to 5.9 nmol m^{-2} day^{-1} (assuming an average depth of 10 m for the Kiel Fjord, this flux is equivalent to an average rate of concentration change of 0.31 pmol L^{-1} day^{-1} with a range of -0.04 to 0.59 pmol L^{-1} day^{-1}). The calculated flux is shown in Figure 3.5. It can be seen that the flux of CH_3I is from the ocean to the atmosphere for most of the year and is

dependent on both the wind speed and oceanic CH_3I concentration. For example, higher wind speeds are seen in the winter of 2009 (>5.0 m s^{-1}) compared to the beginning of summer in 2010 (< 3.0 m s^{-1}), but the calculated fluxes in the winter of 2009 are less than in the beginning of summer of 2010 due to the lower CH_3I concentrations. Sea-to-air fluxes in winter were almost zero.

The sea-to-air flux in this study was almost 9 times lower than the 45.8 nmol m^{-2} day^{-1} calculated by Archer *et al* [2005] in August in the western English Channel and 4 times lower than the mean flux of 23 nmol m^{-2} day^{-1} in the tropical Atlantic (Richter & Wallace, 2004). The major reasons for these differences are the different wind speed regimes in the different studies.

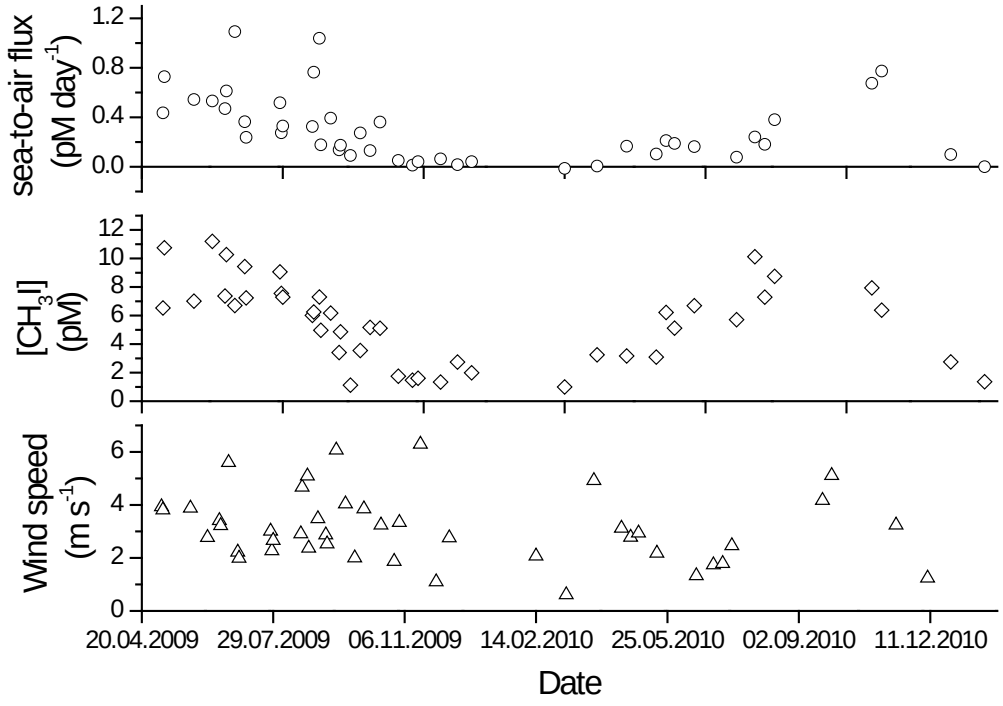

Figure 3. 7: Sea-to-air flux of methyl iodide.

L_{SN2} is the "chemical" loss due to nucleophilic substitution of Cl^- for I and is calculated based on published reaction kinetics (Elliott & Rowland, 1993) using the corresponding monthly mean temperature, salinity and CH3I concentration. The CH_3I loss rate due to the reaction with chloride ions was calculated to be an average of 0.047 pmol L^{-1} day^{-1} in this study. Compared

with the mean chemical loss rate of 0.12 pmol L^{-1} day^{-1} in the western English Channel (Archer et al., 2007) and of 1.0 pmol L^{-1} day^{-1} in the tropical Atlantic, the chemical loss rate in Kiel Fjord was much lower. The possible reasons were because of the difference of SST and SSS. The lowest SST in the western English Channel was higher than 8 °C and the SST in tropical Atlantic ranged from 27 to 29°C, but in Kiel Fjord the SST from November to April was lower than 8 °C (Figure 3.3a). In the western English Channel SSS ranged from 34.8 to 35.5 and in the tropical Atlantic the mean SSS was ca. 35. In Kiel Fjord the highest SSS was 20 (Figure 3.3b). Lower SSS means lower concentration of chloride in the seawater, and lower SST implies the lower chloride ion reaction rates using the Arrhenius type expressions. Taken together, these factors lead to the lower chemical loss rate of CH_3I in our study.

L_{mix} is the loss due to mixing, either lateral or vertical, with waters with lower concentrations of CH_3I. In open ocean waters, the CH_3I concentrations decrease below the euphotic zone, however the downward mixing loss has been shown to be negligible in comparison with the sea-to-air flux (e.g. Richter and Wallace, 2004). In the Kiel Fjord, which is only c. 2 m deep at the sampling site and 12 m deep at the deepest location, we assume that this loss pathway is negligible. Horizontal exchanges, on the other hand, depend on horizontal gradients which we did not measure. We assume that in the absence of tides and significant estuarine flow, that this loss pathway is also negligible.

Figure 3.8 shows that there is very strong seasonality in all terms of equation 3, with the sea-to-air flux being the principal known loss process for CH_3I throughout the year. Cl^- substitution is responsible for only c. 14% of the total loss rate. Further details about the seasonally-varying mass balance and loss processes for CH_3I will be discussed in the light of the incubation experiment results presented in Chapter 4 (see section 4.3.1).

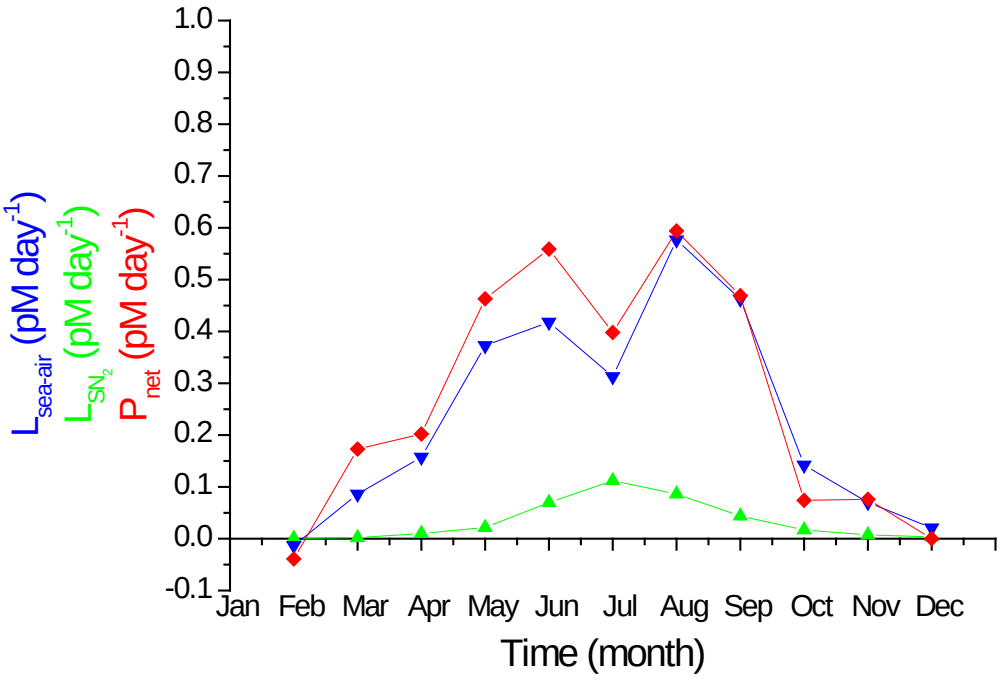

Figure 3.8: Variation of the terms in equation 3 over an annual cycle (L_{mix} is assumed to be negligible). Values represent daily rates calculated from monthly averages. Shown are P_{net} (red diamonds), $L_{air\text{-}sea}$ (blue triangles), L_{SN2} (green triangles). pM means pmol L^{-1}.

3.4 Conclusions

The long-term (Oct.2008-Dec.2010), time-series observations of CH_3I in the Kiel Fjord showed a repeating seasonal cycle of CH_3I with highest concentration in summer (June and July) and lowest concentration in winter (December to February). The correlations of methyl iodide concentration with corresponding biological and physical parameters (e.g. solar radiation) in the Kiel Fjord were investigated. The strongest positive correlation (R=0.93) was observed between CH_3I and solar radiation, with the next strongest correlation (R = 0.79) being between CH_3I and sea surface temperature (SST). Given that SST is, itself, determined strongly by the input of solar radiation, the correlations may suggest that CH_3I production in the Kiel Fjord is controlled primarily by the amount of solar radiation reaching the sea surface and are consistent with a photochemical production pathway.

However, a further consideration is that both SST and light affect the growth rate of phytoplankton and bacteria, which might also produce methyl iodide in seawater (Amachi et al., 2001; Brownell et al., 2010; Hughes et al., 2011; Smythe-Wright et al., 2006). Therefore, the positive correlation with SST may require further experimental investigation.

With respect to possible biological production pathways, the observed significant but weaker (R = 0.68) positive correlation between CH_3I and chlorophyll *a* may be spurious because the seasonal chlorophyll level in the Kiel Fjord is also correlated with solar radiation. Stepwise multiple regression analysis suggested that chlorophyll *a* was not a significant contributor to the CH_3I concentration variations. From this study, there is no compelling evidence for direct biological production of CH_3I, although it cannot be ruled out completely. There is suggestion of a possible role for bacterial degradation which require further testing. However, the biological production pathways of CH_3I via *Prochlorococcus* (Amachi et al., 2001; Brownell et al., 2010; Hughes et al., 2011; Smythe-Wright et al., 2006) have been reported and debated. In the further work, the similar time-series and experimental study could be conducted in a region where *Prochlorococcus* is abundant (e.g. off Cape Verde).

Using the annual cycle of monthly mean concentration, a mass balance for CH_3I in the Kiel Fjord was calculated. Because of the difference of SST and especially salinity, the average chemical loss rate of 0.047 pmol L^{-1} day^{-1} due to the reaction with chloride ions was much lower in the Kiel Fjord than that calculated previously for the western English Channel (Amachi et al., 2001) and the tropical Atlantic (Richter & Wallace, 2004). Based on the gas exchange relationship of Nightingale et. al. [2000] the calculated sea-to-air flux in this study averaged 3.1 nmol m^{-2} day^{-1}. The daily net production rates of CH_3I could be estimated from the field time-series data. They had strong seasonal variability and ranged from 0 to 0.15 pmol L^{-1} day^{-1}.

Chapter 4
Kiel Fjord Incubation Experiments

4.1 Artificial Seawater Experiments

An initial set of experiments was conducted to test ideas concerning controls on methyl iodide formation, including the influence of different sources of inorganic iodine. From March 2009 to June 2009 a set of incubation experiments with artificial seawater was conducted on the roof of GEOMAR´s west shore building. The experiments involved long-term (c. 1 month) incubations under natural sunlight (see Chapter 2, section 2.5.1 for experimental details). Given that the media had been autoclaved, there was no living material in the flasks. In these early experiments, samples were collected and analyzed at only 5 time-points over the course of the incubations.

4.1.1 Results of Artificial Seawater Experiments

Figures 4.1a and b show the temporal variation of methyl iodide during these c. 1 month-long incubations in the various artificial seawater media. The CH_3I concentration in artificial seawater without added inorganic iodine and sodium pyruvate (i.e. the normal media) remained low (0.04 ± 0.02 pmol L^{-1}) over the course of the incubation. In contrast, methyl iodide concentrations increased to 0.22 ± 0.19 pmol L^{-1} in the media with added potassium iodide (KI, red) and reached 0.36 ± 0.21 pmol L^{-1} in the media with added potassium iodide and sodium pyruvate ($C_3H_3NaO_3$, blue). The highest concentrations were recorded after 14-15 days and decreased subsequently. However the time resolution of the sampling does not allow for a more detailed characterization of the time-course.

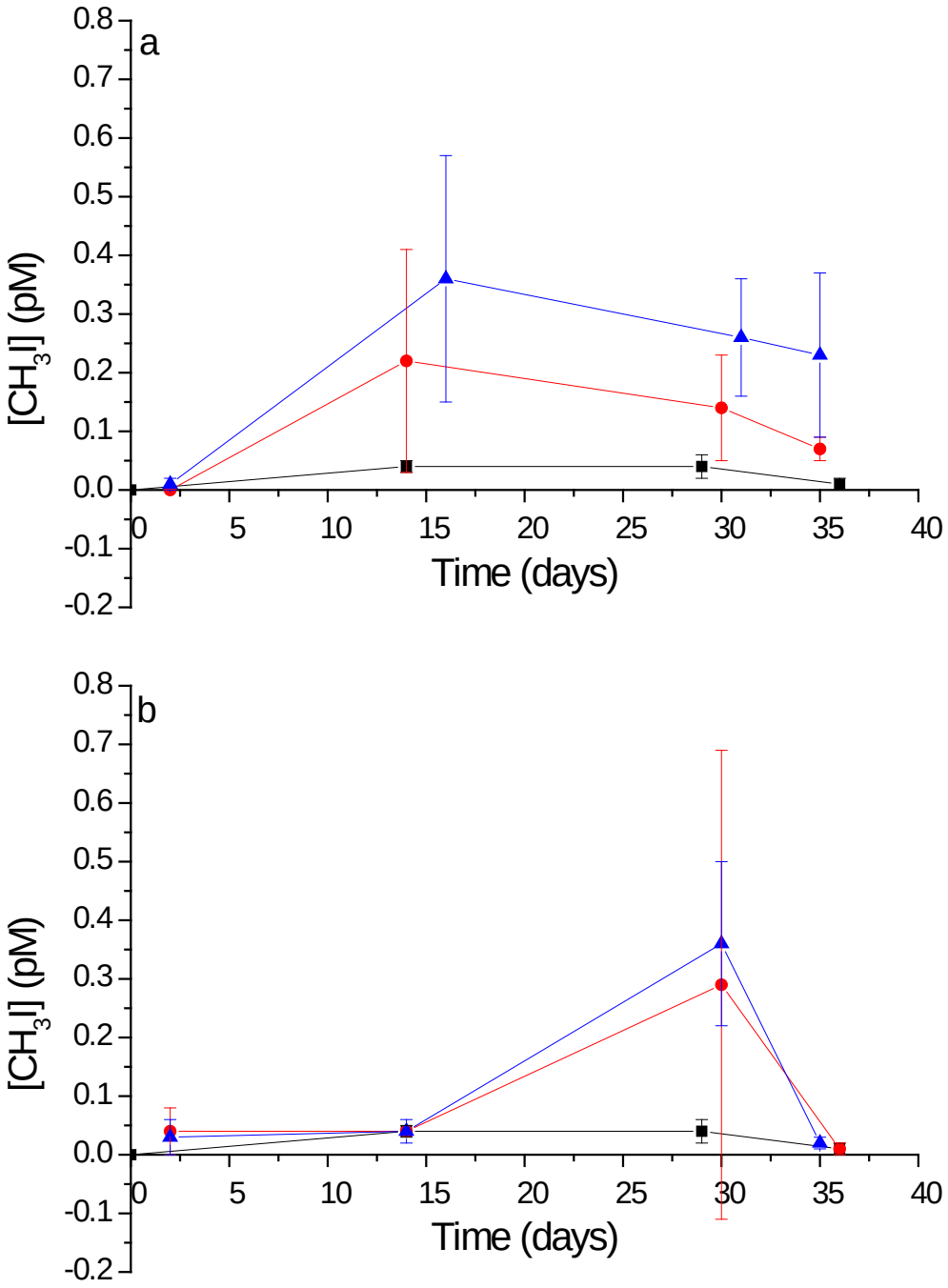

Figure 4.1: Variation of CH_3I concentration during incubations with various artificial seawater media (see Chapter 2). Black squares in both panels are results with the normal media (i.e. without added inorganic iodine and $C_3H_3NaO_3$). Panel a) shows results for additions of inorganic iodine in the form of KI; Panel b) shows results for inorganic iodine added in the form of KIO_3.In both cases, red circles are for the media with added inorganic iodine and blue triangles represent media with added inorganic iodine and pyruvate (a: KI + $C_3H_3NaO_3$; b:KIO_3 + $C_3H_3NaO_3$). Error bars show the 95% confidence intervals of triplicate measurements.

A similar pattern was observed for the samples to which KIO_3 was added (Figure 4.1b). However in this experiment, no significant increase was detected in the samples collected at 14 days and elevated concentrations were measured only at 29 days. Concentrations were close to their low, initial values at the end of the incubation.

Table 4.1: Variation of CH_3I concentration in various artificial seawater media

Media	Incubation time (days)	[CH_3I] (pM)	95% confidence
normal media	0	0.00	0.00
without KI and $C_3H_3NaO_3$	14	0.04	0.01
	29	0.04	0.02
	36	0.01	0.01
media with KI	2	0.00	0.00
	14	0.22	0.19
	30	0.14	0.09
	35	0.07	0.02
media with KI	2	0.01	0.01
and $C_3H_3NaO_3$	16	0.36	0.21
	31	0.26	0.10
	35	0.23	0.14
media with KIO_3	2	0.04	0.04
	14	0.04	0.00
	30	0.29	0.40
	36	0.01	0.01
media with KIO_3	2	0.03	0.03
and $C_3H_3NaO_3$	14	0.04	0.02
	30	0.36	0.14
	35	0.02	0.01

4.1.2 Discussion of Experiments with Artificial Seawater

a) Influence of Inorganic Iodine Species

The principle finding of these experiments was confirmation that there were no observable variations of methyl iodide concentrations in the “normal” artificial seawater media (i.e. artificial seawater without added KI, KIO_3 and pyruvate). The result is not surprising given that the “normal” medium should not have contained significant levels of iodine (see media composition in section 2.5.1.) but it also confirmed that contamination by extraneous sources of CH_3I was not a problem for the incubations.

On the other hand, additions of iodine in the form of both KI and KIO_3 led to production of CH_3I. Therefore, as expected, inorganic iodine plays an important role for the production of methyl iodide in the seawater.

The maximum CH_3I concentration in the medium with added KI was observed after 14 days, and earlier than in the medium with added KIO_3 (although the limited time resolution of the sampling precludes detailed insight into the timing).The results are consistent with the hypothesised pathway of photochemical formation of methyl iodide via radical recombination (Moore & Zafiriou, 1994).

$$CH_3\cdot + I\cdot \longrightarrow CH_3I \qquad (1)$$

As expected, no variation of methyl iodide in the “normal” artificial seawater medium was observed because there should have been no inorganic iodine in the artificial seawater (Figure 4.1, black squares). Addition of inorganic iodine should increase iodine radical formation leading to increased production of methyl iodide in the other two media prepared (i.e. the artificial seawater with added KI or with added KI and $C_3H_3NaO_3$).The dissolved I^- in the water is readily oxidized, and many photochemical oxidants in the water can provide a source of iodine radical, (e.g. the OH radical (Mopper & Zhou, 1990)). On the other hand, iodate (IO_3^-) is typically the dominant form of inorganic iodine

under oxidising conditions (pH 8.0, p*E* 12.5) (Luther et al., 1995; Ullman, Luther, Delange, & Woittiez, 1990). Iodate (IO_3^-) can be reduced through the following reaction to iodide (Spokes & Liss, 1996).

$$IO_3^- + 6H^+ + 6e^- \longrightarrow I^- + 3H_2O \qquad (2)$$

In the oceanic surface layer iodate can also react with dissolved organic material (DOM) under UV-light to form iodide (Truesdale, 1995) (Equation 3 and 4).

$$DOM + h\upsilon \longrightarrow DOM^* \qquad (3)$$

$$DOM^* + IO_3^- \longrightarrow I^- \qquad (4)$$

Additionally, photochemical conversion of iodate to iodide has also been proposed (Jickells et al., 1988). They suggested that iodate reacts with atomic oxygen to form molecular oxygen and an unstable intermediate of unknown structure, which decays to produce iodide and molecular oxygen (Equation 5 and 6). Biological conversion (marine phytoplankton) of iodate to iodide was reported by Wong [2002], Waite and Truesdale [2003] and Chance *et al* [2007].

$$IO_3^- + O \longrightarrow IO_2^- + O_2 \qquad (5)$$

$$IO_2^- \longrightarrow I^- + O_2 \qquad (6)$$

In our artificial seawater, concentrations of particulate and dissolved organic matter should have been low. Iodate might therefore have been reduced to iodide through the photochemical mechanisms with atomic oxygen, with iodide being oxidized to iodine radicals by photochemical oxidants in the water. It can be speculated, that this process may have led to the delayed maximum in CH_3I concentration observed in the medium with added KIO_3.

b) Influence of Pyruvate

With respect to the effect of adding sodium pyruvate, our results appear to be consistent with the findings of Moore and Zafiriou [1994], who had added pyruvate into deoxygenated water, and had observed enhanced production of methyl iodide. Here sodium pyruvate likely acts as a donor of the required methyl-group (Equation 1) because it can be decomposed photochemically according to (Closs & Miller, 1978):

(7)

The highest CH_3I concentration observed in the media with added KI and pyruvate was 0.36 ± 0.21 pmol L^{-1} compared to 0.22 ± 0.19 pmol L^{-1} of methyl iodide in the media with added KI only (Figure 4.1 and Table 4.1). The higher concentrations of CH_3I produced in the media with added KI and pyruvate is consistent with expectations, but the difference is not statistically significant. In the media with added KI but without added pyruvate, CH_3I concentration also increased after 15 days of incubation. Presumably organic material derived from the deionized water system, or salts used in preparation of the media acted as donors of the methyl-group.

These initial experiments with artificial seawater suggested that, overall, the appearance of CH_3I in incubation experiments was consistent with prior understanding of mechanisms and, especially, that the incubations themselves were not subject to major external contamination with CH_3I. However in retrospect, and given the results of the later experiments (see below), the time-resolution of the sampling was too limited to allow more conclusive findings. In particular, the observed CH_3I concentration variation was only c. 0.4 pmol L^{-1} after 15 days incubation, whereas our subsequent experiments with natural seawater revealed diurnal variations of the order of > 1 pmol L^{-1} (see section 4.3.1). Because these initial experiments did not resolve diurnal and possible other, shorter-term variability, our ability to

interpret the reasons for the increase of methyl iodide in the artificial seawater incubations is limited.

4.2 Incubation Experiments with Diurnal Sampling

From July of 2009 to December of 2010 over 20 longer-term (2.5 days or 57 hour duration) incubation experiments were conducted in the Kiel Fjord (see Chapter 2). This set of experiments resolved the seasonal cycle which has been discussed already in Chapter 3. The incubation experiments were designed to give more information about which factors influence CH_3I production in the surface ocean. Goals of the experiments included examination of the variability of production and testing of the relative importance of photochemical production compared to biological production. During the long-term-incubation experiments both treated and untreated samples were analyzed to investigate the diurnal variation of CH_3I concentration. The underlying experimental design has been described in section 2.5.3.

4.2.1 Diurnal Variability of Methyl iodide Concentrations

Figure 4.2 illustrates the variation of CH_3I concentration during a 57-hour incubation experiment conducted in July 2010. Results are presented for samples which were exposed to natural sunlight (i.e. the natural day-night cycle) and for samples that were kept in the dark. This particular experiment included incubations of both unfiltered samples and samples that had been pre-filtered to remove particles greater than 0.2 µm diameter (see section 2.5.3). The results show a clear diurnal variation of methyl iodide under irradiation in both the non-filtered (NF) and filtered (F) samples compared with samples that were kept in the dark (the effects of filtration are discussed in section 4.2.3). The “sunlit” samples showed a clear increase during daylight hours and a decrease at night. Notably, almost all of the CH_3I produced in the day-light was consumed during the night so that the long-term build-up of

CH_3I in the flasks was small or negligible compared to the daytime variations. For instance, the CH_3I concentration in the non-filtered samples (Figure 4.2a) increased by only approximately 0.01 pmol L^{-1} after the first 24 hours of incubation, compared to daytime variation of 1.35 pmol L^{-1} from 8:00 to 17:00. The monthly accumulation rate calculated from the seasonal cycle data discussed in Chapter 3 is plotted on Figure 4.2 for comparison (red line).

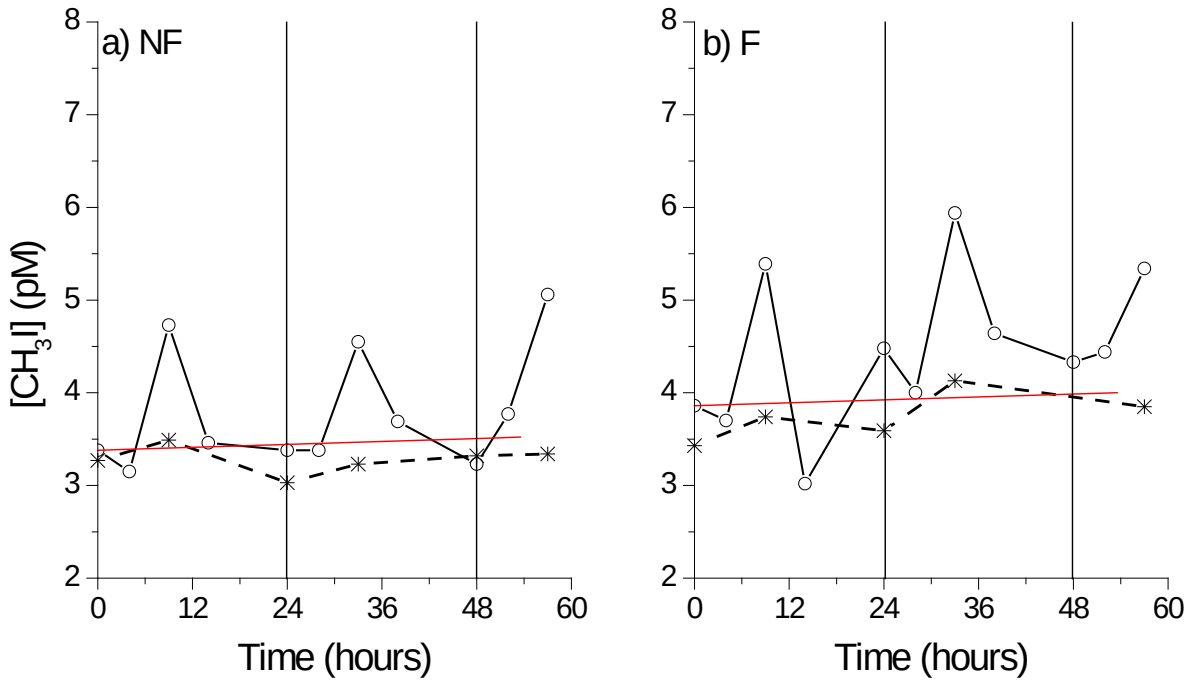

Figure 4.2: Variation of CH_3I concentration during a 57-hour incubation experiment conducted in July 2010. Samples were exposed to natural sunlight (line+circles), or kept in the dark (dash+stars). a): results for non-filtered samples (NF); b): results for filtered samples (F). The red lines show, for comparison, the equivalent long-term trend of CH_3I concentration over the month of July (using the monthly accumulation rate for CH_3I, see section 3.3.4).

Both the absolute values and the amplitude of the daytime variation varied from experiment to experiment. In order to obtain an overall view of the typical daily cycle, the results from all experiments (n=24) were normalized as follows. For each 24-hour time period, an initial concentration and the peak (maximum) concentration were determined. The normalized concentrations for this 24-hour period were then calculated as:

$$[CH_3I]_{nor} = \frac{[CH_3I] - [CH_3I]_{initial}}{[CH_3I]_{peak} - [CH_3I]_{initial}} \quad (8)$$

Where $[CH_3I]_{nor}$ is the normalized concentration of methyl iodide, $[CH_3I]_{initial}$ is the concentration in the "sunlit" samples analyzed at 8:00 for each 24-hour time period, and $[CH_3I]_{peak}$ is the maximum concentration during each 24-hour time period in the "sunlit" samples.

Subsequently, the average values of these normalized concentrations were calculated for each daily sampling time using values from all 24 incubation experiments. These average, normalized values and their error bars (95% confidence) are plotted in Figure 4.3.

On the basis of this normalization, the typical daily cycle for the "sunlit" samples during incubations can be described (Figure 4.3a). From early morning (8:00), the CH_3I concentration increases to a maximum at 17:00 within the samples exposed to natural sunlight. After 17:00 the CH_3I concentration decreases rapidly until near midnight (23:00). From 23:00 to 8:00 of the next day the concentration of CH_3I appeared to change only slightly. On average, over 24 hours of incubation the CH_3I concentration increased only slightly (Figure 4.3a, red line).

Using this "typical" daily cycle as a guide, we have calculated the daytime accumulation ($\Delta[CH_3I]_{day}$) in the "sunlit" samples as the CH_3I concentration increase over the 9 hour interval between 08:00 and 17:00. Similarly, the nighttime loss ($\Delta[CH_3I]_{night}$) was calculated as the concentration decrease measured between 17:00 and 08:00 on the second day.

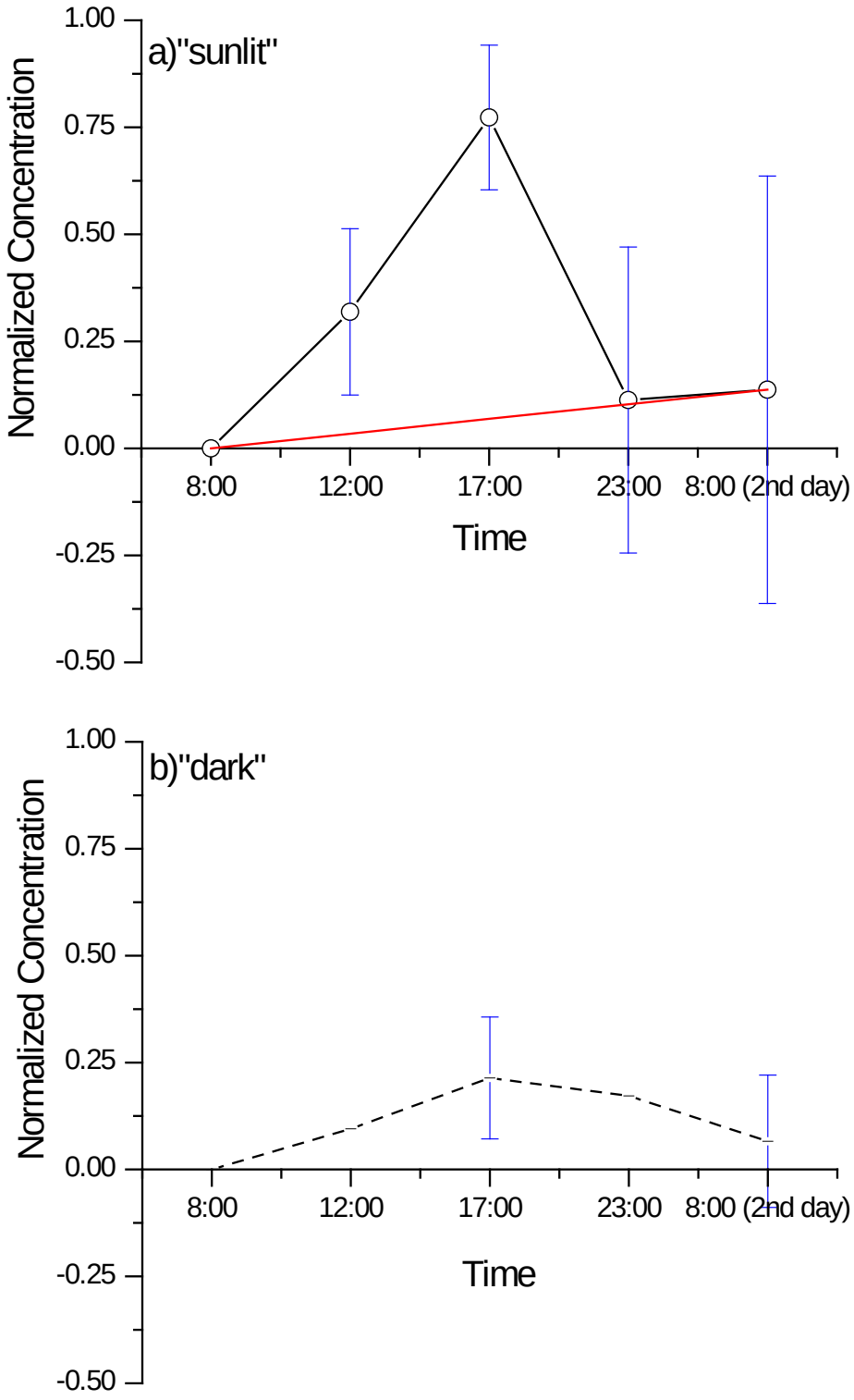

Figure 4.3: Normalized daily cycle of CH_3I (a) in the "sunlit" samples and (b) in the "dark" samples. Red line indicates the trend of CH_3I over 24 hours incubation.

Using the same equation 8, the results of "dark" sample incubations were also normalized for each 24-hour time period. For the "dark" sample plots, $[CH_3I]_{peak}$ was the maximum concentration in the "sunlit" samples during the same 24-hour time period, and $[CH_3I]_{initial}$ was the concentration in the "dark" samples analyzed at 08:00 for each 24-hour time period. The normalized, mean concentrations of "dark" samples are plotted in Figure 4.3b. The CH_3I concentration in the "dark" samples increased very slightly from 08:00 to 17:00, then decreased back to the starting concentration between 17:00 and 08:00 of the following day.

Comparison of the "sunlit" samples and "dark" samples (Figure 4.3) indicates that a significant difference was observed, with samples exposed to sunlight having much higher daytime accumulations compared to the samples kept in the dark.

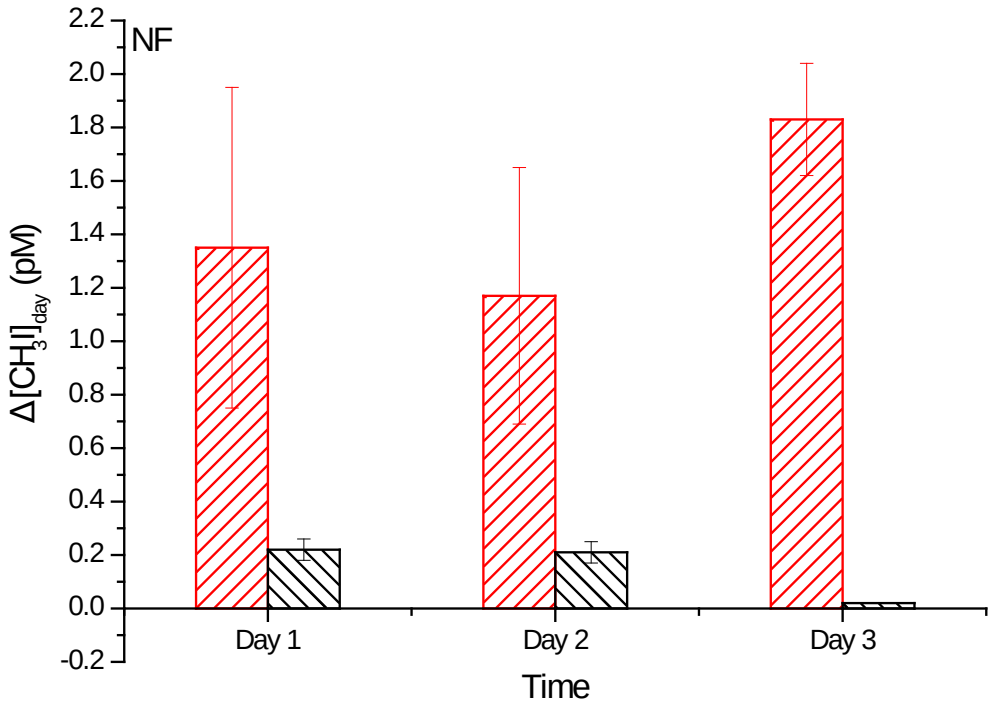

Figure 4.4: Summary presentation of the daytime accumulation of CH_3I concentration in the "sunlit" samples (red slash) and the dark samples (black slash) during the 57 hour incubation shown previously in Figure 4.2a. Error bars show the 95% confidence intervals of triplicate measurements.

The daytime accumulations of CH_3I ($\Delta[CH_3I]_{day}$) in the non-filtered samples (NF), that were already shown in Figure 4.2a, are presented in Figure 4.4. $\Delta[CH_3I]_{day}$ of methyl iodide in the first day from the samples exposed to light was 1.35 pmol L^{-1}, c. 7 times higher than that observed in the dark samples (0.2 pmol L^{-1}). Similar daytime accumulations of methyl iodide and differences between “sunlit” and “dark” samples were observed in the second and third days of the experiment.

4.2.2 Seasonal Variation of the Diurnal CH_3I Variability

Incubation experiments were conducted from Spring through Winter in order to examine seasonal variations in production. The daytime accumulation of CH_3I ($\Delta[CH_3I]_{day}$) during the first day of the incubation experiments from March to November are shown in Figure 4.5. The $\Delta[CH_3I]_{day}$ of CH_3I in samples exposed to sunlight ranged from 0.04 to 1.53 pmol L^{-1}, and from -0.48 to 0.39 pmol L^{-1} in the dark samples. A clear seasonal cycle of $\Delta[CH_3I]_{day}$ with a maximum in summer and a minimum in winter can be seen in the sunlit samples. Values of $\Delta[CH_3I]_{day}$ increased from c. 0.2 pmol L^{-1} at the end of March to maximal values of 1.53 pmol L^{-1} in July, and the daytime accumulation of CH_3I decreased again to a winter minimum of 0.04 pmol L^{-1} (Figure 4.5a).

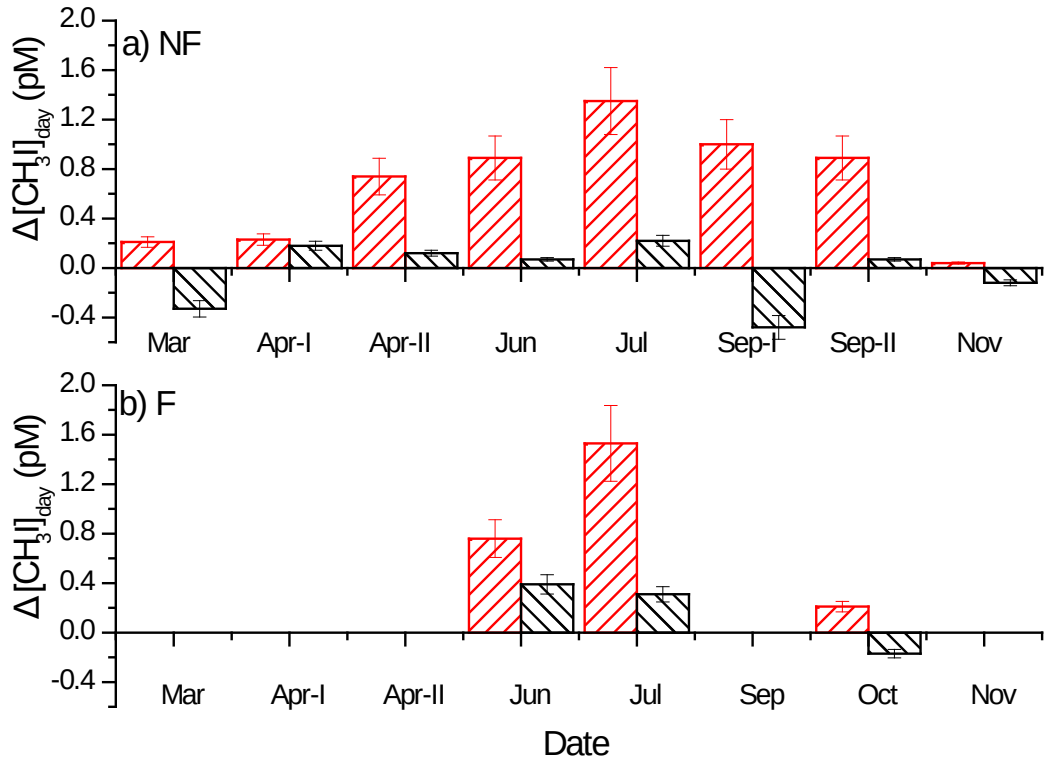

Figure 4.5: Daytime accumulation of CH_3I ($\Delta[CH_3I]_{day}$) during the first day of incubation experiments over the year for a) non-filtered samples (NF) and b) filtered samples (F) (discussed in section 4.3.3). Red shading indicates the samples kept in the light, black shading indicate the samples kept in the dark.

4.2.3 Effects of Filtration and Pre-purging with Nitrogen

a) Filtration Effects

As noted earlier, incubations were conducted with filtered samples in a small subset of the experiments (Figure 4.2b and 4.5b). Figure 4.2b shows that similar diurnal variability of CH_3I was observed in the filtered samples as in the non-filtered samples. The seasonal variation from this limited set of experiments also appeared to be consistent in timing and magnitude with those from the non-filtered experiments. A maximum accumulation of 1.58 pmol L^{-1} of CH_3I was observed in July (summer), whereas only 0.21 pmol L^{-1} of CH_3I accumulated in experiments conducted at the end of October (Fall) (Figure 4.5b).

b) Pre-purging

Most samples used in the incubations had been pre-purged with synthetic air for 5 hours (see section 2.2.1). On 5 occasions the effect of oxygen on the incubation results was investigated through pre-purging of samples with nitrogen (Nitrogen N50 from Air Liquid Company) for 5 hours instead of with air. This caused the dissolved oxygen and carbon dioxide in the samples to be reduced significantly (i.e., measurements showed that only 10% of the initial oxygen was present at the beginning of the incubation) (Figure 4.6 blue line). Under lower oxygen the daytime accumulation of CH_3I in the nitrogen pre-purged samples appeared to be larger (1.6 pmol L^{-1} compared to 0.9 pmol L^{-1}) than in the corresponding samples that had been pre-purged with synthetic air (60% to 70% of initial oxygen remained). The daytime accumulation of CH_3I in the original samples (no pre-purging) was 0.4 pmol L^{-1} in September (Figure 4.6). This result appears to be consistent with the observations of Moore and Zaifirou [1994]. They found higher concentration of CH_3I in deoxygenated water than in the oxygenated water, after the samples had been incubated under natural light (Moore & Zafiriou, 1994).

This experiment was repeated in November, and the daytime accumulation of methyl iodide was very low in both sets of samples (Figure 4.7). However, the surface seawater temperature in the Kiel Fjord had been reduced to 5 °C by that time. In addition, the sunlight intensity was only 500 W m^{-2}. This change in conditions between September and November likely explains both the reduced daytime accumulation of methyl iodide and the smaller difference between samples pre-purged with air and with nitrogen.

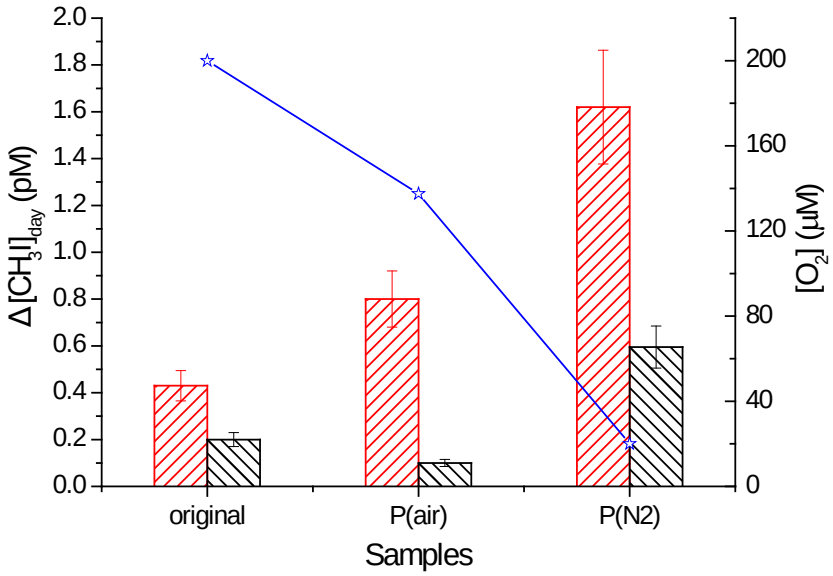

Figure 4.6: Comparison of the daytime accumulations between original samples (i.e. no pre-purging), the samples pre-purged with synthetic air (P_{air}), and those purged with nitrogen (P_{N2}) in the same month. Blue line indicates the oxygen concentration in the sample (right y axis).

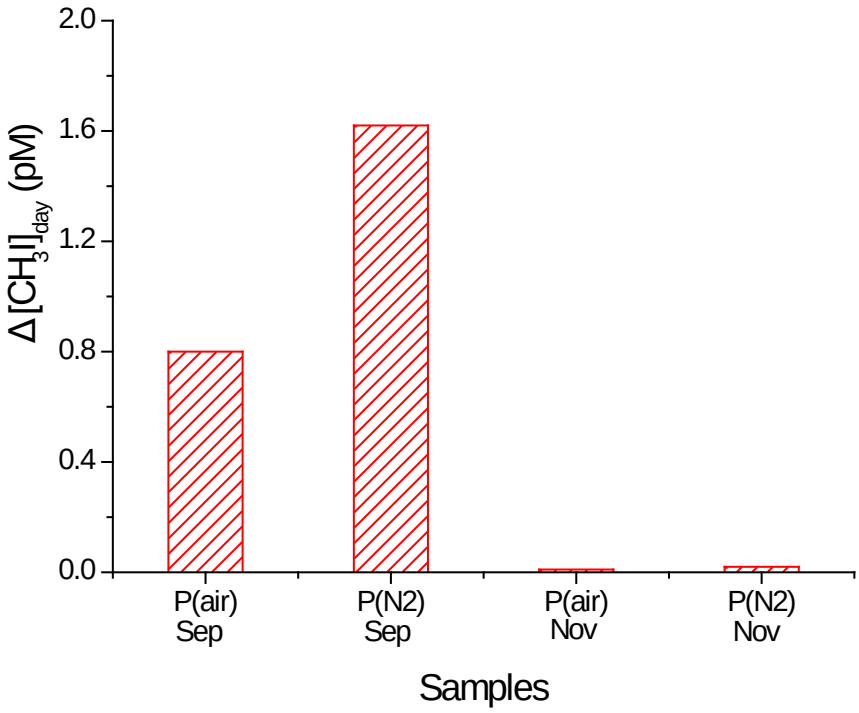

Figure 4.7: Comparison of daytime accumulations between the samples pre-purged with synthetic air (P_{air}) and pre-purged with nitrogen (P_{N2}) in different months. Red shading indicates the samples exposed to sunlight.

4.2.4 Discussion

a) Daytime Accumulation

In this study the diurnal variation of CH_3I has been investigated in incubation experiments that were conducted over a full seasonal cycle. The experiments revealed that samples exposed to a natural light-dark cycle had both higher daytime accumulation than samples kept in the dark, but that most of the CH_3I produced was subsequently degraded at night. In every incubation experiment conducted, a diurnal cycle was observed in the “light”-incubated samples with the average, normalized daily cycle being shown in Figure 4.3a. On the other hand, the CH_3I concentration remained quite stable and invariant in samples that were kept in the dark and neither large gains nor losses were observed (Figure 4.3b). The amplitude of the daytime variation showed a very clear seasonal cycle (see Figure 4.5).

Qualitatively, the results of our experiments are consistent with results from prior incubation experiments reported by Richter and Wallace [2004] and Moore [2006]. Richter and Wallace found that the accumulation of methyl iodide in the dark samples over a 24 hour incubation was only 0.72 pmol L^{-1} (mean) compared with 4.08 pmol L^{-1} (mean) in samples exposed to a natural light-dark cycle (Richter & Wallace, 2004). Moore [2006] reported CH_3I accumulation of 0.02 pmol L^{-1} in “dark” samples after a 48 hour incubation and 10 times higher accumulations of CH_3I in samples exposed to a natural light-dark cycle (Moore, 2006). All of these studies provide evidence that solar radiation promotes the production of CH_3I in surface seawater. However, Richter and Wallace [2004] and Moore [2006] analyzed the incubation samples in a long-term interval (24 hours and 15 hours, respectively) and did not resolve the diurnal variability which was observed in our experiments.

b) Filtration and Pre-purging Effects

The processes underlying methyl iodide production in the ocean are still not well characterised. Several investigations have attempted to evaluate the role of algae and phytoplankton in producing methyl iodide (Brownell et al., 2010; Hughes et al., 2011; Smythe-Wright et al., 2006). In the literature the possibility of abiotic, photochemical production has been proposed repeatedly (Bell et al., 2002; Happell & Wallace, 1996; Moore & Zafiriou, 1994; Richter & Wallace, 2004). In order to help determine if methyl iodide production is mainly associated with biological activity or abiotic photochemistry, incubations of natural seawater samples, both filtered and unfiltered, were performed. Details of incubation experiments were already described in Chapter 2. The filtered water contained no plankton cells (size >0.2 µm) because of the 0.2 µm filter used, but may have contained some bacteria which passed the filter or came from the walls of the incubation flask (which had not been autoclaved before the experiments). The disruption of cells during filtration may also have increased the DOC content of the water.

No significant difference of the daytime accumulation of CH_3I (ΔC_{day}) was observed between the non-filtered and filtered samples with the natural sunlight incubations (Figure 4.8 and Table 4.2), when the incubation experiments were conducted in the same month (June and July). In June, the concentration of methyl iodide increased 0.89 pmol L^{-1} in the first 9 hours for the non-filtered samples and by 0.76 pmol L^{-1} the filtered samples. In July, methyl iodide increased 1.35 pmol L^{-1} for the non- filtered samples and, 1.22 pmol L^{-1} for the filtered samples. The difference of daytime accumulation of methyl iodide between the non-filtered and filtered samples was therefore small (Table 4.2). These observations appear to be consistent with the arguments expressed in earlier studies (e.g. Moore and Zifiriou [1994]; Happell and Wallace [1996]; Richter and Wallace [2004] and Moore [2006]) that the production of methyl iodide in the ocean is not directly biological but rather photochemical in nature. On the other hand, Richter and Wallace [2004] observed that the accumulation in filtered samples from the tropical

Atlantic was 30% lower than in unfiltered samples, which they suggested may be have been a result of removal of organic precursors via filtration rather than a difference in biological activity due to filtration per se. Note that Richter and Wallace used a 0.1 µm membrane filter. In our study the daily accumulation in filtered samples was 11% (mean) lower than that in the unfiltered samples (Table 4.2). Note that we used a membrane filter with larger pore size (0.2 µm), than that used by Richter and Wallace. However there were also several other important differences between the experiments, including the light intensity which was much higher in the tropical Atlantic (10°N) than in Kiel (53°N).

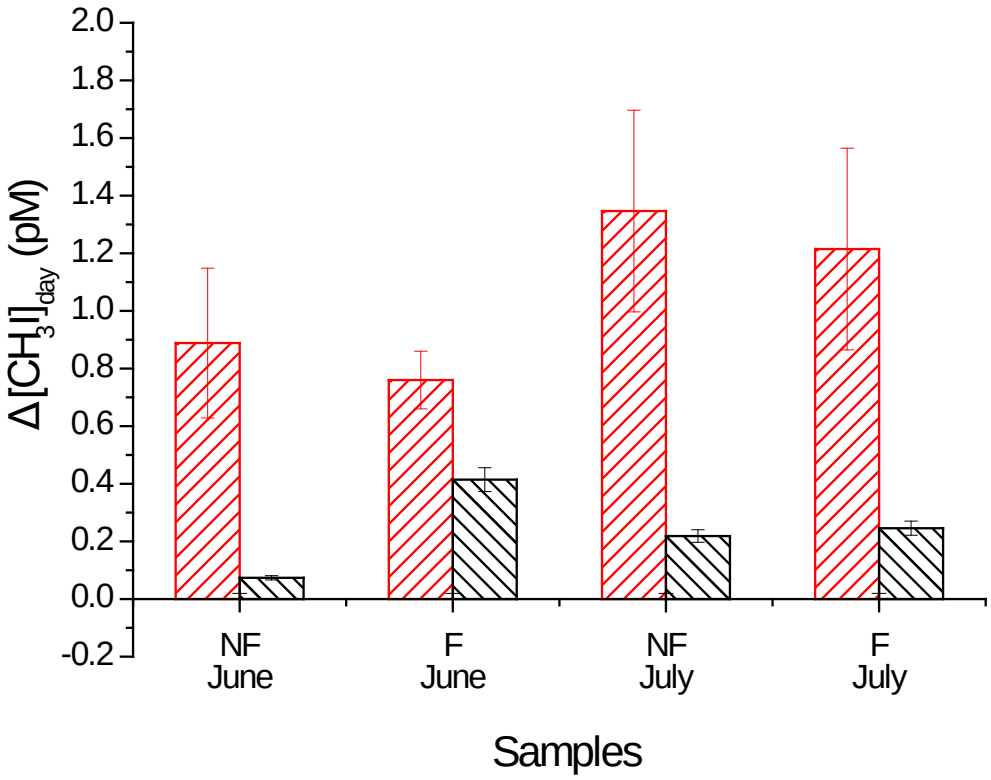

Figure 4.8: Comparison of daytime accumulations of CH_3I between non filtered (NF) and filtered samples (F). Red and black shading denote light and dark samples, respectively.

Table 4.2: Daytime accumulation of CH_3I in the non-filtered samples (NF) and the filtered (F) samples.

$\Delta(CH_3I]_{day}$(pM)	NF	F	Difference
June	0.89	0.76	14 %
July	1.35	1.22	10 %
mean	1.12	0.99	11 %

As shown in Figure 4.11, the daytime accumulation of CH_3I during the incubations increased with decreasing oxygen concentration. Similar results were observed by Moore and Zaifirou (Moore & Zafiriou, 1994) who reported that the rates of methyl iodide production in oxygenated waters were much lower than in deoxygenated samples. Zafiriou *et al.* [1990] argued that, the major obstacle for methyl iodine formation from these precursors is the large sink of methyl radicals through their reaction with oxygen (Zafiriou et al., 1990).

$$CH_3^{\cdot} + O_2 \longrightarrow CH_3OO \qquad (9)$$

This might explain the observed variation of methyl iodide in the samples that were pre-purged with nitrogen versus those pre-purged with synthetic air.

c) Loss Processes

In our experiments, the loss of CH_3I during the night was also larger for the samples that had been incubated under daylight, suggestive of first order loss processes. The consequence was that despite the daytime accumulation, the net production of methyl iodide over a full 24 hour period was low and generally not measurable given the daily variability and analytical uncertainty. Further, the accumulations over 24 hours in the incubations were not noticeably different than the long-term accumulation rates measured in the field (see Chapter 3 and the red lines on Figure 3.7).

The commonly considered removal processes for CH_3I in field studies are sea-to-air flux and nucleophilic substitution. Of these two loss processes, the sea-to-air flux tends to dominate for surface waters (see Figure 3.8 in Chapter 3). However during our incubation experiments, this loss process (sea-to-air flux) was excluded because the flasks were sealed. This would imply that nucleophilic substitution should have been the major removal process during the incubations. Using the reaction rates of Elliott and Rowland [1993], nucleophilic substitution by chloride ions averaged 0.047 pmol L^{-1} day^{-1} and ranged from 0.001 to 0.147 pmol L^{-1} day^{-1} in Kiel Fjord from May 2009 to July 2010 (see section 3.3.4). In this study, however, the observed loss rate of CH_3I during the night was 1-2 orders of magnitude higher than this, averaging 0.124 pmol L^{-1} $hour^{-1}$ (0.019 to 0.340 pmol L^{-1} $hour^{-1}$) (equivalent to an average of 2.98 pmol L^{-1} day^{-1} and a range of 0.46 to 8.16 pmol L^{-1} day^{-1}).

It seems that either the Elliot and Rowland loss rate parameterisation does not match the conditions in our bottles, or that an additional loss pathway was operating during the incubation experiments. There are two main possibilities for this additional loss pathway:

(1) One possibility is bacterial degradation: some bacteria are likely to have passed through the 0.2 micron filters and our incubation experiments were not axenic. However, Richter [2004] conducted alternative incubation experiments using samples that had been poisoned with mercury (II) chloride (the poisoned water still contains bacterial cells and organic matter, but without metabolism). In their study no significant difference was observed between these two treatments (filtered and poisoned).

(2) Another, more speculative loss mechanism is chemical oxidation by compounds that are produced during the day and which accelerate the degradation of CH_3I during the night. However, up until now the stronger loss rates of methyl iodide during incubation experiments have not been reported. Richter and Wallace [2004] incubated their tropical Atlantic seawater for 24 hours which did not allow for detection of the stronger loss rates of methyl

iodide during the incubations. They calculated an accumulation of CH_3I of 4.08 pmol L^{-1} (mean) over a 24 hour incubation for the non-filtered samples, which was ca. 40 times higher than that observed in this study (mean of the net production over 24 hours: 0.14 pmol L^{-1}). The higher daily accumulation in their study might due to the lower loss rate in the night. Richter and Wallace [2004] incubated their tropical Atlantic seawater for 24 hours which did not allow for detection of the stronger loss rates of methyl iodide during the incubations. On the other hand, it might due to the higher production rates of their incubations experiment in the tropical region.

d) Correlations of Diurnal Variability with Seasonally-varying Parameters

In Chapter 3 the seasonal variation of methyl iodide concentrations in the Kiel Fjord, including the strong summertime maximum, was discussed. During our long-term incubation experiments, the daytime accumulation of methyl iodide was investigated and was also shown to have a pronounced seasonal cycle with higher daytime accumulations in summer months (Figure 4.5a). Qualitatively, the higher summertime concentrations of CH_3I in the Kiel Fjord appear to be consistent with the higher daytime accumulation of CH_3I in summer observed in the incubation experiments. In section 3.3.2 the likely parameters underlying the seasonal variation (solar radiation, SST, SSS etc.), were examined. The strongest correlations of CH_3I concentrations were found with incident solar radiation and SST (see section 3.3.2).

Similar correlations were found with the daytime accumulations from the incubations. Figure 4.9 a and b show the amplitude of the daytime variations of CH_3I concentrations measured in the incubation experiments ($\Delta[CH_3I]_{day}$) plotted against values of the daily solar irradiation and SST. Figure 4.9 c and d show the regressions of daily irradiation and SST with $\Delta[CH_3I]_{day}$ ($R = 0.75$ and 0.81 respectively). These regressions show, again, that solar radiation and SST are closely linked to the daily production of methyl iodide in our incubations.

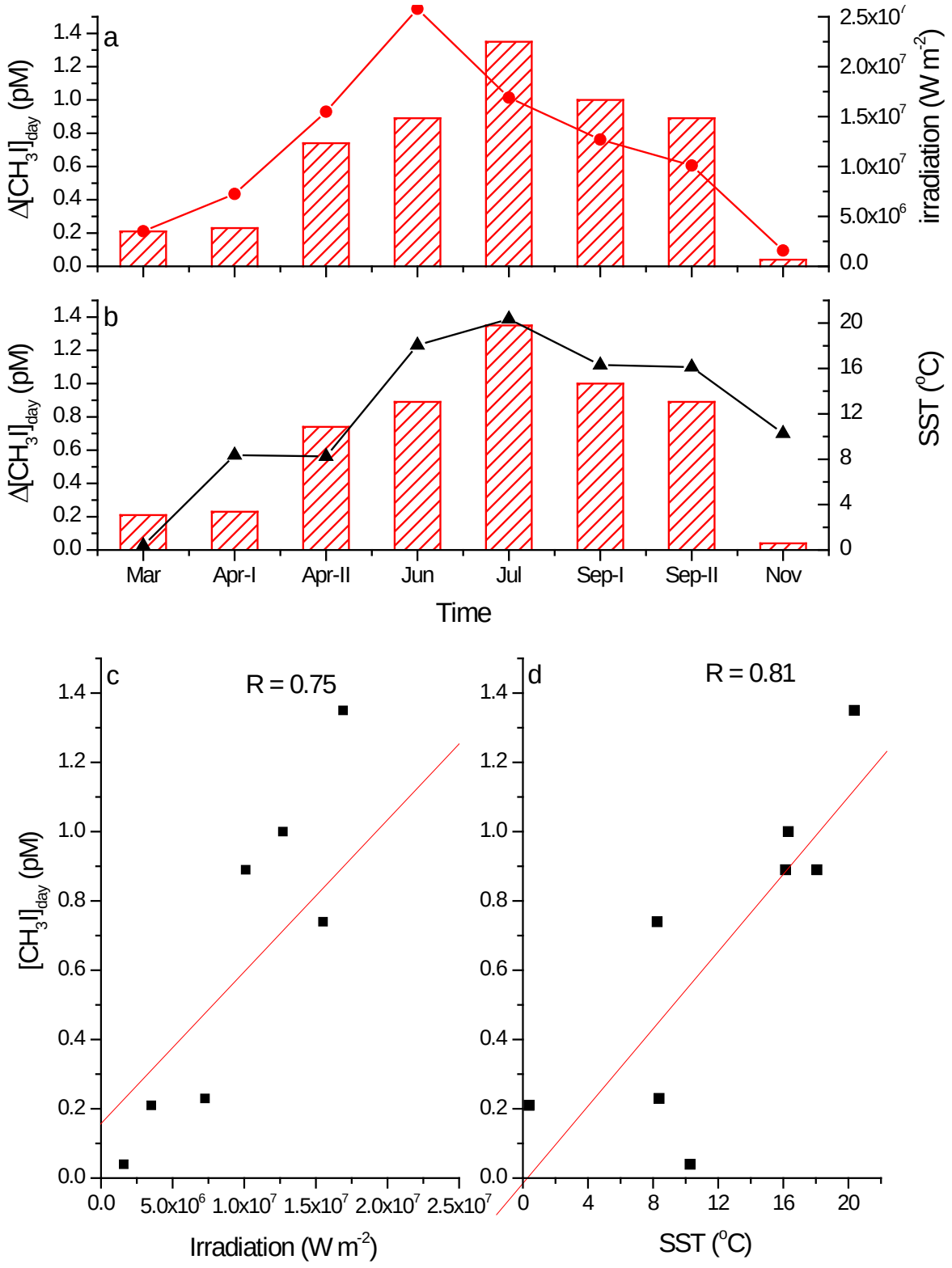

Figure 4.9: Daytime accumulation of CH_3I ($\Delta[CH_3I]_{day}$, red shaded bars), daily irradiation (a: red circles) and daily mean SST (b: black triangles) from March to September. c and d are scatterplots of $\Delta[CH_3I]_{day}$ versus solar radiation and SST during the incubation.

4.3 Rates of CH_3I Production

4.3.1 Mass Balances and Term Definition

In Chapter 3, the seasonal variations of a number of terms in the CH_3I mass balance for the Kiel Fjord were estimated based on data from the annual time-series. The results of the incubation experiments can be compared with this seasonal mass balance. As in Chapter 3 (equation 3), we can write the daily mass balance for CH_3I for surface waters in the Kiel Fjord as

$$\Delta[CH_3I]_{24hr} = P_{net} - L_{sea-air} - L_{SN_2} - L_{Mix} \qquad (10)$$

Where $\Delta[CH_3I]_{24hr}$ is the daily accumulation rate (i.e. over a 24 hour period), $L_{air\text{-}sea}$ is the daily loss associated with the sea-to-air flux, and L_{SN2} is the loss due to substitution of I by Cl^-. L_{mix} is the loss due to mixing, either lateral or vertical, with waters with lower concentrations of CH_3I. As in Chapter 3, P_{net} represents the average daily net production of CH_3I and is the difference between gross (or total) daily production of CH_3I (e.g. due to photochemical and/or biological processes) and any losses due to uncharacterized loss processes (i.e. in addition to mixing, gas exchange and Cl^- substitution). In Chapter 3, the in-situ time-series concentration data were used to define average values for daily accumulations over 24 hours ($\Delta[CH_3I]_{24hr}$). The loss terms $L_{air\text{-}sea}$ and L_{SN2} were estimated and L_{mix} was assumed to be negligible (see section 3.3.4) so that estimates of the average daily net production of CH_3I, P_{net}, could be derived.

The incubation experiments presented in this chapter revealed a pronounced diurnal cycle of CH_3I that was tied closely to the diurnal light cycle. Concentrations of CH_3I increased rapidly during the day and decreased at night. Applying equation 10 to the incubation experiments conducted in sealed flasks it is obvious that $L_{air\text{-}sea} = L_{mix} = 0$, so that equation 10 reduces to

$$\Delta[CH_3I]_{24hr} = P_{net} - L_{SN_2} \qquad (11)$$

This allows P_{net} to be estimated directly from the incubation experiment data, and these values can be compared with P_{net} estimates derived from the field sampling (see section 4.3.3 below).

Further, both the incubation experiments and the time-series revealed a very close relationship between CH_3I production and light intensity. This suggests, in analogy to the estimation of biological primary production from incubation studies, that we could consider P_{net} to be a combination of gross production (P_{gross}) which occurs only in the presence of sunlight, and uncharacterized losses (L_{other}) that take place in both the light and the dark periods so that:

$$P_{gross} = P_{net} + L_{other} \qquad (12)$$

(The "other" losses might include microbial degradation or the oxidation of CH_3I by other chemical species in seawater). Hence the accumulation in the incubation flasks during the daytime can be defined as:

$$\Delta[CH_3I]_{day} = P_{gross} - L_{SN_2} - L_{other} \qquad (13)$$

Where $\Delta[CH_3I]_{day}$ represents the accumulation within the incubation flasks during the daytime period only (approximately 8:00 to 17:00). For the remaining nighttime period, we assume that P_{gross}= 0 and that the loss rate remains unchanged so that:

$$\Delta[CH_3I]_{night} = -L_{SN_2} - L_{other} \qquad (14)$$

L_{other} can therefore be estimated from the nighttime decreases in CH_3I concentration observed during the incubations, and if we assume that L_{other} remains invariant over a 24 hour period, then P_{gross} can be estimated from equation 13.

In principle, the terms derived from the mass balance for the incubation flasks (when integrated over a full 24 hours), can be related to terms in the monthly

mass balance given in equation 3 of Chapter 3. Specifically, we can compare estimates of P_{net} derived from the long-term field study (equation 11), to estimates derived from the daily (24 hour) accumulation rates observed during the incubation experiments.

4.3.2 Comparison of Hourly Rates

According to the previous term definition, the daytime accumulation rate was calculated based on the accumulation ($\Delta[CH_3I]_{day}$) during the daytime period only (i.e. over 9 hours, approximately 08:00 to 17:00), and the daily accumulation rate was calculated based on the accumulation of methyl iodide over 24 hours ($\Delta[CH_3I]_{24hr}$). Such that:

$$Rate = \frac{\Delta[CH_3I]}{\Delta T(hour)} \qquad (15)$$

Using equation 15, the daytime accumulation rates and the daily accumulation rates of different samples in different season were calculated as hourly rates and are presented in Table 4.3 (The daytime accumulation rates were c. 10 times higher than the daily accumulation rates because the methyl iodide was produced in the daytime and largely degraded at night).

The daytime accumulation rates calculated in this study (0.1-0.2 pmol L^{-1} h^{-1}) are lower than the 1.0-1.5 pmol L^{-1} h^{-1} reported by Moore and Zafiriou [1994] for a study with incubations conducted under artificial light. Their higher levels may have been due to the very short incubation times of 0.5 to 2 hours used in their experiments.

Our daily accumulation rates ranged from 0.008 to 0.03 pmol L^{-1} h^{-1} (in Table 4.3). These results are similar in magnitude to the results of Moore [2006] (0.005-0.015 pmol L^{-1} h^{-1}), but are 10 times lower than the rates reported by Richter and Wallace [2004] (0.17 pmol L^{-1} h^{-1} for the NF samples and 0.10 pmol L^{-1} h^{-1} for the F samples) in the tropical Atlantic. The latter difference

Table 4.3: Comparison with other Data of previous study using non-filtered samples (NF) or filtered samples (F). The orange columns denote the daytime accumulation rates, the other 3 columns are the daily accumulation rates.

Accumulation Rates (pmol L^{-1} h^{-1})	$\Delta[CH_3I]_{day}$		$\Delta[CH_3I]_{day}$		$\Delta[CH_3I]_{24hr}$		$\Delta[CH_3I]_{24hr}$		$\Delta[CH_3I]_{24hr}$	
	Moore and Zafirou (1994)		This study (2009-2010)		Moore (2006)		Richter and Wallace (2004)		This study (2009-2010)	
Incubation time	3 h		9 h		50 h		24 h		24 h	
Sample source	coastal North Sea water		costal Kiel Fjord water		off shore water		the tropic Atlantic		costal Kiel Fjord water	
Latitude			54.3° N		50-55° N		10° N		54.3° N	
Irradiation (W m^-2)	1325 (artificial)[1]		532 (summer)[2]		0.5 (with fog)[3]				532 (summer)[2]	
Samples	Light	Dark	Light	Dark	Light	Dark	Light	Dark	Light	Dark
F	1.11	0.15	0.14	0.04	0.005-0.015		0.1	0.02	0.03	0.01
NF							0.17	0.03	0.008-0.01	-0.006-0.002

(1): at a solar zenith angle of 48°, over 280-1100 nm

(2): measured at 12:05 pm of all short wave

(3): only at 411 nm

might be attributable, at least in part, to the differences in irradiation during these studies, as well as the different water types used in the experiments. The Richter and Wallace [2004] study was conducted in open ocean, oligotrophic waters at 10°N under clear skies (they did not report actinic measurements, however the irradiation at 10°N is typically 8 times higher than at 50°N, especially the UV). Moore [2006] conducted the more than 50 hour incubation experiment during two cruises in the N. Atlantic during the spring and summer of 2003. They found rates of only 0.005 to 0.015 pmol L^{-1} h^{-1} in "sunlit" samples using off shore water (station T5: 50°N, 45°W). The irradiations during their incubation period were reduced by frequent fog.

4.3.3 Comparison of Incubation Experiments and Field Accumulation Rates

In section 3.3.4, estimates of a net production rate of CH_3I (P_{net}) derived from field sampling was discussed. Its magnitude reflects the excess of CH_3I production over loss by uncharacterised processes such as microbial degradation and chemical oxidation. P_{net} exhibits strong seasonality, varying from near-zero in winter months to maximum values of ca. 0.02 pmol L^{-1} hr^{-1} in summer (Figure 4.10, black line).

As was already noted in section 4.2.4, the loss rate of methyl iodide during the night time was high (up to 0.09 pmol L^{-1} $hour^{-1}$) indicating that there was an additional (uncharacterised) loss pathway for CH_3I, at least in the incubation experiments. It seems probable that the loss is due to either bacterial degradation or chemical oxidation. The magnitude of this loss rate appears to correlate with the CH_3I concentration. However, there is no direct evidence of bacterial methyl iodide degradation reported in the literature. Using equation 14, L_{other} can be estimated from the nighttime decrease in CH_3I concentration observed during the incubations. Hence a gross production rate can be calculated based on the field-derived estimates of P_{net} and this is plotted in Figure 4.10.

Even the maximum values of P_{net} calculated from the field data would be difficult to estimate from our incubation experiments which were only 57 hours in duration. If the field based estimates of P_{net} were appropriate to conditions within the incubation flasks, then the mean accumulation rates would be expected to follow the solid line (red) which is plotted on the experimental data in Figure 4.2. This figure shows that the high-amplitude diurnal variability observed during the incubations masks the long-term trend expected given the field-derived estimates of $P_{net.}$ On the other hand, the incubation experiment data appear to be quite consistent with the field-derived estimates of P_{net} .

In summary, the diurnal variability in the incubation flasks shows that short-term production (and loss) rates can be very much higher than the rates estimated from long-term, low frequency trends and budgets. This has important implications for the interpretation of rates calculated from prior incubation studies using natural light, which have not resolved the diurnal cycle, as well as for the design of future field and experimental studies.

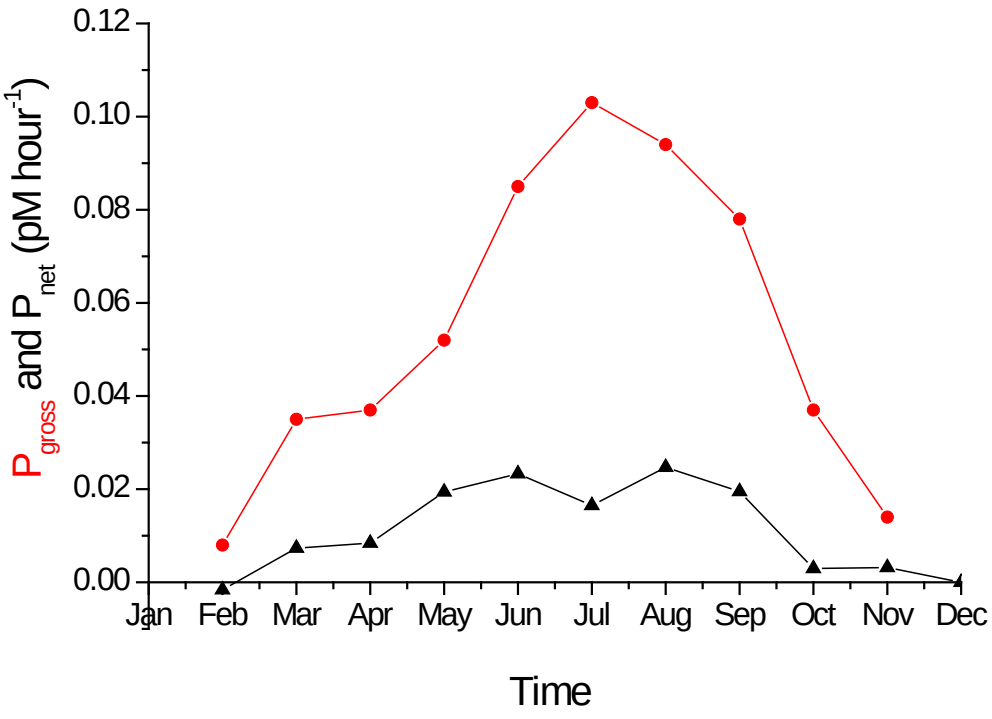

Figure 4.10: Seasonal variations of gross CH_3I production rates based on incubation experiments (red line) and net production based on the field samplings (black line).

4.4 Results for Other Measured Compounds:

A number of other halogen compounds ($CHCl_3$, CH_2Br_2, CH_2ClI and $CHBr_3$) were analyzed during the incubation experiments. These results are discussed briefly in this section.

Figure 4.11 and 4.12 show the results of other halogen compounds. Two compounds (CH_2Br_2, CH_2ClI) showed a seasonal pattern in daytime accumulation similar to that observed for CH_3I, but the seasonal maximum appeared to occur in September, later in the year than for CH_3I. Daytime accumulations of CH_2ClI gradually increased from June to end of September and dropped sharply to winter-minimum levels (Figure 4.11b). CH_2Br_2 daytime accumulations also increased from June to September, but dropped slowly down to spring-minimum levels (Figure 4.11c). The daytime accumulations of $CHBr_3$ increased rapidly from March to April, and the daytime accumulation rates continued to increase from April to July (Figure 4.11d). The daytime accumulation of $CHBr_3$ in the winter was lower than 0.2 pmol L^{-1}. No seasonal pattern was observed for $CHCl_3$ (Figure 4.11a).

In the most cases the “light” samples had higher daytime accumulation for CH_2Br_2 and CH_2ClI compared with the “dark samples”, which is similar to the observation for CH_3I (Figure 4.11b). It seems, that light plays a role of the production of CH_2Br_2 and CH_2ClI. Archer *et al.* [2007] suggested that CH_2I_2 can be photolyzed, partly to CH_2ClI, in the seawater based on their observation of the correlation between CH_2I_2 and CH_2ClI concentration in the English Channel. The higher daytime accumulation of CH_2ClI in the “light” samples in our study might due to the photolysis of CH_2I_2. However, the variations of CH_2I_2 were not measured in our study. Moore *et al.* [1996] presented that the CH_2ClI production has been observed in an algal culture of *Porosira glacialis* when no CH_2I_2 appeared to be produced. Photolysis of CH_2I_2 is not the only source of CH_2ClI in the seawater. However, we did not observe a significant difference of daytime accumulations between non-filtered and filtered samples for CH_2ClI in this study (Figure 4.12b) arguing against biological production as the main source of CH_2ClI in our study.

Oceanic production of CH_2Br_2 by phytoplankton and macro algae has been presented (Carpenter et al., 2000; Quack et al., 2004; Salawitch, 2006; Yang et al., 2005).

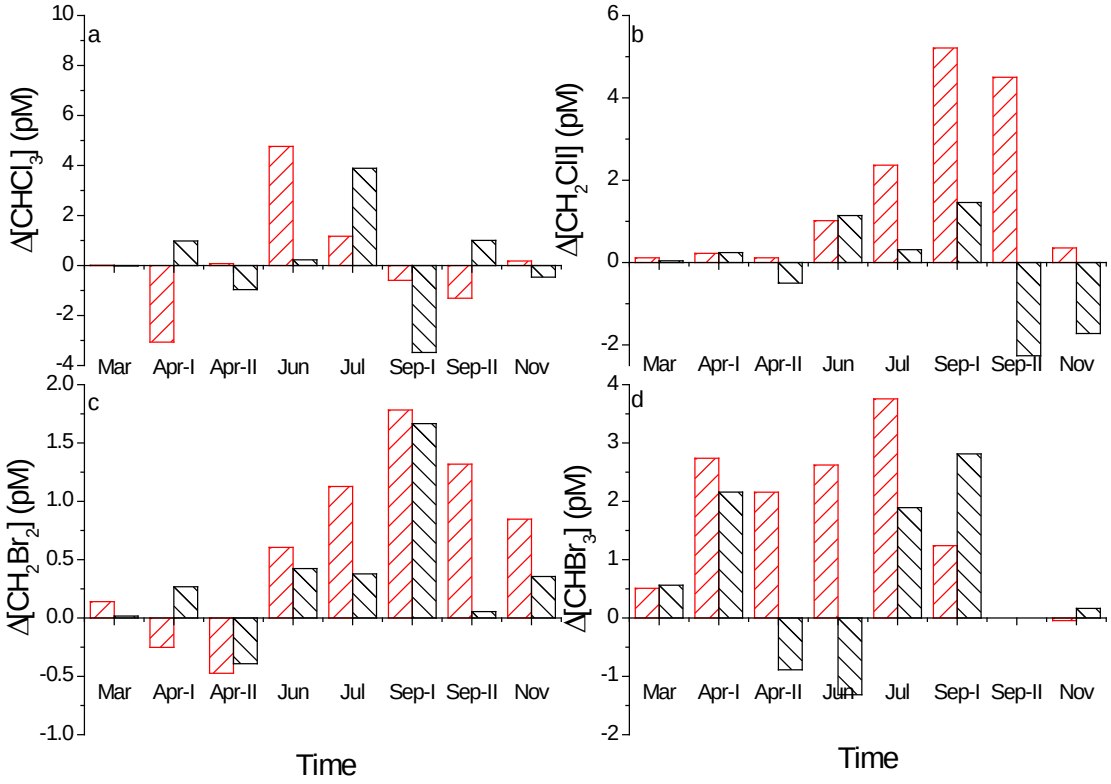

Figure 4.11: Seasonal variability of daytime accumulation of $CHCl_3$ (a), CH_2ClI (b), CH_2Br_2 (c), $CHBr_3$ (d) in the non-filtered samples. Red shading indicates the samples kept in the light, black shading indicate the samples kept in the dark.

Concerning the filtration effect, no significant differences were observed for $CHCl_3$, CH_2Br_2 and CH_2ClI suggesting that the production pathways of these 3 compounds ($CHCl_3$, CH_2Br_2 and CH_2ClI) were not biological. A significant difference was observed for $CHBr_3$ between the filtered and non-filtered samples (Figure 4.12d). The concentration of bromoform in the non-filtered samples increased 4 pmol L^{-1} under irradiation in July, with only a 0.8 pmol L^{-1} increase for the filtered samples under irradiation. This may be consistent with production of bromoform as a result of biological activity. Reports by Klick and Abrahamsson [1992] and Baker *et al.* [1999] implied production of bromoform associated with the abundance of diatoms. Tokarczyk and Moore [1994]

reported that bromoform can be produced through phytoplankton culture in the laboratory. Quack *et al.* [2004] observed the maximum concentration of bromoform was at the same depth as the maximum concentration of chlorophyll *a* in the water column. All these lines of evidence are suggestive of a biological production pathway for bromoform.

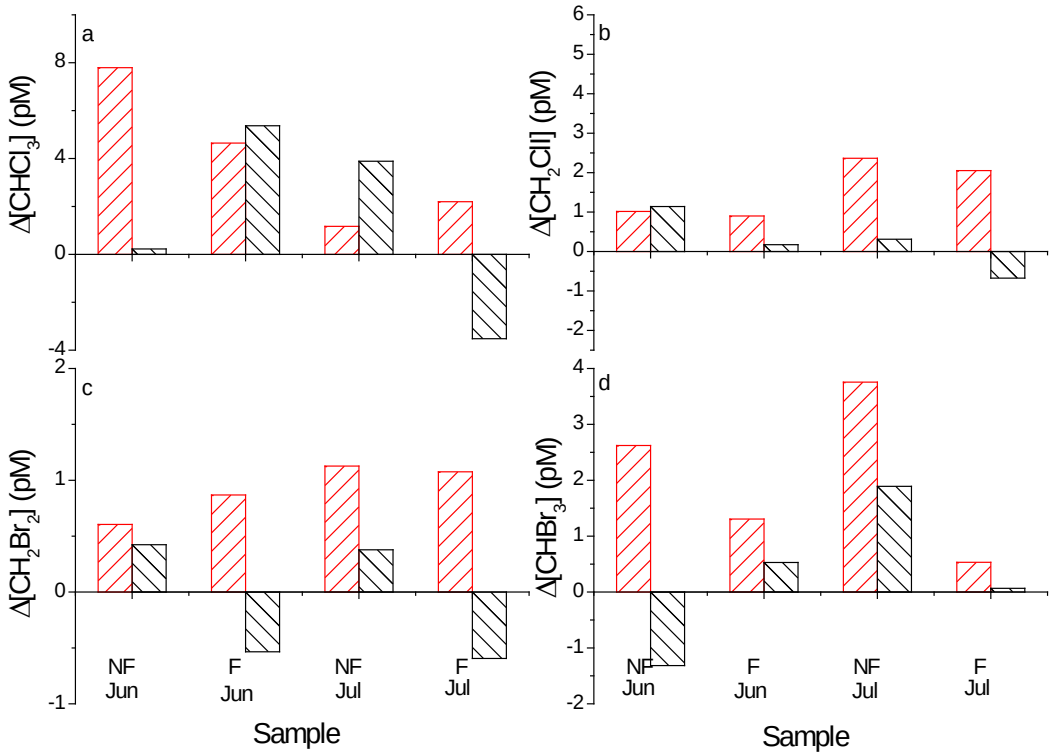

Figure 4.12: Comparison of daytime accumulations between non-filtered and filtered samples (F) of four halogen compounds (a: $CHCl_3$; b: CH_2ClI; c: CH_2Br_2; d: $CHBr_3$). Red and black shading denote light and dark samples, respectively.

4.5 Conclusion

"Whole-bottle" (quartz-flask) long-term (57 hours) incubation experiments were conducted to examine production of methyl iodide from July 2009 to July 2010. These experiments were conducted in the context of the time-series sampling program discussed in Chapter 3, allowing for the first time a direct comparison of production experiments with field-based sampling and empirical correlations over an annual cycle.

A clear diurnal variation of methyl iodide was observed in the samples incubated under natural light conditions. On average, the concentration of methyl iodide in the "sunlit" samples increased between 08:00 and 17:00, and decreased from 17:00 to 08:00 of the second day. Compared to the "sunlit" samples, the CH_3I concentration in the "dark" control samples varied only very slightly. This implies again that solar radiation plays an important, direct role in the CH_3I production process, and is consistent with the suggestion that CH_3I production in the Kiel Fjord is controlled by a photochemical mechanism. The strong diurnal cycle within incubations has not been observed before, likely because measurement of diurnal variations over short time scales (e.g. every 5 hours) has not been attempted previously.

No significant difference was observed between filtered and non-filtered samples with the natural sunlight incubations, when the incubation experiments were conducted in the same month, suggesting again that the daytime accumulation of CH_3I production is not directly biological but is consistent with photochemical production. The daytime accumulation of CH_3I did appear to be affected by pre-purging with oxygen-free gas, with the daytime accumulation increasing with decreasing oxygen concentrations. Oxygen can be an obstacle for methyl iodide formation by a photochemical pathway with radical combined mechanism.

However, methyl iodide loss during the night was unexpectedly large, and larger in the samples that had been incubated under daylight. These large night-time losses caused the daily net production of methyl iodide over 24 h periods to be low. The daily net production rates could not be estimated reliably from the incubation experiments due to their short duration coupled with strong diurnal variability. However the inferred low rates were consistent with the net production rates that had been estimated in Chapter 3 from the time-series data set.

The commonly considered removal processes for CH_3I in field studies are sea-to-air flux and nucleophilic substitution. However during our incubation experiments, a sea-to-air flux was excluded because the flasks were sealed.

The mean, calculated chemical loss rate of 0.047 pmol L^{-1} day^{-1} was 1-2 orders of magnitude lower than the observed loss rate of CH_3I during the night, which averaged 2.98 pmol L^{-1} day^{-1}. Hence an additional loss pathway was operating during the incubation experiments. There are two main possibilities for this additional loss pathway. One possibility is bacterial degradation because some bacteria are likely to have passed through the 0.2 micron filters used, and our incubation experiments were not axenic. Another possibility is chemical oxidation by unknown compounds produced during the day and which accelerate degradation of CH_3I during the night. The reason for the night-time loss rates clearly requires further experimental study.

By combining loss rates estimated from the incubation experiments with net production rates estimated from the field time-series data, the gross production rates for CH_3I were calculated on a monthly basis. These calculations implied highest gross production rates in summer and much lower production rates in winter and were consistent with a seasonal cycle of CH_3I driven primarily by variations in light intensity.

Chapter 5
Conclusions and Outlook

Methyl iodide is a major carrier of gas phase iodine from the ocean into the atmosphere. In the atmosphere, methyl iodide is photodissociated by near-UV light, with an absorption between 260-350 nm (Tsao and Root 1972; Roehl, Burkholder et al. 1997) and generates iodide atoms, which participate in ozone destruction and aerosol formation in the troposphere. In the ocean, the production sources and sinks, including air-sea flux, of methyl iodide must be investigated to improve the understanding of the methyl iodide global cycle. This thesis aims at elucidating the sources and mechanisms of methyl iodide in the surface seawater. From October 2008 to November 2010 a set of incubation experiments was designed to identify and quantify the sources of methyl iodide in the marine environment, in the context of a time-series of methyl iodide concentrations and other parameters (e.g. concentration of iodine species/chlorophyll) in the Kiel Fjord.

In Chapter 3, the results of long-term (Oct. 2008-Dec. 2010), time-series observations were presented to reveal indications about the processes controlling CH_3I concentrations (e.g. through correlation). They show a repeating seasonal cycle of methyl iodide in the Kiel Fjord with higher concentrations in summer (June and July) and lowest concentrations in winter (December to February). We examined methyl iodide correlations with solar radiation, SST, SSS, chlorophyll *a*, nutrients, CDOM and inorganic iodine species (iodide and iodate) via a simple statistical approach of Spearmann´s Rank correlations. The strongest positive relationship was observed between CH_3I and solar radiation (R=0.93), and suggested that CH_3I production in the Kiel Fjord is controlled primarily by the amount of solar radiation reaching the sea surface, and likely by a photochemical mechanism.

A strong correlation between CH_3I and SST (R=0.79) also was observed. However since the temporal and geographical variation in SST is determined

strongly by input of solar radiation to the sea surface, the positive correlation with SST could be due to the influence of light and be consistent with a photochemical mechanism. Hence the correlation with SST might be spurious in part. Increased SST can enhance the sea-to-air flux of methyl iodide (DeBruyn & Saltzman, 1997; Yamamoto et al., 2001; Yokouchi et al., 2001; Yokouchi et al., 2008), and the chemical loss reaction rate of methyl iodide in surface water (Elliott & Rowland, 1993; Moore, 2006). Thus, the positive correlation implies that one or more production processes of methyl iodide have to be enhanced by increased temperature in order to counteract the above mentioned negative effects. If the production of methyl iodide is a secondary photochemical process, SST could have a direct temperature effect on the production rate. A further consideration is that increased SST might increase the growth rate of phytoplankton and bacteria, which might produce methyl iodide in seawater (Amachi et al., 2001; Brownell et al., 2010; Hughes et al., 2011; Smythe-Wright et al., 2006). Therefore, the reason for the positive correlation with SST requires further experimental investigation.

A moderately strong positive correlation between chlorophyll *a* and CH_3I (R= 0.68) might suggest that CH_3I production involves a biological pathway. However, the observed correlation between chlorophyll *a* and CH_3I concentration may be spurious because the seasonal chlorophyll is also correlated with solar radiation. Future work will include the investigation of seasonal variation of diatoms in Kiel Fjord, which has been shown to produce methyl iodide in the laboratory (Smythe-Wright et al., 2006), to examine the possible bio-production of methyl iodide in the seawater.

Chapter 4 focuses on the “whole-bottle” (quartz-flask) long-term (57 hours) incubation experiments, which were conducted to examine production of methyl iodide from July 2009 to July 2010. A clear diurnal variation of methyl iodide was observed in the samples exposed to natural light. On average, the concentration of methyl iodide in the “sunlit” samples increased between 08:00 and 17:00, and decreased from 17:00 to 08:00 of the second day. Compared to the “sunlit” samples, the CH_3I concentration in the “dark” control

samples varied only very slightly. This implies again that solar radiation plays an important, direct role in the CH_3I production process, and is consistent with the suggestion that CH_3I production in the Kiel Fjord is controlled by a photochemical mechanism. The strong diurnal cycle within incubations has not been observed before, likely because measurement of diurnal variations in experiments forced with diurnal light variability has not been attempted previously. No significant difference was observed between filtered and non-filtered samples with the natural sunlight incubations, when the incubation experiments were conducted in the same month, suggesting again that the daytime accumulation of CH_3I production is not directly biological but is consistent with photochemical production.

However, methyl iodide loss during the night was unexpectedly large, and larger in the samples that had been incubated under daylight. These large night-time losses caused the daily net production of methyl iodide over 24 h periods to be low. Previous studies showed the main sinks of methyl iodide in seawater were sea-to-air flux and nucleophilic substitution. During our incubation experiments, the sea-to-air flux loss process was excluded because the flasks were sealed. The Elliot and Rowland loss rate parameterisation does not match the conditions in our bottles (nucleophilic substitution by chloride ions averaged 0.047 pmol L^{-1} day^{-1}, the observed loss rate of CH_3I during the night was 2.98 pmol L^{-1} day^{-1}). At the moment there is no firm explanation for this observation. One possibility is that unknown chemical species produced during the day can accelerate the degradation of CH_3I during the night, another possibility is degradation by bacteria. Thus, future work needs to investigate the loss process of methyl iodide during incubations and the controlling factors. During the incubation experiments, four samples were analysed every day to examine the diurnal cycle of methyl iodide. Only one sample was measured during the night (12 hours). To investigate the loss process of methyl iodide, I would like to analyse more samples during the night.

A pronounced seasonal cycle of the daytime accumulation of methyl iodide was observed during the incubation experiments. Qualitatively, the higher summertime concentrations of CH_3I in the Kiel Fjord appear to be consistent with the higher daytime accumulation of CH_3I in summer observed in the incubation experiments. Similar correlations were found with the daytime accumulations from the incubations. Solar radiation, and perhaps SST, is closely linked to the daily production of methyl iodide in our incubations.

For the pre-purging effect, the results of a few experiments in September showed that the daytime accumulation of methyl iodide increased with decreasing oxygen concentration. We repeated the experiments in November 2010, but the results were not replicated. A possible explanation is the much lower production of methyl iodide in the winter. To confirm this observation we need do more work in summer under more controlled conditions.

In Chapters 3 and 4 we already discussed the mass balance for CH_3I in the Kiel Fjord according to the equation:

$$\Delta[CH_3I]_{24hr} = P_{net} - L_{sea-air} - L_{SN_2} - L_{Mix}$$

The daytime accumulation rate of methyl iodide during the incubation experiments was much higher than the daily production rate (24 hour) of methyl iodide based on the field sampling in the Kiel Fjord. For a better understanding of the budget of methyl iodide, the best approach is likely to get a better understanding of the factors influencing production and loss of methyl iodide. As discussed it seems that the surface water concentration of methyl iodide is strongly influenced by solar radiation reaching the sea surface, as well as, perhaps SST and biomass. Future research should repeat the incubation experiments in different regions at different times of the year, particularly in the tropics and sub-tropics where CH_3I fluxes can be very large (Moore & Groszko, 1999; Richter & Wallace, 2004). In addition similar experiments under controlled conditions (e.g. light intensity, SST and the DOM concentration) should be carried out to investigate which factors

influence and/or control CH_3I production and loss and to evaluate the reaction mechanisms leading to the formation of methyl iodide. Further, the role of bacteria as a source or sink of methyl iodide in the ocean needs to be investigated to complete the methyl iodide cycle.

Overall, the approach of combining repeated experiments in the context of a field-based time-series, which was demonstrated here for the first time, looks promising and could be extended to other, non-coastal situations (e.g. Bermuda or Cape Verde).

Appendix
SHIVA Sonne Cruise: Results and Discussion

App.1.1 Introduction

A set of incubation experiments were conducted to qualify and quantify the marine source of methyl iodide in the Kiel Fjord from 2009 to 2010. The results suggested that the production pathway of methyl iodide in the surface seawater is not directly biological but rather photochemical. A research cruise aboard R/V Sonne was performed in order to investigate a suite of halogenated gas emissions (e.g. CH_3I, $CHCl_3$, CH_2Br_2, $CHBr_3$) from the western Pacific (and upwelling waters) and their subsequent atmospheric transport/transformation. This cruise was used to improve understanding of the photochemical source of methyl iodide in seawater. The SHIVA Sonne (SO218) cruise was conducted in November 2011, starting in Singapore and ending, via the South China Sea and Sulu Sea, in Manila (Philippines). The track is shown in Figure 1.

App.1.2 Sampling and Analytical Methods

Water samples for CH_3I measurements were collected every 3 hours via a well pump in the hydrographic shaft of the ship at 5 m depth. The seawater flow was approximately 30 L min^{-1}. Water samples for CH_3I measurements were analysed on board using the purge & trap GC-ECD method described in Chapter 2. The samples were generally analyzed immediately after collection and, in cases where storage was necessary, were stored in the refrigerator until analysis, a period averaging about 3 hours. Sea surface temperature (SST), sea surface salinity (SSS) and wind speed were measured by on-board sensors, while chlorophyll *a* and concentrations of phytoplankton pigments, including Zeaxanthin (Zea) the marker pigment for cyanobacteria,

were analysed by colleagues from the Alfred Wegener Institute (AWI) in Bremerhaven. Sea water samples for iodide and iodate were transferred back to Kiel and analysed by Kathrin Wuttig.

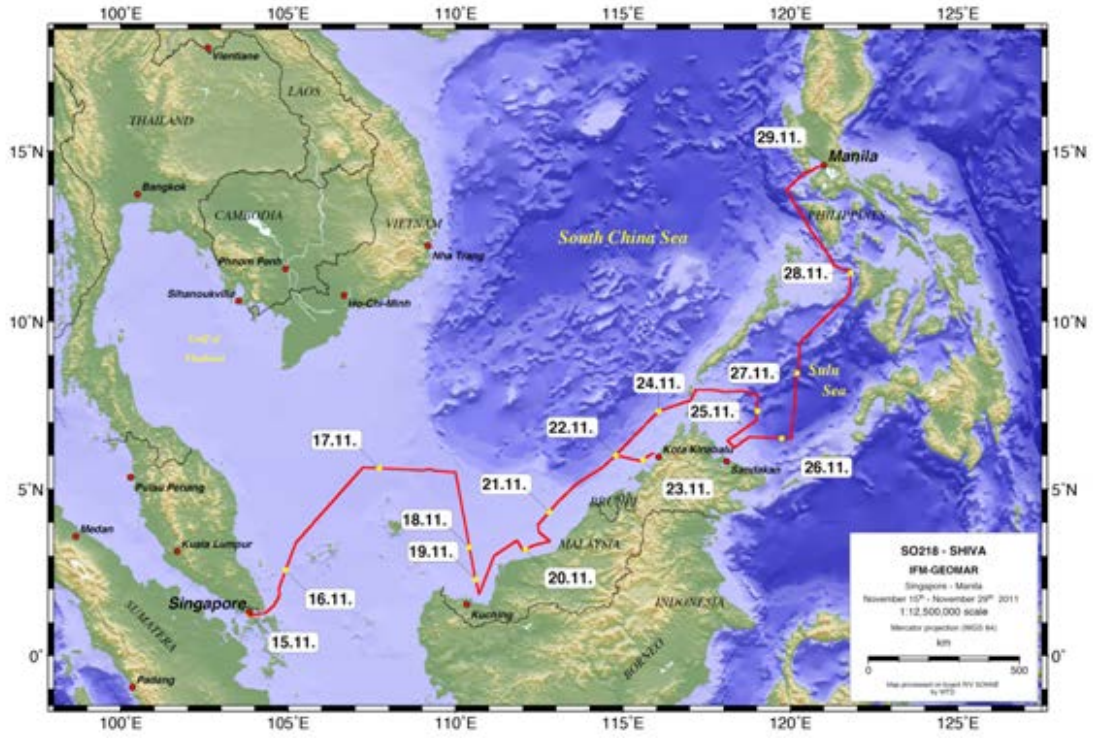

Figure 1: The track of the SHIVA Sonne Cruise.

There were two diurnal stations in shelf waters during the cruise, each roughly 20 km off coast from Kuching and Kota Kinabalu (KK) (diurnal stations: 2.41°N, 111.57°E; 6.01° N, 114.77° E respectively; Figure 2). Additionally local boats sampled near shore waters at 1 km, 5 km, 10 km, 15 km, and 20 km off coast. In order to investigate sources and sinks, vertical profiles of methyl iodide were measured along the cruise track. Only the samples from stations 3, 5, 6, and 11 were analysed with the GC-ECD system. The other profiles were analysed by gas chromatography coupled to mass spectrometry (GC-MS) from Helmke Hepach and Stefan Raimund. Stations 3, 5 and 6 lie in the South China Sea and Station 11 lies in the Sulu Sea (see Figure 2).

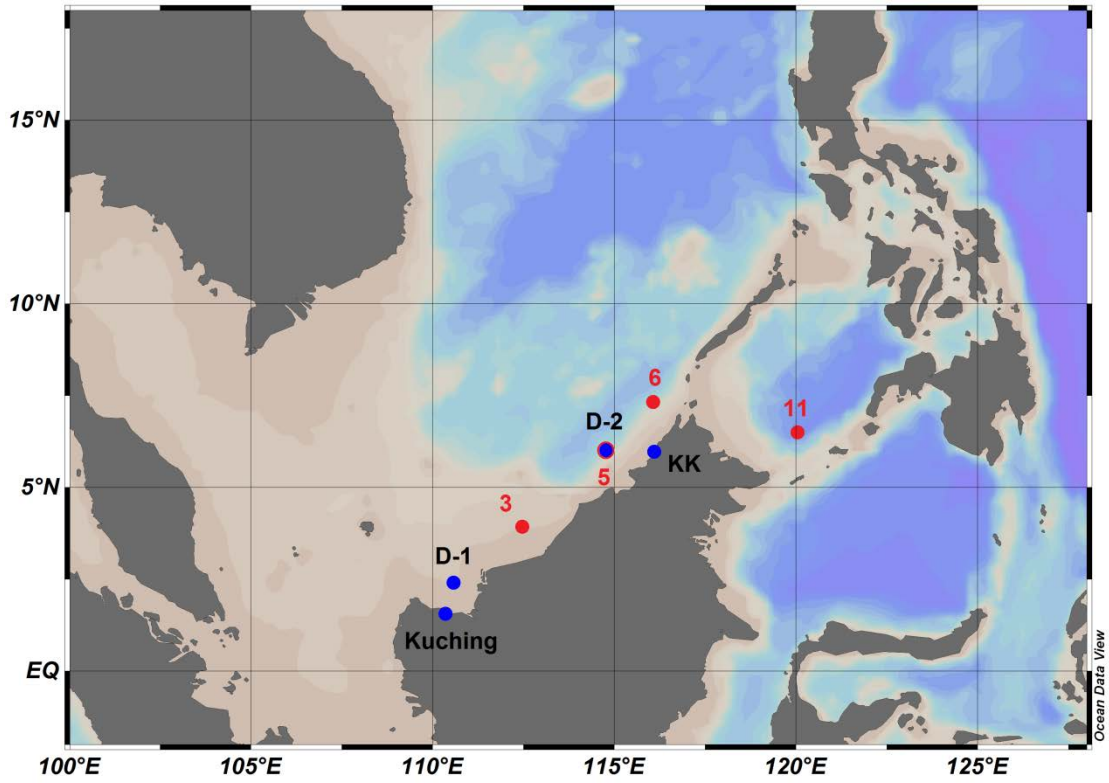

Figure 2: Locations of two diurnal stations (D-1and D-2), one was close to Kuching, the other was close to Kota Kinabalu (KK). Also pictured are the locations of CTD stations 3, 5, 6 and 11.

During the Sonne cruise, quantification of the compounds was carried out using liquid standards prepared on board. A stock standard solution contained 7.73 nmol μl^{-1} of CH_3I, 6.24 nmol μl^{-1} of $CHBr_3$, 7.77 nmol μl^{-1} of CH_2Br_2, 7.16 nmol μl^{-1} $CHCl_3$ and 7.03 nmol μl^{-1} CH_2ClI in 10 ml pentane. The stock solution was diluted stepwise to 1: 500000, 1:100000, 1: 50000 and 1:10000 in 10 ml methanol. Standard (volumes between 1 and 2 µl) were injected via a septum port into the purge vessel. Resulting calibration curves were linear (Figure 3). A blank was established each day by running the system with a repeatedly purged water sample (i.e. free of dissolved methyl iodide). Average blanks for the water analyses were equivalent to 1.16 ±0.12 pmol L^{-1}. A possible source of the blank was contamination of organic matter from water samples in the purge and trap system. The standard deviation of triplicate measurements of water samples on the cruise (mean concentration: 2.83 pmol L^{-1}) was 0.81 pmol L^{-1}.

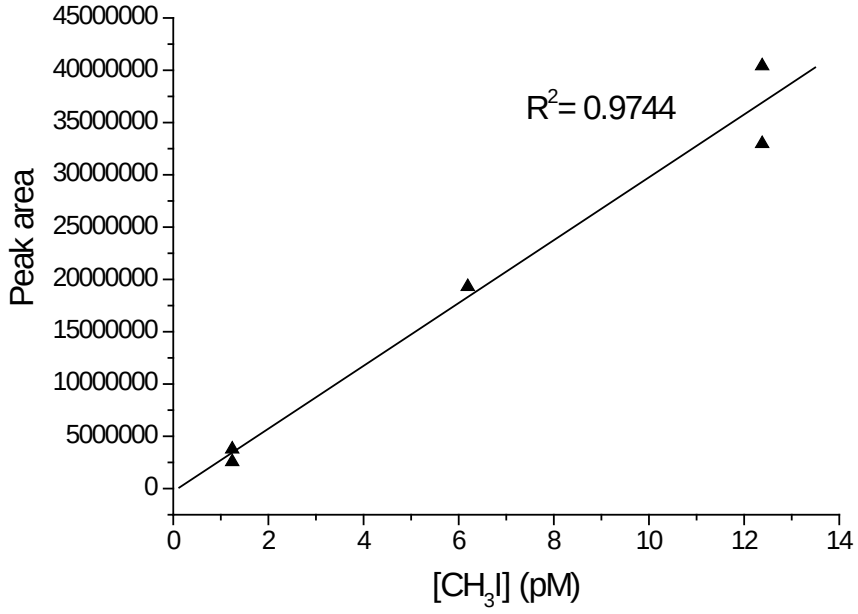

Figure 3: Calibration curve of methyl iodide in standard solution.

App.1.3 Results

App. 1.3.1 Variability of CH_3I Concentrations in the South China Sea

The measured concentrations of methyl iodide in surface waters of the South China Sea are shown in Figure 4. The concentrations ranged from 1.21 to 9.60 pmol L^{-1} (mean: 4.56 pmol L^{-1}). The higher concentrations of CH_3I were observed in the area around 111°E and 115°E, approaching the island of Borneo. These higher CH_3I concentrations are most likely related to a coastal influence, details will be discussed in section 6.4.3. The eastern part of the cruise between 10°N and 15°N show lower CH_3I concentrations from 2.50 to 4.50 pmol L^{-1}. This area is close to Manila, a possible explanation for these lower methyl iodide concentrations is given in the discussion in Section 6.5.3.
The surface concentrations of methyl iodide are plotted over the cruise dates along with chlorophyll *a*, SST, SSS, iodide and wind speed, starting in Singapore on 15 November 2011 and finishing in Manila on 29 November 2011 in Figure 5. During the cruise, SST varied from 27.5 °C to 31.1°C and SSS was low, ranging from 30.5 to 33.3. The concentration of chlorophyll *a* varied from 0.07 to 1.8 µg L^{-1}, reflecting an overall low phytoplankton

abundance in the region during that time. The wind speed ranged from 0.9 to 17.1 m s^{-1}. The highest concentration of methyl iodide was 9.59 pmol L^{-1} around 111°E (Figure 5, in pink circle), where SSS was reduced from 32.6 to 32.1. The highest concentration of chlorophyll *a* was observed 7 hours later than the highest CH_3I concentration. It is possible that coincidence between peaks in chlorophyll *a* and CH_3I was not seen because not enough overlapping measurements were made at this time. The two lowest CH_3I concentrations of 1.21 and 1.55 pmol L^{-1} were observed (Figure 5a, blue circles). It seems that the methyl iodide may have been lost during the purge and trap process, because the system blank was subtracted during the calibration.

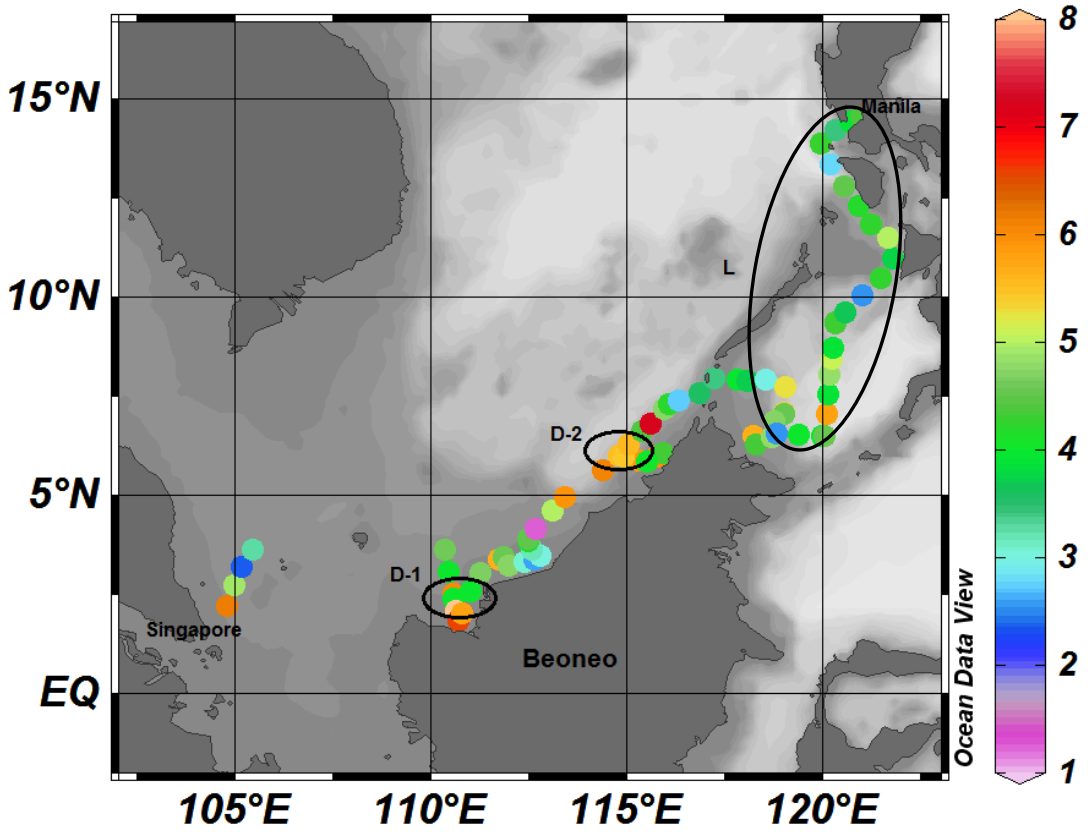

Figure 4: Surface water concentrations of CH_3I (pM) during the SO218 cruise. D-1 (18 Dec – 19 Dec) and D-2 (21 Dec – 22 Dec) show the results of the two diurnal stations. "L" circle shows the lower concentration region.

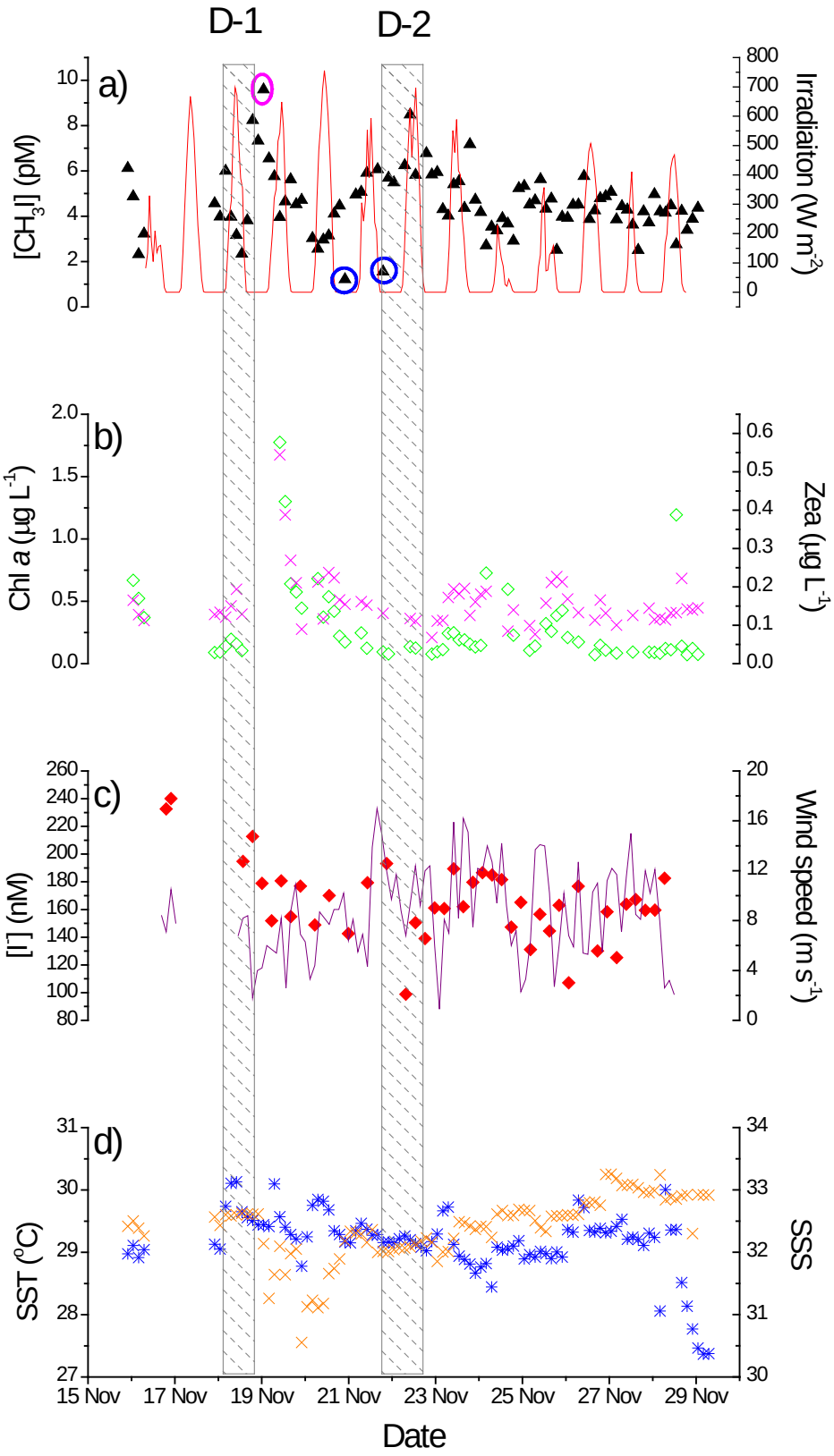

Figure 5: Variation of CH_3I (a; triangles), irradiation (a: red line), chlorophyll *a* (b; diamonds), zea pigment (b; crosses), iodide (c; diamonds), wind speed (c; purple line), SST (d; stars) and SSS (d; crosses) during the cruise (in local time, UTC+

8hours). Box D-1 shows the results from the first diurnal station, D-2 shows the results in the second diurnal station. The pink circle shows the highest concentration of underway samples. The blue circles show the lowest concentration of underway samples.

App. 1.3.2 Diurnal Variability of CH_3I Concentration in Surface Seawater

There were two diurnal stations in shelf waters during the cruise, each roughly 20 km off coast from Kuching and KK (locations marked in Figure 2). The diurnal variation of CH_3I concentrations in the surface seawater at these two stations is shown in Figures 4, 5 and 6. Concentrations of methyl iodide varied between 2.30 to 8.30 pmol L^{-1} at Kuching (mean: 4.81 pmol L^{-1}, Figure 6a), and 5.48 to 8.50 pmol L^{-1} at KK (mean: 6.41 pmol L^{-1}, Figure 6b). The lowest concentration (first value, 19:00) at KK was thrown out because it was at the limit of detection. At Kuching, the CH_3I concentration varied more strongly than at KK. The peak in concentrations at the two diurnal stations was observed at different times: 19:00 at Kuching; 10:00 at KK.

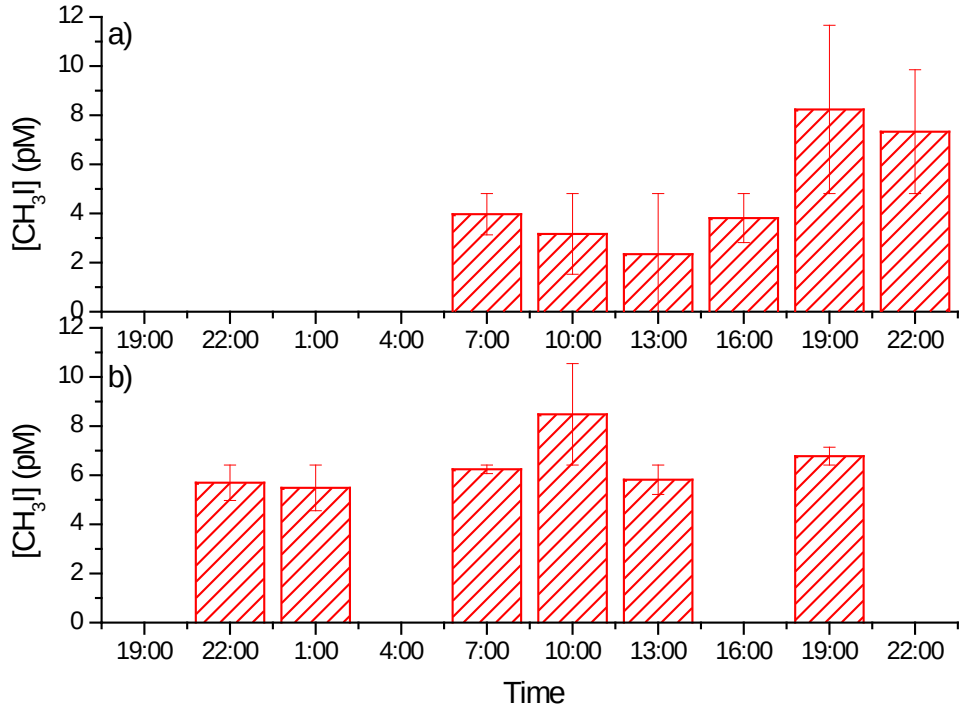

Figure 6: Diurnal variation (in local time) of methyl iodide in surface seawater, a): close to Kuching (2.41 °N, 110.57 °E); b): close to KK (6.01 °N, 114.77 °E).

App. 1.3.3 Depth Profiles of CH_3I

Vertical profiles of methyl iodide were measured along the cruise track in order to investigate sources and sinks. The samples at 4 stations, 3, 5, 6 and 11, were analyzed on board (locations marked in Figure 2). The samples at station 3 and 5 were collected in the night and the samples at station 6 and 11 were collected in the daytime. Figure 7 illustrates the vertical profiles of methyl iodide. A pronounced subsurface maximum of CH_3I concentration was observed in the profiles at about 15 - 20 m, except at station 6, with concentrations decreasing into deeper waters. At station 6, a small maximum was seen around 50 m (Figure 7, green line). The maximum concentration of methyl iodide in the South China Sea was 7.5 pmol L^{-1} (station 5, red line) and in the Sulu Sea it was 5.1 pmol L^{-1} (station 11, blue line).

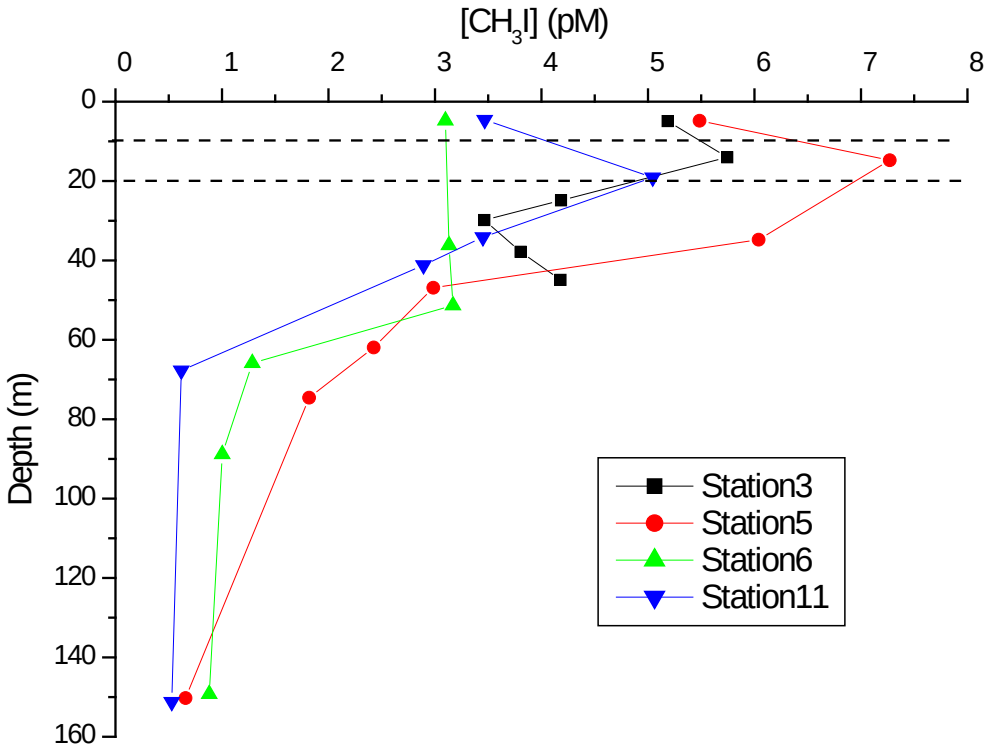

Figure 7: Vertical profiles of CH_3I concentrations from different stations. Dashed line shows the highest CH_3I concentration depth range.

Figure 8 illustrates the variation of salinity, temperature, iodide, iodate, chlorophyll *a* and cyanobacteria (pigment: zeaxanthin) in the water column at

each station. Station 3 is one shallow station with 50 m depth (Figure 7a). At ca. 15 m a maximum concentration of CH_3I was observed. A peak of iodate (IO_3^-) was found at the same depth. From 15 m deep the concentration of zea decreased and chlorophyll *a* increased slightly.

At station 5 (150 meter deep) a similar variation of CH_3I in the water column was found with a maximum concentration at ca. 15 m deep (Figure 8b). At the same depth the salinity started to increase slightly. Beneath 40 meter the iodide concentration decreased in the water column and the iodate concentration increased into the deep water. At 50 m a pronounced peak of chlorophyll *a* (green triangles) was found.

Station 6 (Figure 8c) was 750 meter deep. At this station CH_3I concentrations varied slightly from the surface to ca. 50 m. From 50 m depth, CH_3I concentration decreased to 0.5 pmol L^{-1}. Beneath 90 m no change was observed in CH_3I concentrations. Salinity started to increase at 35 m. Beneath the mixed layer, iodide concentrations decreased rapidly and iodate increased from 120 nmol L^{-1} to 350 nmol L^{-1}. One wide peak (50-60 m) was found in chlorophyll *a*.

One significant peak of CH_3I at 20 meter depth was found at station 11 (Figure 8d). At the same depth the concentration of the zea pigment showed a maximum, and salinity started to increase. No peaks were observed for iodide and iodate at 20 meter deep. Chlorophyll *a* showed a small peak at 50 meter depth.

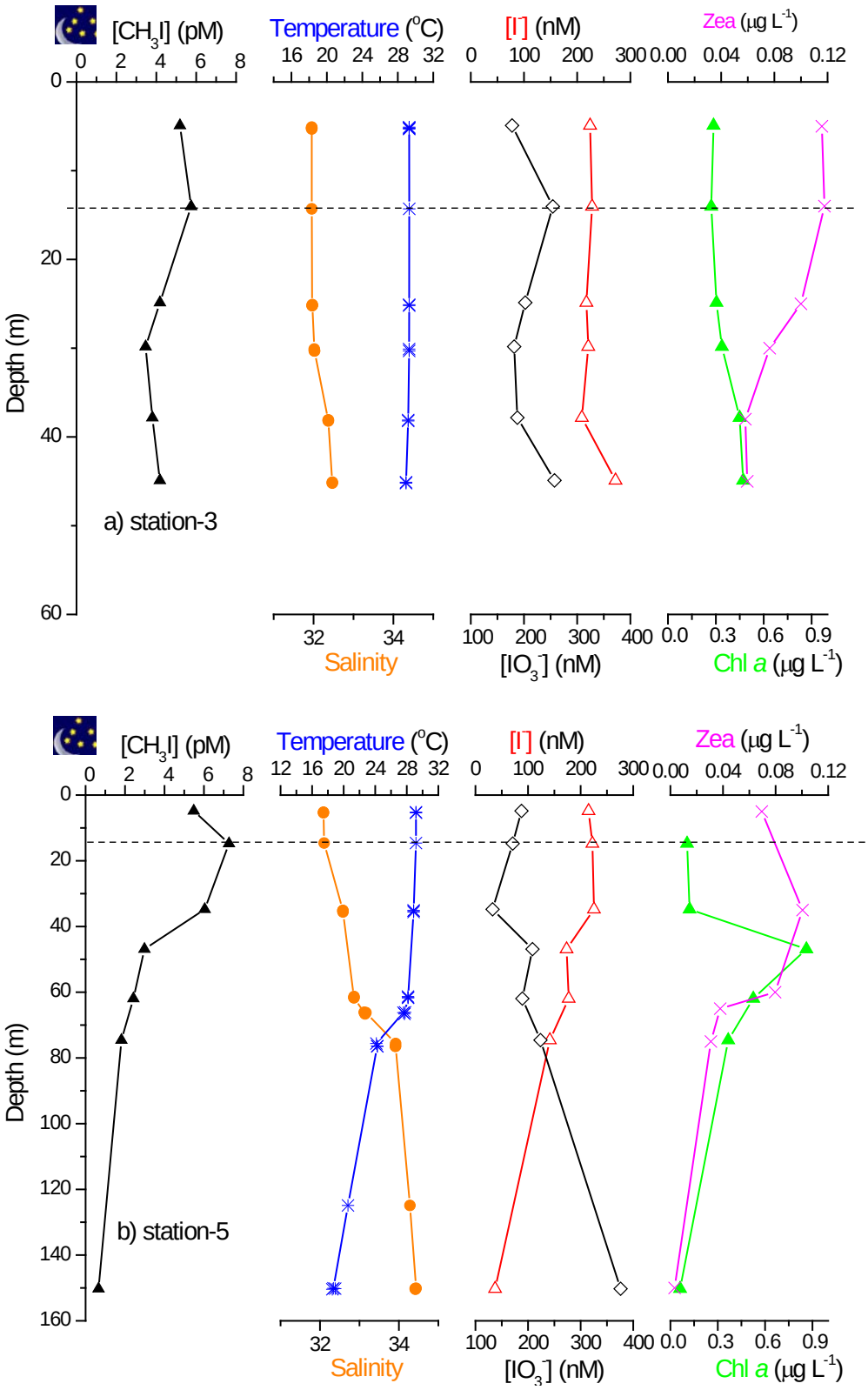
[CH3I] (pM)
Temperature (°C)
[I⁻] (nM)
Zea (µg L-1)
Depth (m)
a) station-3
Salinity
[IO3⁻] (nM)
Chl a (µg L-1)
b) station-5

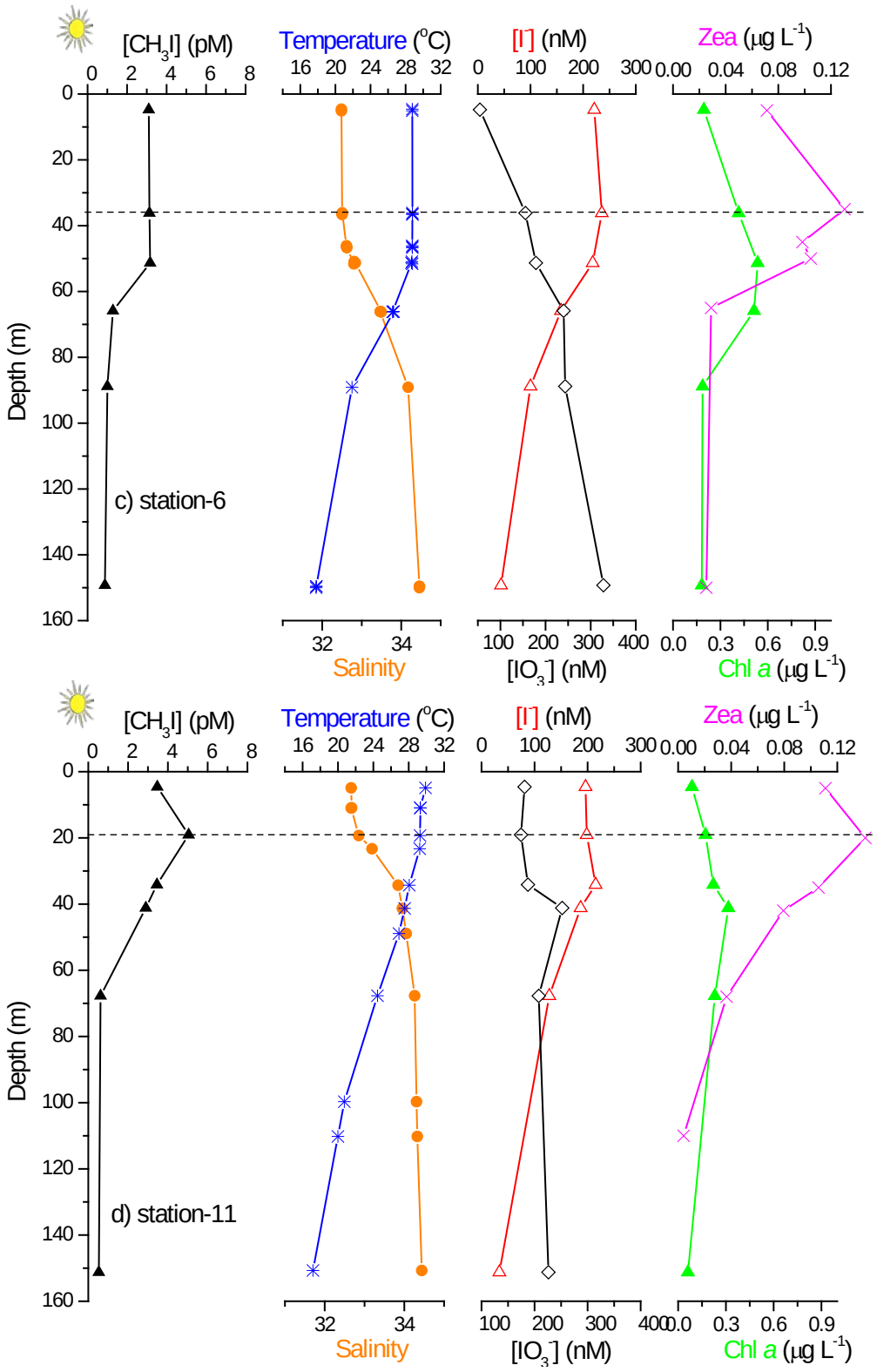

Figure 8: Vertical profiles of CH_3I (black triangles), salinity (orange circles), temperature (blue stars), iodide (red triangles), iodate (black diamonds), chlorophyll *a* (green triangles) and cyanobacteria (zea, purple crosses) in the water column at the same stations pictured in Figure 7. Dashed line shows the depth of highest CH_3I

concentration in the water column. Station 3 and 5 were conducted at night, Station 6 and 11 were in the day.

App. 1.3.4 Variation of CH_3I Concentration with the Distance to the Coast.

Two sample exchanges between 'local boats' and the R/V Sonne were performed during the cruise. Seawater samples were taken at 5 stations between the R/V Sonne and the coast by the 'local boats'. The measured concentrations of methyl iodide, sea surface temperature, salinity, iodide and chlorophyll *a* from these stations are plotted along the distance to the coast in the Figure 9. All samples were taken at 1 m depth except for the station closest to the R/V Sonne, where the sample was taken at 5 m depth (in red circle).

The main feature seen in these samples is the general decrease in CH_3I concentrations with distance from the coast. The CH_3I concentration ranged from 3-7 pmol L^{-1} at Kuching and 5-9 pmol L^{-1} at KK. After 16 km off coast the concentrations of CH_3I in the surface seawater varied less, remaining at ca. 4 pmol L^{-1} at Kuching and 5.5 pmol L^{-1} at KK. Methyl iodide concentrations in samples taken at 1 m depth were higher than in the sample collected at 5 m.

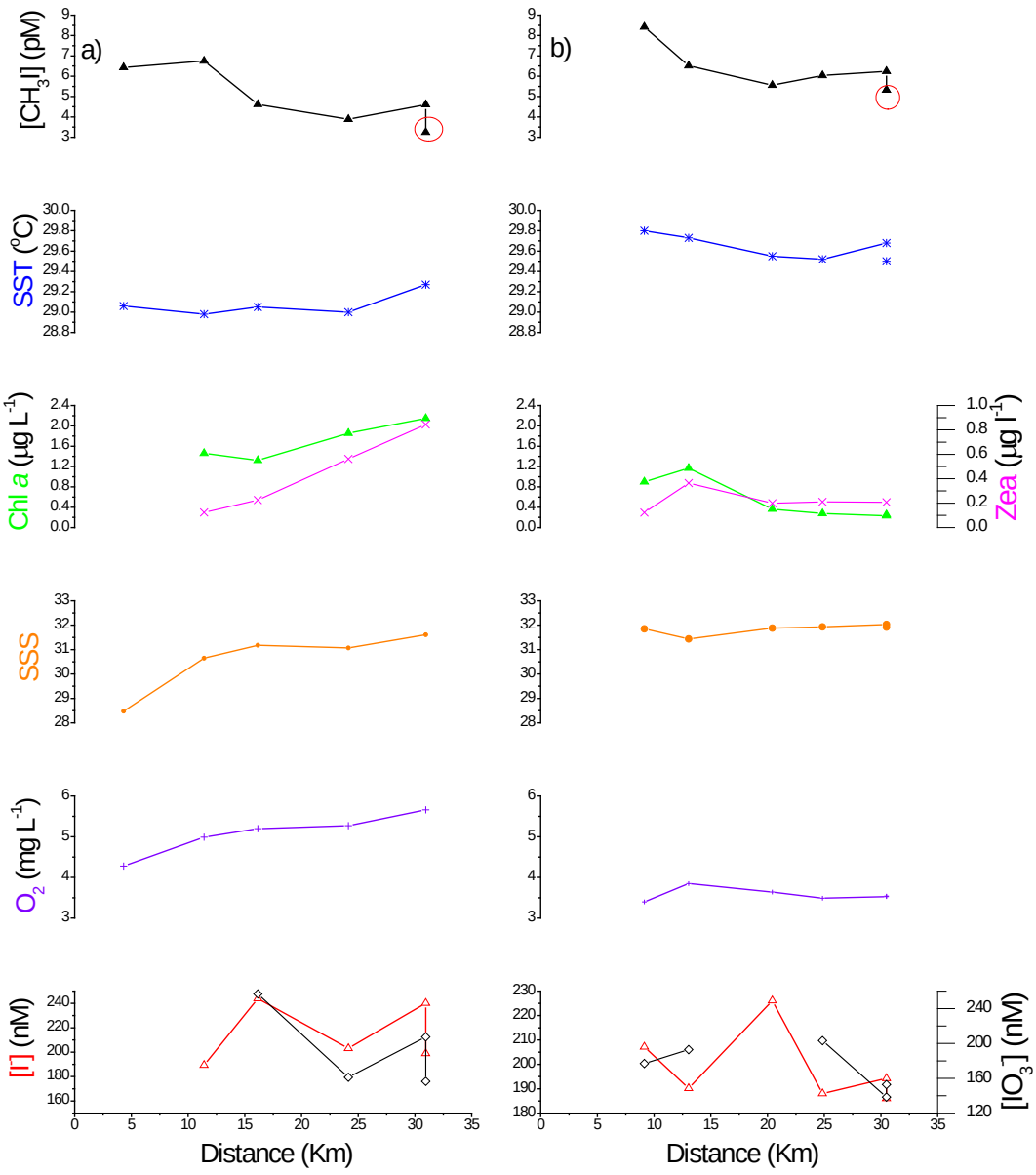

Figure 9: Variation of CH_3I (black triangles), salinity (orange circles), temperature (blue stars), iodide (red squares), iodate (black diamonds), oxygen (violet crosses), chlorophyll *a* (green triangles) and zea (purple crosses) along the distance from the coast. The last sample (in red circle) was taken at 5 m depth, others were taken at 1 m depth: a) at Kuching; b) at KK.

App.1.4 Discussion

In this chapter methyl iodide data from the tropical Pacific has been presented. The mean concentration of methyl iodide in the tropical Pacific seawater during SO218 was 4.56 ± 0.30 pmol L^{-1}.This is lower than 11.3 ± 9.9 pmol L^{-1} for the eastern Pacific (40°N-35°S), within the range of 2-47.9 pmol L^{-1} reported by Singh et al. [1983], and higher than those presented by Moore and Groszko [1999] (range 2 - 4 pmol L^{-1} between 40°S to 40°N in the Pacific) (Table 1). Richter reported a mean concentration of 6.7 ± 2.7 pmol L^{-1} (range 0.8-14.7 pmol L^{-1}) for the tropical Atlantic (Richter & Wallace, 2004), which looks similar to the results from this study. Happell [1999] reported 8.2 ± 0.6 pmol L^{-1} of CH_3I (range 6.1-12.3 pmol L^{-1}) for the southern tropical Atlantic (Happell & Wallace, 1996).

Table 1: Methyl iodide concentrations in surface seawater from the previous studies compared to this work (in pmol L^{-1}).

mean	Range	Area	Source
4.2	1.5-8.2	Atlantic	Tanzer and Heumann [1992]
8.2 (0.6)	6.1-12.3	southern tropical Atlantic	Happell and Wallace [1996]
6.7 (2.7)	0.8-7.9	western tropical Atlantic	Richter and Wallace [2003]
11.3 (9.9)	2.8-47.9	Eastern Pacific	Singh et al. [1983]
6.3	4.9-8.5	Ocean(Weddell)	Fogelqvist and Tanhua[1995]
2.1	0.08-8.8	Southern Pacific Ocean 62°-72°S	Schall et al. [1997]
	2.0-6.0	Pacific	Moore and Groszko [1999]
4.56 (0.30)	1.21-9.60	western tropical Pacific	**this work**

App. 1.4.1 Correlations between CH_3I and Other Parameters

The correlation of the seasonal variability of CH_3I in the Kiel Fjord, with corresponding biological and physical data, was discussed in Chapter 3 (Figure 5 in section 3.2.3). Strong positive temporal correlations of SST with CH_3I and chlorophyll *a* with CH_3I were observed, and a negative linear relationship between CH_3I and nitrate was found. The same statistical approach using scatterplots was used to investigate the correlations between methyl iodide and other biological and physical parameters on board the SHIVA cruise (Figure 10).

No significant correlation between methyl iodide and other parameters was observed. It seems that the results from the western Pacific are different from the previous study. The SST in the Kiel Fjord ranged from 0 to 22 °C, while the SST (27 to 31°C) during the Sonne cruise was higher with less variaiton. Groszko [1999] observed that the methyl iodide concentrations appeared to rise with temperature from 0 to 15°C. Above 18 °C, methyl iodide had no strong trend with temperature. As the geographical variation in sea surface temperature is determined mainly by the incoming irradiation to the sea surface, increased SST indicates that more solar energy reach the sea surface, and remains consistent with a photochemical production of CH_3I. Under the temperature limit SST has positive influence on the growth rate of phytoplankton and bacteria, which might produce CH_3I in sea water (Amachi et al., 2001; Brownell et al., 2010; Hughes et al., 2011; Smythe-Wright et al., 2006). On the other hand, increased SST reduces the solubility of gas. Taken together, these factors might explain why no significant correlation between CH_3I and SST was observed during this cruise.

The difference of other biological and physical parameters between the Sonne cruise and the Kiel Fjord experiment are presented in Table 2. As for SST, there are significant differences between SSS, chlorophyll *a* and nitrate data. In the Kiel Fjord, nitrate concentrations and chlorophyll *a* concentrations were ca. 10 times higher than during the Sonne cruise, and SSS was much lower

than during the Sonne cruise. The observations and correlations with biological, chemical and physical parameters in the Kiel Fjord were made over a long time period, thus reflecting temporal variations, while the observations during the Sonne cruise reflect spatial variations. Taken together, these factors lead to no significant correlations being observed in this study.

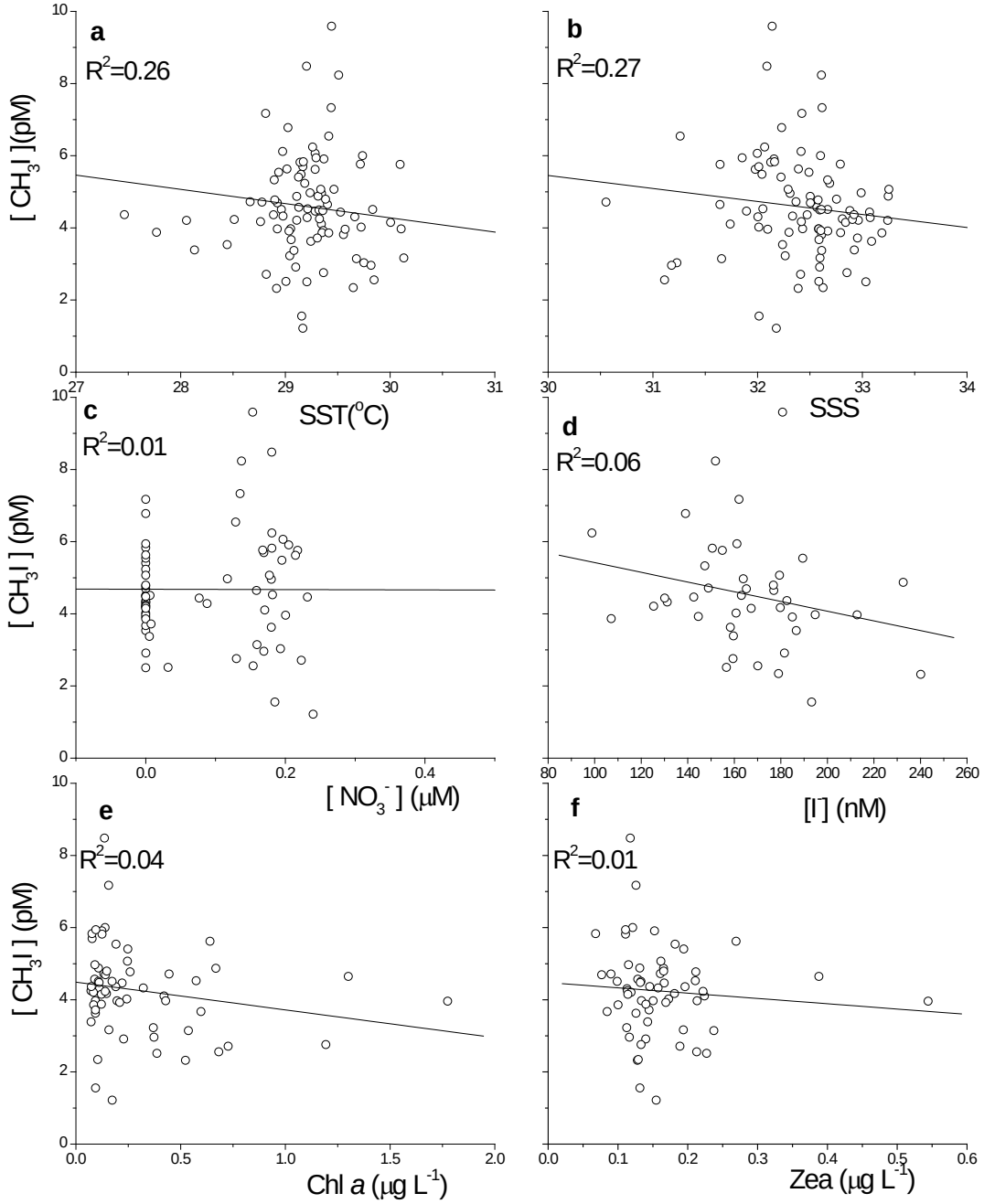

Figure 10: Scatter plots of CH_3I concentrations of underway samples against physical, chemical, and biological parameters a) SST, b) SSS, c) nitrate, d) iodide, e) Chl *a* and f) zea pigment.

The iodide concentrations were approximately the same level in both locations. Manley [1994] and Moore et al. [1994] found that the addition of iodide enhanced CH_3I production during incubations. No correlation between CH_3I and iodide was observed in the Kiel Fjord or on the Sonne cruise. Since iodide concentration in the seawater is 10000 times higher than CH_3I concentration, the fraction of iodide acting as a source of iodine radicals is only a minimal part of the total iodide concentration in the seawater. The concentration changes might be so low that no correlation between CH_3I and iodide can be observed.

Table 2: CH_3I and other parameters measured in underway samples from the Sonne cruise compared with the data from the Kiel Fjord (2009-2010)

Location	Kiel Fjord 54.3°N		Sonne cruise 1.8°N-14.7°N	
	mean	range	mean	range
SST (°C)	11.1	0-21.7	29.2	27.4-30.2
SSS	15.4	10.3-20.0	32.4	30.5-33.3
Nitrate (µM)	6.0	0.3-28.5	0.5	0-16
Iodide (nM)	151.4	50.3-272.6	165.6	98-240
Chl *a* (µg L)	4.3	0.6-11.5	0.3	0.07-1.8
Wind speed (m s^{-1})			8.8	0.9-17
CH_3I (pM)	5.0	0.4-12.3	4.6	2.0-9.5

App. 1.4.2 Vertical Profiles

The samples of depth profiles collected during the cruise demonstrated the existence of subsurface maxima in methyl iodide concentrations just in the mixed layer in the South China Sea. The CH_3I concentration maximum in the water column was located between 15 and 25 m deep (Figure 7). This is at a similar depth as that reported by Wang et.al. [2009]. Wang et al. [2009] observed a maximum of CH_3I concentration beneath the mixed layer (20-30 m

deep) in the Labrador Sea. However, that is at a much shallower depth than the observation by Moore and Groszko [1999]. They found the maximum concentration of CH_3I about 50 m deep in the Pacific, and suggested that the observed deep chlorophyll maximum (also at 50m) might explain the large maximum in methyl iodide through a biological production pathway. Overall, they hypothesize that higher biological production coupled to a lower chemical loss rate (depending on temperature) and a minimum sea-to-air flux lead to the maximum of CH_3I in the water column around 50 m. Archer et al. [2007] reported that the concentration of methyl iodide in the western English Channel varied slightly with depth in general. They did not observe the pronounced subsurface maximum.

In our data there is no correlation of the chlorophyll and the CH_3I maximum. The depth of CH_3I maximum was shallower than the observation of chlorophyll *a* maximum in the water column. One very likely explanation for the subsurface maximum of methyl iodide is simply the relationship between the depth of the zone of production and gas exchange. In the following we investigate the possibilities of photochemical and biological production of methyl iodide.

If methyl iodide production is a photochemical process involving the reaction of radicals produced through UV absorption (Happell & Wallace, 1996; Moore & Zafiriou, 1994; Richter & Wallace, 2004), then the depth of production could depend primarily on the attenuation coefficient of the water at the maximum wavelength of the actinic spectrum. Richter and Wallace [2004] showed that the light intensity at 20 m depth was lower than 20% of the surface light intensity. This indicated that the light dependent photochemical production rate would reduce rapidly in the water column.

If methyl iodide production is indeed biological (Brownell et al., 2010; Hughes et al., 2011; Smythe-Wright et al., 2006), the high concentrations of methyl iodide with depth in the water column are possibly due to the increasing number of cyanobacteria. Smythe-Wright [2006] reported that CH_3I in the

open ocean was biologically produced by marine cyanobacteria (i.e. *Prochlorococcus*). In this study a peak of the cyanobacteria pigment (zea) was observed in the same depth range as the CH_3I maximum. More methyl iodide might be produced via cyanobacteria in this zone. However, only at station 3 and 11 the maximum concentration of CH_3I and the pigment were found at the same depth (Figure 8). At station 5 the peak of CH_3I concentration was observed at 15 meter depth, which was higher than the depth (ca. 40 m) of the maximum pigment concentration. At station 6 no peak of CH_3I was observed at ca. 35 meter depth, where a pigment peak of was found. Here it should be noted that no pigment samples at 15 m at station 5 and no samples of any type are available for 15-25 meter depth at station 6. Therefore, it is possible that critical pieces of information are missing for these profiles and may not be directly comparable to the others (e.g. the zea peak was missed).

The commonly considered removal processes for CH_3I in the surface seawater are sea-to-air flux, nucleophilic substitution and loss due to mixing with waters with lower concentrations of CH_3I. In open ocean waters, the downward mixing loss has been shown to be negligible in comparison with the sea-to-air flux (e.g. Richter and Wallace, 2004). The loss by nucleophilic substitution with chloride ions is much lower than the loss via sea-to-air flux in the surface seawater in the previous studies (Archer et al., 2007; Moore & Groszko, 1999; Richter & Wallace, 2004). Sea-to-air flux is the major removal process for CH_3I in the surface seawater, which depends on the wind speed (Nightingale et al., 2000). Beneath the surface mixed layer, the rates of loss by efflux to the atmosphere are reduced (Moore & Groszko, 1999). The light depended photochemical production, biological production and sea-to-air flux should lead to the observed variation of CH_3I concentration in the water column.

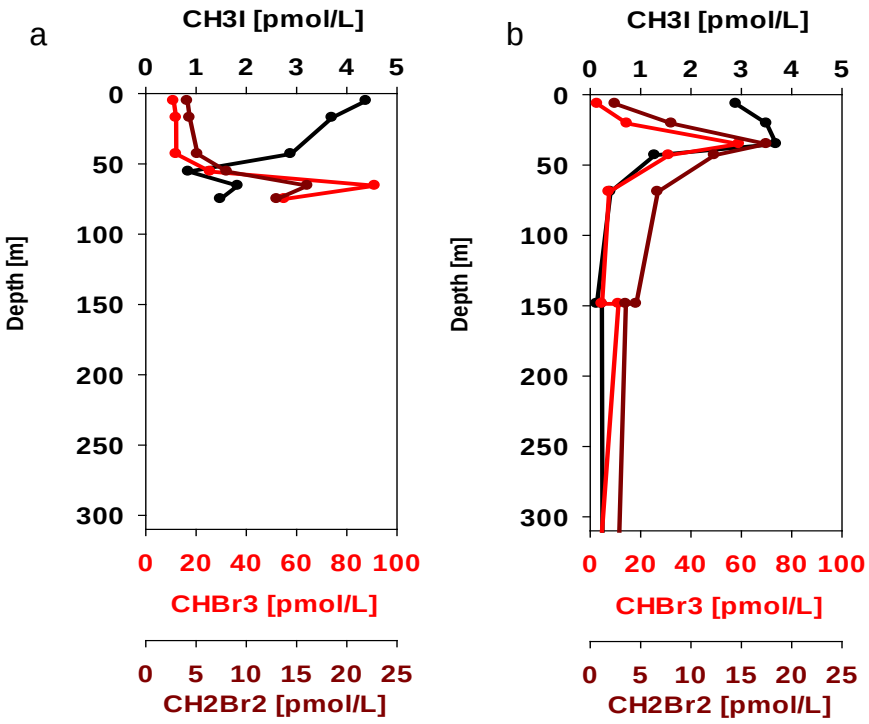

Figure 11: Typical observation of methyl iodide with depth in a) South China Sea and b) Sulu sea.

The results of additional CTD samples analysed on the cruise with GC-MS by Helmke Hepach and Stefan Raimund are summarized in Figure 11, which shows the general features of CH_3I profiles observed during the cruise (Figure 11). The CH_3I concentrations in the South China Sea generally decreased with depth, while maximum concentrations were observed deeper in the water column in the Sulu Sea. The depth profiles of methyl iodide in the South China Sea imply that the production process of methyl iodide is photochemical, depending on the attenuation of light intensity. The observed peak in the CH_3I concentration in the water column in Sulu Sea might be due to the decreasing of the sea-to-air flux, which is the major removal process for CH_3I in surface seawater. In this study a peak of the zea pigment was found in the same depth range as the CH_3I maximum (Figure 8a and d), and suggested that the production of CH_3I also could be biological, perhaps by *Prochlorococcus*.

App. 1.4.3 Daily Variation of CH_3I Concentration

A clear diurnal pattern in the CH_3I concentrations was observed at the two 24 hour stations. The concentration of CH_3I in surface seawater of the Kiel Fjord correlate with the solar radiation, SST, SSS, Chlorophyll *a* (as discussed in Chapter 3) and wind speeds (sea-to-air exchange). The reported sinks of CH_3I in the surface ocean are sea-to-air exchange and chemical loss via reaction with chloride. The computation of the loss processes was applied to the data of the South China Sea as it was to the Kiel Fjord. As in Chapter 3 (equation 3), the mass balance for CH_3I for surface water in the diurnal stations is calculated as

$$P_{net} = \Delta[CH_3I]_{3hour} + L_{sea-air} + L_{SN_2} + L_{Mix} \qquad (1)$$

where P_{net} represents the average net production rate of CH_3I, $\Delta[CH3I]_{3hour}$ is the accumulation or loss of CH_3I in 3 hours, $L_{sea\text{-}air}$ is the average sea-to-air flux of CH_3I in 3 hours, L_{SN2} is the " chemical" loss rate, and L_{Mix} is the loss due to mixing, which is assumed to be negligibe (see section 3.3.4).

Figure 12 illustrates daily variation of the net production rate of CH_3I (red line), the sea-to-air flux (blue line) depending on the wind speed, and the chemical loss rate (green line) depending on temperature. As already discussed in Chapter 3 (see section 3.3.4) and Chapter 4 (see section 4.3.3), the net production rate of CH_3I (P_{net}) based on the field sampling ranged from 0-0.03 pmol L^{-1} $hour^{-1}$, and the daytime accumulation rates during the 57 hours incubations were up to 0.14 pmol L^{-1} $hour^{-1}$ in summer in the Kiel Fjord. In Figure 12b, the production rates of CH_3I from 02:30 to 08:30 ranged from 0.05 to 0.2 pmol L^{-1} $hour^{-1}$ and were a similar magnitude of the daytime accumulation rates of the incubation experiments. From Figure 12a it is evident that significant production of methyl iodide occurred between 14:00 to 19:00 at the first diurnal station, which is supported by the observation in the incubation experiments in the Kiel Fjord in Chapter 4 (Figure 3 in Section 4.2.1). The significant increase of CH_3I concentration in the incubation was

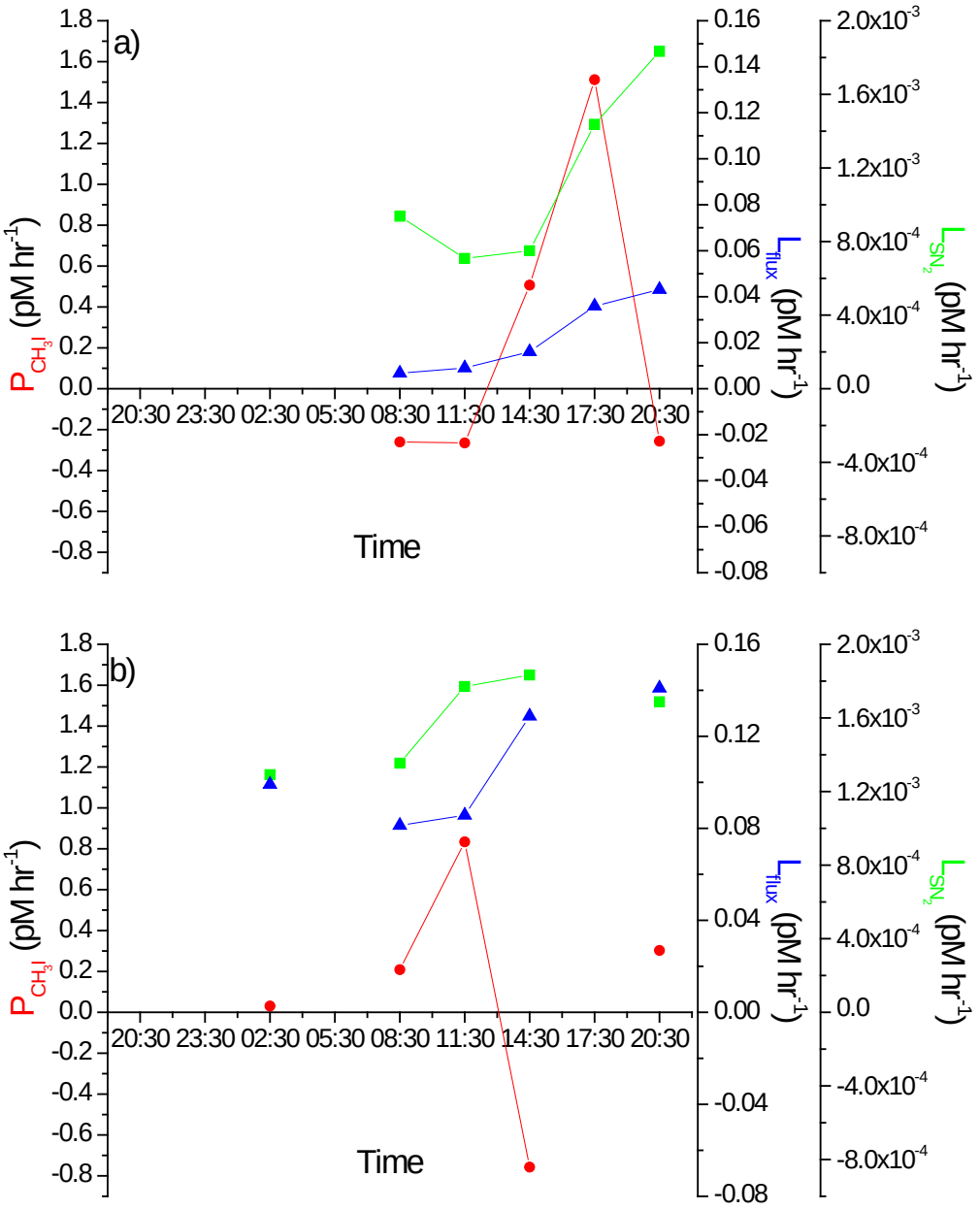

Figure 12: Daily variation of the sea-to-air-flux (blue line), the chemical loss rate (green line) and production rate of methyl iodide (red line). a) Kuching; b) KK.

observed between 12:00 to 17:00. However, Figure 12b shows the highest production rate of methyl iodide at the second diurnal station is between 10:00 and 13:00. By comparing sea-to-air flux during the two diurnal stations, it is clear that the flux at the second diurnal station (>0.08 pmol L^{-1} $hour^{-1}$, Figure 12b blue line) was much higher than at the first station (<0.05 pmol L^{-1} $hour^{-1}$,

Figure 12a blue line). It is possible that more methyl iodide was lost from the ocean surface at the second diurnal station, especially at 19:00, than at the first, which may explain why a maximum between 14:00 to 19:00 at the second diurnal station was not observed.

In both stations, negative production rates were computed. This might suggest another major removal process for methyl iodide in the surface ocean in addition to the sea-to-air flux and the “chemical” loss due to nucleophilic substitution of chloride (Cl^-). During the incubation experiments in the Kiel Fjord large loss rates (mean: 0.04 pmol L^{-1} $hour^{-1}$) at night were observed. This loss rate appears to correlate with the CH_3I concentration. Of course it is possible that the losses calculated are underestimated relative to actual conditions. However, it also possible that bacterial degradation and/or chemical oxidation could contribute to additional CH_3I loss in the water column. There is no direct evidence of bacterial methyl iodide degradation reported in the literature to date.

App. 1.4.4 Coastal Effect

A coastal effect on the CH_3I concentration was observed (Figure 9), where concentrations decreased with distance from the coast at Kuching and KK. The high levels of CH_3I were observed between 1 and 10 km off the coast and may be related to a source of methyl iodide from the mainland. Additionally, more dissolved organic matter in the coastal water could be a source of methyl radicals for photochemical production.

Figure 13 shows the geographical environment of Kuching and KK (the location of both day-long stations are marked in Figure 2). The first station (near Kuching, see Figure 11A) was 30 km from the estuary mouths of 6 rivers. These six rivers could offer prolific precursor species of photochemical production (dissolved organic matter) into the ocean, enhancing the photochemical production of methyl iodide in the nearshore water zone. The second diurnal station, which was near Kota Kinabalu (Figure 11B), was not

as influenced by runoff water. However, there are more than 100 rice paddies surrounding Kota Kinabalu. Muramatsu and Yoshida [1995] reported that 0.18 Gmol yr^{-1} of methyl iodide can be produced by rice paddies (Muramatsu & Yoshida, 1995). Redeker *et al.* [2000] found ca. 0.5 Gmol yr^{-1} emission of methyl iodide from rice paddies. In addition, there is evidence for a biological source of CH_3I from macro algae production ($4 \cdot 10^{-3}$ Gmol yr^{-1}) in the coastal water (Nightingale, Malin, & Liss, 1995). Despite the low global input of CH_3I by macro algae, it may locally be the dominant source, e.g. in coastal areas with large algae beds (Carpenter et al., 2000; Manley & delaCuesta, 1997). This may explain the higher concentration of methyl iodide near shore during the SHIVA Sonne cruise.

Figure 13: Geographical environment of the two day-long stations: A) close to Kuching; B) close to KK (adapted from Google map).

App.1.5 Conclusion and Outlook

The seawater concentrations of methyl iodide showed a spatial variation between 1.8°N and 14.7°N, with higher concentrations west of Borneo (Kuching). The South China Sea is a high concentration region of methyl iodide.

During the cruise, an increase of the CH_3I concentrations towards the coasts was observed. The highest concentration of CH_3I was observed close to Kuching around 110°E. The CH_3I concentration in the coastal water could be elevated because of river run off, introducing more DOC for photochemical production, and coastal biota, including rice paddies. Furthermore, sample exchanges between 'local boat' and the R/V Sonne confirm the coastal effect on two separate occasions. In the future, samples of DOM or CDOM should be analyzed in order to investigate the effect of organic matter input on the CH_3I production.

Depth profiles helped to determine the sources of methyl iodide. The main feature in the South China Sea was continuously decreasing CH_3I concentrations with depth, while in the Sulu Sea maximum concentrations were sometimes observed in the water column (ca.15-20 m deep). The depth profiles of methyl iodide in the South China Sea imply that the production process of methyl iodide might be photochemical depending on the attenuation of light intensity. The maximum of CH_3I in deeper water and a collocated maximum of cyanobacteria concentrations in the water column might imply another source of methyl iodide in the seawater (biological production via cyanobacteria). Both production processes may occur in parallel and it cannot be decided from this data set which one is more important in this region. Both production pathways need more investigation to improve the understanding of their role in the marine environment. Future work should involve the collection of repeated CTD profiles during day- and nighttime, collected at the same location. Also data about the attenuation of light intensity should be measured.

It is clear that the measurements performed for this body of work in the Kiel Fjord, incubation experiments, and in the South China and Sulu Seas are not directly comparable. However, after taking the differences into account, some clear trends emerge. There is evidence for an additional important sink for CH_3I in the surface ocean that may be related to bacteria. This mechanism needs further direct investigation. In addition, the daytime production rates observed in the incubation experiments are similar to those observed in the diurnal stations aboard the SHIVA cruise. In future studies, “whole-bottle” incubation experiments can be conducted during 24-hour stations to look more deeply into the mechanisms in different water masses. Again, non-filtered seawater and filtered seawater could be incubated to compare biological and photochemical processes. At the same time, CDOM, iodide and iodate should be analyzed in a diurnal cycle.

However, the Kiel Fjord study shows that correlations within one month could be weak and difficult to interpret. The correlations were strong because the data set encompassed an entire year and covered a wide range of conditions.

References

Amachi, S., Kamagata, Y., Kanagawa, T., & Muramatsu, Y. 2001. Bacteria Mediate Methylation of Iodine in Marine and Terrestrial Environments. ***Applied and Environmental Microbiology***, 67(6): 2718-2722.

Anderson, J. G., Toohey, D. W., & Brune, W. H. 1991. Free-Radicals within the Antarctic Vortex - the Role of Cfcs in Antarctic Ozone Loss. ***Science***, 251(4989): 39-46.

Andreae, M. O., Atlas, E., Harris, G. W., Helas, G., deKock, A., Koppmann, R., Maenhaut, W., Mano, S., Pollock, W. H., Rudolph, J., Scharffe, D., Schebeske, G., & Welling, M. 1996. Methyl halide emissions from savanna fires in southern Africa. ***Journal of Geophysical Research-Atmospheres***, 101(D19): 23603-23613.

Archer, S. D., Goldson, L. E., Liddicoat, M. I., Cummings, D. G., & Nightingale, P. D. 2007. Marked seasonality in the concentrations and sea-to-air flux of volatile iodocarbon compounds in the western English Channel. ***Journal of Geophysical Research-Oceans***, 112(C8).

Baker, J. M., Reeves, C. E., Nightingale, P. D., Penkett, S. A., Gibb, S. W., & Hatton, A. D. 1999. Biological production of methyl bromide in the coastal waters of the North Sea and open ocean of the northeast Atlantic. ***Marine Chemistry***, 64(4): 267-285.

Bell, N., Hsu, L., Jacob, D. J., Schultz, M. G., Blake, D. R., Butler, J. H., King, D. B., Lobert, J. M., & Maier-Reimer, E. 2002. Methyl iodide: Atmospheric budget and use as a tracer of marine convection in global models. ***Journal of Geophysical Research-Atmospheres***, 107(D17).

Berges, J. A., Franklin, D. J., & Harrison, P. J. 2004. Evolution of an artificial seawater medium: Improvements in enriched seawater, artificial water over the last two decades (vol 37, pg 1138, yr 2003). ***Journal of Phycology***, 40(3): 619-619.

Bluhm, K., Croot, P., Wuttig, K., & Lochte, K. 2010. Transformation of iodate to iodide in marine phytoplankton driven by cell senescence. ***Aquatic Biology***, 11(1): 1-15.

Bluhm, K., Croot, P. L., Huhn, O., Rohardt, G., & Lochte, K. 2011. Distribution of iodide and iodate in the Atlantic sector of the southern ocean during austral summer. ***Deep-Sea Research Part Ii-Topical Studies in Oceanography***, 58(25-26): 2733-2748.

Bricaud, A., Morel, A., & Prieur, L. 1981. Absorption by Dissolved Organic-Matter of the Sea (Yellow Substance) in the Uv and Visible Domains. ***Limnology and Oceanography***, 26(1): 43-53.

Brownell, D. K., Moore, R. M., & Cullen, J. J. 2010. Production of methyl halides by Prochlorococcus and Synechococcus. ***Global Biogeochemical Cycles***, 24.

Campos, M. L. A. M. 1997. New approach to evaluating dissolved iodine speciation in natural waters using cathodic stripping voltammetry and a storage study for preserving iodine species. ***Marine Chemistry***, 57(1-2): 107-117.

Campos, M. L. A. M., Farrenkopf, A. M., Jickells, T. D., & Luther, G. W. 1996. A comparison of dissolved iodine cycling at the Bermuda Atlantic Time-Series station and Hawaii Ocean Time-Series Station. ***Deep-Sea Research Part Ii-Topical Studies in Oceanography***, 43(2-3): 455-466.

Campos, M. L. A. M., Nightingale, P. D., & Jickells, T. D. 1996. A comparison of methyl iodide emissions from seawater and wet depositional fluxes of iodine over the southern North Sea. ***Tellus Series B-Chemical and Physical Meteorology***, 48(1): 106-114.

Carpenter, L. J., Malin, G., Liss, P. S., & Kupper, F. C. 2000. Novel biogenic iodine-containing trihalomethanes and other short-lived halocarbons in the coastal East Atlantic. ***Global Biogeochemical Cycles***, 14(4): 1191-1204.

Carpenter, L. J., Sturges, W. T., Penkett, S. A., Liss, P. S., Alicke, B., Hebestreit, K., & Platt, U. 1999. Short-lived alkyl iodides and bromides at Mace Head, Ireland: Links to biogenic sources and halogen oxide production. ***Journal of Geophysical Research-Atmospheres***, 104(D1): 1679-1689.

Chameides, W. L., & Davis, D. D. 1980. Iodine - Its Possible Role in Tropospheric Photochemistry. ***Journal of Geophysical Research-Oceans and Atmospheres***, 85(Nc12): 7383-7398.

Chance, R., Malin, G., Jickells, T., & Baker, A. R. 2007. Reduction of iodate to iodide by cold water diatom cultures. ***Marine Chemistry***, 105(1-2): 169-180.

Chance, R., Weston, K., Baker, A. R., Hughes, C., Malin, G., Carpenter, L., Meredith, M. P., Clarke, A., Jickells, T. D., Mann, P., & Rossetti, H. 2010. Seasonal and interannual variation of dissolved iodine speciation at a coastal Antarctic site. ***Marine Chemistry***, 118(3-4): 171-181.

Chuck, A. L., Turner, S. M., & Liss, P. S. 2005. Oceanic distributions and air-sea fluxes of biogenic halocarbons in the open ocean. ***Journal of Geophysical Research-Oceans***, 110(C10).

Closs, G. L., & Miller, R. J. 1978. Photo-Reduction and Photodecarboxylation of Pyruvic-Acid - Applications of Cidnp to Mechanistic Photochemistry. ***Journal of the American Chemical Society***, 100(11): 3483-3494.

Crutzen, P. J., & Arnold, F. 1986. Nitric-Acid Cloud Formation in the Cold Antarctic Stratosphere - a Major Cause for the Springtime Ozone Hole. ***Nature***, 324(6098): 651-655.

Davis, D., Crawford, J., Liu, S., McKeen, S., Bandy, A., Thornton, D., Rowland, F., & Blake, D. 1996. Potential impact of iodine on tropospheric levels of ozone and other critical oxidants. ***Journal of Geophysical Research-Atmospheres***, 101(D1): 2135-2147.

DeBruyn, W. J., & Saltzman, E. S. 1997. Diffusivity of methyl bromide in water. ***Marine Chemistry***, 57(1-2): 55-59.

Dimmer, C. H., Simmonds, P. G., Nickless, G., & Bassford, M. R. 2001. Biogenic fluxes of halomethanes from Irish peatland ecosystems. ***Atmospheric Environment***, 35(2): 321-330.

Dister, B., & Zafiriou, O. C. 1993. Photochemical Free-Radical Production-Rates in the Eastern Caribbean. ***Journal of Geophysical Research-Oceans***, 98(C2): 2341-2352.

Elderfield, H., & Truesdale, V. W. 1980. On the Biophilic Nature of Iodine in Seawater. ***Earth and Planetary Science Letters***, 50(1): 105-114.

Elliott, S., & Rowland, F. S. 1993. Nucleophilic-Substitution Rates and Solubilities for Methyl Halides in Seawater. ***Geophysical Research Letters***, 20(11): 1043-1046.

Eppley, R. W. 1972. Temperature and Phytoplankton Growth in Sea. ***Fishery Bulletin***, 70(4): 1063-1085.

Farrenkopf, A. M., Dollhopf, M. E., NiChadhain, S., Luther, G. W., & Nealson, K. H. 1997. Reduction of iodate in seawater during Arabian Sea shipboard incubations and in laboratory cultures of the marine bacterium Shewanella putrefaciens strain MR-4. ***Marine Chemistry***, 57(3-4): 347-354.

Fogelqvist, E., & Tanhua, T. 1995. Iodinated C-1-C-4 hydrocarbons released from ice algae in Antarctica. ***Naturally-Produced Organohalogens***, 1: 295-305.

Green, S. A., & Blough, N. V. 1994. Optical-Absorption and Fluorescence Properties of Chromophoric Dissolved Organic-Matter in Natural-Waters. ***Limnology and Oceanography***, 39(8): 1903-1916.

Grob, K., & Habich, A. 1983. Trace Analysis of Halocarbons in Water - Direct Aqueous Injection with Electron-Capture Detection. ***Journal of High Resolution Chromatography & Chromatography Communications***, 6(1): 11-15.

Grosskopf, T., Mohr, W., Baustian, T., Schunck, H., Gill, D., Kuypers, M. M. M., Lavik, G., Schmitz, R. A., Wallace, D. W. R., & LaRoche, J. 2012. Doubling of marine dinitrogen-fixation rates based on direct measurements. ***Nature***, 488(7411): 361-364.

Groszko, W. 1999. An Estimate of the Global Air-sea Flux of Methyl Chloride, Methyl Bromide, and Methyl Iodide. pp79-80.

Happell, J. D., & Wallace, D. W. R. 1996. Methyl iodide in the Greenland/Norwegian Seas and the tropical Atlantic Ocean: Evidence for photochemical production. ***Geophysical Research Letters***, 23(16): 2105-2108.

Heller, M. I., & Croot, P. L. 2010a. Application of a superoxide (O-2(-)) thermal source (SOTS-1) for the determination and calibration of O-2(-) fluxes in seawater. ***Analytica Chimica Acta***, 667(1-2): 1-13.

Heller, M. I., & Croot, P. L. 2010b. Kinetics of superoxide reactions with dissolved organic matter in tropical Atlantic surface waters near Cape Verde (TENATSO). ***Journal of Geophysical Research-Oceans***, 115.

Heller, M. I., & Croot, P. L. 2010c. Superoxide Decay Kinetics in the Southern Ocean. ***Environmental Science & Technology***, 44(1): 191-196.

Heumann, K. G., Gall, M., & Weiss, H. 1987. Geochemical Investigations to Explain Iodine-Overabundances in Antarctic Meteorites. ***Geochimica Et Cosmochimica Acta***, 51(9): 2541-2547.

Hughes, C., Chuck, A. L., Rossetti, H., Mann, P. J., Turner, S. M., Clarke, A., Chance, R., & Liss, P. S. 2009. Seasonal cycle of seawater bromoform and dibromomethane concentrations in a coastal bay on the western Antarctic Peninsula. ***Global Biogeochemical Cycles***, 23.

Hughes, C., Franklin, D. J., & Malin, G. 2011. Iodomethane production by two important marine cyanobacteria: Prochlorococcus marinus (CCMP 2389) and Synechococcus sp (CCMP 2370). ***Marine Chemistry***, 125(1-4): 19-25.

Jickells, T. D., Boyd, S. S., & Knap, A. H. 1988. Iodine Cycling in the Sargasso Sea and the Bermuda Inshore Waters. ***Marine Chemistry***, 24(1): 61-82.

Jones, C. E., Hornsby, K. E., Sommariva, R., Dunk, R. M., Von Glasow, R., McFiggans, G., & Carpenter, L. J. 2010. Quantifying the contribution of marine organic gases to atmospheric iodine. ***Geophysical Research Letters***, 37.

Jordan, A., Harnisch, J., Borchers, R., Le Guern, F. N., & Shinohara, H. 2000. Volcanogenic halocarbons. ***Environmental Science & Technology***, 34(6): 1122-1124.

Kennedy, H. A., & Elderfield, H. 1987. Iodine Diagenesis in Pelagic Deep-Sea Sediments. ***Geochimica Et Cosmochimica Acta***, 51(9): 2489-2504.

Klick, S. 1992. Seasonal-Variations of Biogenic and Anthropogenic Halocarbons in Seawater from a Coastal Site. ***Limnology and Oceanography***, 37(7): 1579-1585.

Klick, S., & Abrahamsson, K. 1992. Biogenic Volatile Iodated Hydrocarbons in the Ocean. ***Journal of Geophysical Research-Oceans***, 97(C8): 12683-12687.

Laturnus, F. 1995. Release of Volatile Halogenated Organic-Compounds by Unialgal Cultures of Polar Macroalgae. ***Chemosphere***, 31(6): 3387-3395.

Liss, P. S., & Slater, P. G. 1974. Flux of Gases across Air-Sea Interface. ***Nature***, 247(5438): 181-184.

Lovelock, J. E. 1974. Electron-Capture Detector - Theory and Practice. ***Journal of Chromatography***, 99(Nov6): 3-12.

Lovelock, J. E. 1975. Natural Halocarbons in Air and in Sea. ***Nature***, 256(5514): 193-194.

Lovelock, J. E., & Maggs, R. J. 1973. Halogenated Hydrocarbons in and over Atlantic. ***Nature***, 241(5386): 194-196.

Luther, G. W., Swartz, C. B., & Ullman, W. J. 1988. Direct Determination of Iodide in Seawater by Cathodic Stripping Square-Wave Voltammetry. ***Analytical Chemistry***, 60(17): 1721-1724.

Luther, G. W., Wu, J. F., & Cullen, J. B. 1995. Redox Chemistry of Iodine in Seawater - Frontier Molecular-Orbital Theory Considerations. ***Aquatic Chemistry***, 244: 135-155.

Maggs, R. J., Joynes, P. L., Davies, A. J., & Lovelock, J. E. 1971. Electron Capture Detector - New Mode of Operation. ***Analytical Chemistry***, 43(14): 1966-&.

Manley, S. L. 1994. The Possible Involvement of Methylcobalamin in the Production of Methyl-Iodide in the Marine-Environment. ***Marine Chemistry***, 46(4): 361-369.

Manley, S. L., & delaCuesta, J. L. 1997. Methyl iodide production from marine phytoplankton cultures. ***Limnology and Oceanography***, 42(1): 142-147.

Manley, S. L., Goodwin, K., & North, W. J. 1992. Laboratory Production of Bromoform, Methylene Bromide, and Methyl-Iodide by Macroalgae and Distribution in Nearshore Southern California Waters. ***Limnology and Oceanography***, 37(8): 1652-1659.

Martino, M., Mills, G. P., Woeltjen, J., & Liss, P. S. 2009. A new source of volatile organoiodine compounds in surface seawater. ***Geophysical Research Letters***, 36.

McFiggans, G., Plane, J. M. C., Allan, B. J., Carpenter, L. J., Coe, H., & O'Dowd, C. 2000. A modeling study of iodine chemistry in the marine boundary layer. ***Journal of Geophysical Research-Atmospheres***, 105(D11): 14371-14385.

Miyake, Y., & Tsunogai, S. 1963. Evaporation of Iodine from Ocean. ***Journal of Geophysical Research***, 68(13): 3989-&.

Moore, L. R., Coe, A., Zinser, E. R., Saito, M. A., Sullivan, M. B., Lindell, D., Frois-Moniz, K., Waterbury, J., & Chisholm, S. W. 2007. Culturing the marine cyanobacterium Prochlorococcus. ***Limnology and Oceanography-Methods***, 5: 353-362.

Moore, R. M. 2006. Methyl halide production and loss rates in sea water from field incubation experiments. ***Marine Chemistry***, 101(3-4): 213-219.

Moore, R. M., & Groszko, W. 1999. Methyl iodide distribution in the ocean and fluxes to the atmosphere. ***Journal of Geophysical Research-Oceans***, 104(C5): 11163-11171.

Moore, R. M., & Tokarczyk, R. 1992. Chloro-Iodomethane in North-Atlantic Waters - a Potentially Significant Source of Atmospheric Iodine. ***Geophysical Research Letters***, 19(17): 1779-1782.

Moore, R. M., & Tokarczyk, R. 1993. Volatile Biogenic Halocarbons in the Northwest Atlantic. ***Global Biogeochemical Cycles***, 7(1): 195-210.

Moore, R. M., Webb, M., Tokarczyk, R., & Wever, R. 1996. Bromoperoxidase and iodoperoxidase enzymes and production of halogenated methanes in marine diatom cultures. ***Journal of Geophysical Research-Oceans***, 101(C9): 20899-20908.

Moore, R. M., & Zafiriou, O. C. 1994. Photochemical Production of Methyl-Iodide in Seawater. ***Journal of Geophysical Research-Atmospheres***, 99(D8): 16415-16420.

Mopper, K., & Zhou, X. L. 1990. Hydroxyl Radical Photoproduction in the Sea and Its Potential Impact on Marine Processes. ***Science***, 250(4981): 661-664.

Muramatsu, Y., & Yoshida, S. 1995. Volatilization of Methyl-Iodide from the Soil-Plant System. ***Atmospheric Environment***, 29(1): 21-25.

Nelson, N. B., Carlson, C. A., & Steinberg, D. K. 2004. Production of chromophoric dissolved organic matter by Sargasso Sea microbes. ***Marine Chemistry***, 89(1-4): 273-287.

Nelson, N. B., Siegel, D. A., Carlson, C. A., Swan, C., Smethie, W. M., & Khatiwala, S. 2007. Hydrography of chromophoric dissolved organic matter in the North Atlantic. ***Deep-Sea Research Part I-Oceanographic Research Papers***, 54(5): 710-731.

Nelson, N. B., Siegel, D. A., & Michaels, A. F. 1998. Seasonal dynamics of colored dissolved material in the Sargasso Sea. ***Deep-Sea Research Part I-Oceanographic Research Papers***, 45(6): 931-957.

Newman, P. A., Daniel, J. S., Waugh, D. W., & Nash, E. R. 2007. A new formulation of equivalent effective stratospheric chlorine (EESC). ***Atmospheric Chemistry and Physics***, 7(17): 4537-4552.

Nightingale, P. D., Malin, G., Law, C. S., Watson, A. J., Liss, P. S., Liddicoat, M. I., Boutin, J., & Upstill-Goddard, R. C. 2000. In situ evaluation of air-sea gas exchange parameterizations using novel conservative and volatile tracers. ***Global Biogeochemical Cycles***, 14(1): 373-387.

Nightingale, P. D., Malin, G., & Liss, P. S. 1995. Production of Chloroform and Other Low-Molecular-Weight Halocarbons by Some Species of Macroalgae. ***Limnology and Oceanography***, 40(4): 680-689.

O'Dowd, C. D., Jimenez, J. L., Bahreini, R., Flagan, R. C., Seinfeld, J. H., Hameri, K., Pirjola, L., Kulmala, M., Jennings, S. G., & Hoffmann, T. 2002. Marine aerosol formation from biogenic iodine emissions. ***Nature***, 417(6889): 632-636.

Ooki, A., Tsuda, A., Kameyama, S., Takeda, S., Itoh, S., Suga, T., Tazoe, H., Okubo, A., & Yokouchi, Y. 2010. Methyl halides in surface seawater and marine boundary layer of the northwest Pacific. ***Journal of Geophysical Research-Oceans***, 115.

Pellizza.Ed. 1974. Electron-Capture Detection in Gas-Chromatography. ***Journal of Chromatography***, 98(2): 323-361.

Pi, Y. Z., Schumacher, J., & Jekel, M. 2005a. Decomposition of aqueous ozone in the presence of aromatic organic solutes. ***Water Research***, 39(1): 83-88.

Pi, Y. Z., Schumacher, J., & Jekel, M. 2005b. The use of para-chlorobenzoic acid (pCBA) as an ozone/hydroxyl radical probe compound. ***Ozone-Science & Engineering***, 27(6): 431-436.

Quack, B., Atlas, E., Petrick, G., Stroud, V., Schauffler, S., & Wallace, D. W. R. 2004. Oceanic bromoform sources for the tropical atmosphere. ***Geophysical Research Letters***, 31(23).

Rasmussen, R. A., Khalil, M. A. K., Crawford, A. J., & Fraser, P. J. 1982. Natural and Anthropogenic Trace Gases in the Southern-Hemisphere. ***Geophysical Research Letters***, 9(6): 704-707.

Rasmussen, R. A., Khalil, M. A. K., Gunawardena, R., & Hoyt, S. D. 1982. Atmospheric Methyl-Iodide (Ch3i). ***Journal of Geophysical Research-Oceans and Atmospheres***, 87(Nc4): 3086-3090.

Ratkowsky, D. A., Olley, J., Mcmeekin, T. A., & Ball, A. 1982. Relationship between Temperature and Growth-Rate of Bacterial Cultures. ***Journal of Bacteriology***, 149(1): 1-5.

Redeker, K. R., Wang, N. Y., Low, J. C., McMillan, A., Tyler, S. C., & Cicerone, R. J. 2000. Emissions of methyl halides and methane from rice paddies. ***Science***, 290(5493): 966-969.

Reifenhauser, W., & Heumann, K. G. 1992. Bromochloromethanes and Bromochloromethanes in the Antarctic Atmosphere and the South Polar Sea. ***Chemosphere***, 24(9): 1293-1300.

Rhee, G. Y., & Gotham, I. J. 1981. The Effect of Environmental-Factors on Phytoplankton Growth - Light and the Interactions of Light with Nitrate Limitation. ***Limnology and Oceanography***, 26(4): 649-659.

Richter, U., & Wallace, D. W. R. 2004. Production of methyl iodide in the tropical Atlantic Ocean. ***Geophysical Research Letters***, 31(23).

Roehl, C. M., Burkholder, J. B., Moortgat, G. K., Ravishankara, A. R., & Crutzen, P. J. 1997. Temperature dependence of UV absorption cross sections and atmospheric implications of several alkyl iodides. ***Journal of Geophysical Research-Atmospheres***, 102(11D): 12819-12829.

Scarratt, M. G., & Moore, R. M. 1996. Production of methyl chloride and methyl bromide in laboratory cultures of marine phytoplankton. ***Marine Chemistry***, 54(3-4): 263-272.

Schall, C., Heumann, K. G., & Kirst, G. O. 1997. Biogenic volatile organoiodine and organobromine hydrocarbons in the Atlantic Ocean from 42 degrees N to 72 degrees S. ***Fresenius Journal of Analytical Chemistry***, 359(3): 298-305.

Shaw, S. L., Chisholm, S. W., & Prinn, R. G. 2003. Isoprene production by Prochlorococcus, a marine cyanobacterium, and other phytoplankton. ***Marine Chemistry***, 80(4): 227-245.

Siegel, D. A., & Michaels, A. F. 1996. Quantification of non-algal light attenuation in the Sargasso Sea: Implications for biogeochemistry and remote sensing. ***Deep-Sea Research Part Ii-Topical Studies in Oceanography***, 43(2-3): 321-345.

Siegel, D. A., Michaels, A. F., Sorensen, J. C., Obrien, M. C., & Hammer, M. A. 1995. Seasonal Variability of Light Availability and Utilization in the Sargasso Sea. ***Journal of Geophysical Research-Oceans***, 100(C5): 8695-8713.

Singh, H. B., Salas, L. J., & Stiles, R. E. 1983a. Methyl Halides in and over the Eastern Pacific (40-Degrees-N-32-Degrees-S). ***Journal of Geophysical Research-Oceans and Atmospheres***, 88(Nc6): 3684-3690.

Singh, H. B., Salas, L. J., & Stiles, R. E. 1983b. Selected Man-Made Halogenated Chemicals in the Air and Oceanic Environment. ***Journal of Geophysical Research-Oceans and Atmospheres***, 88(Nc6): 3675-3683.

Sioris, C. E., Kovalenko, L. J., McLinden, C. A., Salawitch, R. J., Van Roozendael, M., Goutail, F., Dorf, M., Pfeilsticker, K., Chance, K., von Savigny, C., Liu, X., Kurosu, T. P., Pommereau, J. P., Bosch, H., & Frerick, J. 2006. Latitudinal and vertical distribution of bromine monoxide in the lower stratosphere from Scanning Imaging Absorption Spectrometer for Atmospheric Chartography limb scattering measurements. ***Journal of Geophysical Research-Atmospheres***, 111(D14).

Smythe-Wright, D., Boswell, S. M., Breithaupt, P., Davidson, R. D., Dimmer, C. H., & Diaz, L. B. E. 2006. Methyl iodide production in the ocean: Implications for climate change. ***Global Biogeochemical Cycles***, 20(3).

Solomon, S. 1990. Progress Towards a Quantitative Understanding of Antarctic Ozone Depletion. ***Nature***, 347(6291): 347-354.

Solomon, S., Garcia, R. R., & Ravishankara, A. R. 1994. On the Role of Iodine in Ozone Depletion. ***Journal of Geophysical Research-Atmospheres***, 99(D10): 20491-20499.

Spokes, L. J., & Liss, P. S. 1996. Photochemically induced redox reactions in seawater .2. Nitrogen and iodine. ***Marine Chemistry***, 54(1-2): 1-10.

Steinberg, D. K., Nelson, N. B., Carlson, C. A., & Prusak, A. C. 2004. Production of chromophoric dissolved organic matter (CDOM) in the open ocean by zooplankton and the colonial cyanobacterium Trichodesmium spp. ***Marine Ecology-Progress Series***, 267: 45-56.

Tanzer, D., & Heumann, K. G. 1992. Gas-Chromatographic Trace-Level Determination of Volatile Organic Sulfides and Selenides and of Methyl-Iodide in Atlantic Surface-Water. ***International Journal of Environmental Analytical Chemistry***, 48(1): 17-31.

Tessier, E., Amouroux, D., Abril, G., Lemaire, E., & Donard, O. F. X. 2002. Formation and volatilisation of alkyl-iodides and -selenides in macrotidal estuaries. ***Biogeochemistry***, 59(1-2): 183-206.

Tokarczyk, R., & Moore, R. M. 1994. Production of Volatile Organohalogens by Phytoplankton Cultures. ***Geophysical Research Letters***, 21(4): 285-288.

Truesdale, V. W. 1978. Automatic-Determination of Iodate-Iodine and Total-Iodine in Seawater. ***Marine Chemistry***, 6(3): 253-273.

Truesdale, V. W. 1995. The Distribution of Dissolved Iodine in Hebridean Waters during Midwinter. ***Marine Environmental Research***, 40(3): 277-288.

Truesdale, V. W., Luther, G. W., & Canosamas, C. 1995. Molecular-Iodine Reduction in Seawater - an Improved Rate-Equation Considering Organic-Compounds. ***Marine Chemistry***, 48(2): 143-150.

Tsao, C.-W., & Root, J. W. 1972. New primary process in the ultraviolet photolysis of methyl iodide. Direct photolysis to :CHI. ***The Journal of Physical Chemistry***, 76(3): 308-311.

Turner, N. H., & Deitz, V. R. 1975. Investigation of Adsorbent Charcoal Containing Iodine by Electron-Spectroscopy. ***Abstracts of Papers of the American Chemical Society***, 170(Aug24): 56-56.

Ullman, W. J., Luther, G. W., Delange, G. J., & Woittiez, J. R. W. 1990. Iodine Chemistry in Deep Anoxic Basins and Overlying Waters of the Mediterranean-Sea. ***Marine Chemistry***, 31(1-3): 153-170.

Vogt, R., Sander, R., Von Glasow, R., & Crutzen, P. J. 1999. Iodine chemistry and its role in halogen activation and ozone loss in the marine boundary layer: A model study. ***Journal of Atmospheric Chemistry***, 32(3): 375-395.

Waite, T. J., & Truesdale, V. W. 2003. Iodate reduction by Isochrysis galbana is relatively insensitive to de-activation of nitrate reductase activity - are phytoplankton really responsible for iodate reduction in seawater? ***Marine Chemistry***, 81(3-4): 137-148.

Wang, L., Moore, R. M., & Cullen, J. J. 2009. Methyl iodide in the NW Atlantic: Spatial and seasonal variation. ***Journal of Geophysical Research-Oceans***, 114.

Wong, G. T. F. 1991. The Marine Geochemistry of Iodine. ***Reviews in Aquatic Sciences***, 4(1): 45-73.

Wong, G. T. F., Piumsomboon, A. U., & Dunstan, W. M. 2002. The transformation of iodate to iodide in marine phytoplankton cultures. ***Marine Ecology-Progress Series***, 237: 27-39.

Yamamoto, H., Yokouchi, Y., Otsuki, A., & Itoh, H. 2001. Depth profiles of volatile halogenated hydrocarbons in seawater in the Bay of Bengal. ***Chemosphere***, 45(3): 371-377.

Yang, X., Cox, R. A., Warwick, N. J., Pyle, J. A., Carver, G. D., O'Connor, F. M., & Savage, N. H. 2005. Tropospheric bromine chemistry and its impacts on ozone: A model study. ***Journal of Geophysical Research-Atmospheres***, 110(D23).

Yokouchi, Y., Mukai, H., Yamamoto, H., Otsuki, A., Saitoh, C., & Nojiri, Y. 1997. Distribution of methyl iodide, ethyl iodide, bromoform, and dibromomethane over the ocean (east and southeast Asian seas and the western Pacific). ***Journal of Geophysical Research-Atmospheres***, 102(D7): 8805-8809.

Yokouchi, Y., Nojiri, Y., Barrie, L. A., Toom-Sauntry, D., & Fujinuma, Y. 2001. Atmospheric methyl iodide: High correlation with surface seawater temperature and its implications on the sea-to-air flux. ***Journal of Geophysical Research-Atmospheres***, 106(D12): 12661-12668.

Yokouchi, Y., Osada, K., Wada, M., Hasebe, F., Agama, M., Murakami, R., Mukai, H., Nojiri, Y., Inuzuka, Y., Toom-Sauntry, D., & Fraser, P. 2008. Global distribution and seasonal concentration change of methyl iodide in the atmosphere. ***Journal of Geophysical Research-Atmospheres***, 113(D18).

Zafiriou, O. C. 1974. Photochemistry of Halogens in Marine Atmosphere. ***Journal of Geophysical Research***, 79(18): 2730-2732.

Zafiriou, O. C. 1975. Reaction of Methyl Halides with Seawater and Marine Aerosols. ***Journal of Marine Research***, 33(1): 75-81.

Fortgeschrittenen-Praktikum Analytische Chemie, Prof. Heumann, Analytik von „Ozonkillern“ in der Umwelt mit Gaschromatographie und Elektroneneinfangdetektion (GC-ECD).

Acknowledgments

First of all I would like to thank my dear supervisor Prof. Dr. D.W.R. Wallace. I have learned so many things from him! I am so grateful for his encouragement, for teaching me British English and a positive life attitude.

I would like to thank Prof. Dr. C. Marandino and Dr. B. Quack for their helpful discussion and comments. It was a great pleasure to work on this topic with all of my co-authors. I am grateful to Gert Petrick for providing the technical support and helpful suggestions in the laboratory work.

I would also like to express my gratitude to GEOMAR offering the chance for me to study here and the SOPRAN project, which supported my PhD work financially. Likewise, I would like to thank the department secretary Codula Zenk for standing by my side whenever I needed advice, and my colleague Evgenia Ryabenko for providing helpful advice and encouragement.

Special thanks to my parents for their support and understanding. Without them I couldn´t concentrate on studying for nine years in Germany (for my Diploma and PhD).

In the end, I have to say something to my all friends in Kiel: Life in Kiel is so wonderful because of you!

Erklärung

Hiermit erkläre ich, dass die Dissertation “Seasonal Variability of Iodomethane (CH_3I) Production in the Surface Ocean of North Atlantic“ nach Inhalt und Form meine eigene Arbeit ist, abgesehen von der üblichen Beratung durch den Betreuer, Prof. Dr. D.W.R. Wallace. Ich habe die Dissertation selbstständig und ohne unerlaubte Hilfe angefertigt. Alle benutzen Quellen und Hilfsmittel habe ich vollständig angegeben. Die Zusammenarbeit mit anderen Wissenschaftlern habe ich kenntlich gemacht. Die Arbeit ist unter Einhaltung der Regeln guter wissenschaftlicher Praxis der Deutschen Forschungsgemeinschaft entstanden. Ferner habe ich weder diese noch eine ähnliche Arbeit an einer anderen Abteilung oder Hochschule im Rahmen eines Prüfungsverfahrens vorgelegt, veröffentlicht oder zur Veröffentlichung vorgelegt.

Kiel. 18. Dezember 2012 _____

(Qiang Shi)